



# VCU

Virginia Commonwealth University  
VCU Scholars Compass

---

Theses and Dissertations

Graduate School

---

2011

## Age Dependent Spatial Characteristics of Epileptiform Activity in Malformed Cortex

L. Andrew Bell  
*Virginia Commonwealth University*

Follow this and additional works at: <https://scholarscompass.vcu.edu/etd>



Part of the [Neurosciences Commons](#)

© The Author

---

Downloaded from

<https://scholarscompass.vcu.edu/etd/2614>

This Dissertation is brought to you for free and open access by the Graduate School at VCU Scholars Compass. It has been accepted for inclusion in Theses and Dissertations by an authorized administrator of VCU Scholars Compass. For more information, please contact [libcompass@vcu.edu](mailto:libcompass@vcu.edu).

© L. Andrew Bell 2011

All Rights Reserved

AGE DEPENDENT SPATIAL CHARACTERISTICS OF EPILEPTIFORM ACTIVITY  
IN MALFORMED CORTEX

A dissertation submitted in partial fulfillment of the requirements for the degree of Doctor of  
Philosophy in Neuroscience at Virginia Commonwealth University.

by

L. Andrew Bell  
B.A. Hampden-Sydney College, 2005

Director: Kimberle Jacobs, Ph.D.  
Associate Professor  
Department of Anatomy and Neurobiology

Virginia Commonwealth University  
Richmond, VA  
November 28, 2011

### **Acknowledgment**

The author wishes to thank several people. I would like to thank my very patient wife, Katie, for her love and support during the past six years and beyond. I would also like to thank my parents for their support and their academic genes. Last but not least, I would like to thank the many Virginia Commonwealth University faculty, students, and staff who have helped me with this project. They include my advisor, Dr. Kimberle Jacobs, my graduate committee members, Drs. Rory McQuiston, Alex Medina, Jason Chen, Margaret Biber, fellow students of the Anatomy and Neurobiology department, and members of the Povlishock lab.

## Table of Contents

	Page
List of Figures .....	iv
List of Abbreviations .....	vi
Abstract .....	1
Chapter 1    Introduction to Epilepsy and the Timeline of Seizure Susceptibility .....	3
1.1 Introductory statement .....	3
1.2 Introduction to epilepsy .....	4
1.3 Normal cortical development .....	9
1.4 Cortical malformations associated with cortical development .....	13
1.5 Polymicrogyria - clinical observations and freeze lesion model.....	19
1.6 Postnatal maldevelopment - timeline of hyperexcitability .....	37
1.7 General Methods .....	46
Chapter 2    Early Susceptibility to Epileptiform Activity in Malformed Cortex .....	61
Introduction .....	62
Methods .....	63
Results .....	66
Discussion .....	72
Chapter 3    Developmental Characteristics of Spontaneous Epileptiform Activity in Malformed Cortex .....	88
Introduction .....	89
Methods .....	90
Results .....	93
Discussion .....	99
Chapter 4    Characterization of the Spatial Dynamics of Epileptiform Events in the Cortical Malformation of Microgyria .....	118
Introduction .....	119
Methods .....	122
Results .....	124
Discussion .....	130
Chapter 5    General Discussion .....	150
List of References .....	158
Vita .....	197

## List of Figures

Figure	Page
1.1 Timing of Neurogenesis in Rat .....	49
1.2 Cortical Radial Migration .....	51
1.3 Interneuron Neurogenesis and Tangential Migration .....	53
1.4 Five Types of Developmental Cortical Malformations .....	55
1.5 Human Polymicrogyria and Freeze Lesion Model of Microgyria .....	57
1.6 Types of Epileptiform Activity in Low Magnesium aCSF Recorded for Dissertation ...	59
2.1 Intrinsic Excitability Changes in Normal aCSF During Development .....	76
2.2 Example of Automated Epileptiform Activity Detection .....	78
2.3 Threshold for Epileptiform Activity Visualized by Spectrogram .....	80
2.4 Increased Incidence of Epileptiform Sweeps in PMR Cortex .....	82
2.5 Time to First Epileptiform Sweep After Low-Mg <sup>2+</sup> Application .....	84
2.6 Magnitude of Late Field Potential Activity .....	86
3.1 Type of Activity Induced by Low-Mg <sup>2+</sup> aCSF in P12 Neocortex .....	106
3.2 Developmental Changes in Low-Mg <sup>2+</sup> aCSF-induced Epileptiform Activity .....	108
3.3 Duration of SLE and Interval Between SLEs Does Not Predict Emergence of CRI ....	110
3.4 Spontaneous Epileptiform Events in PMR are Dependent on Glutamatergic Transmission .....	112
3.5 Pharmacological Manipulation of CRI Persistence and Spectral Properties in P9 PMR cortex .....	114

3.6	CRI Rhythmicity After Pharmacological Manipulation Does Not Change .....	116
4.1	Voltage-sensitive Dyes Used to Assess Neuronal Activity For Distances of Over 4 mm .....	136
4.2	Spatiotemporal Characteristics of Evoked Responses Prior to Low-Mg <sup>2+</sup> in PMR and Control Cortex .....	138
4.3	Examples of MG- and PMR-Initiated Epileptiform Activity .....	140
4.4	Influence of Malformation Induction Timing on Evoked Epileptiform Activity Initiation Site .....	142
4.5	The Location of Epileptiform Activity Initiation Site Relative to the Induced Sulcus Varies Depending on the Timing of the Malformation Induction .....	144
4.6	The Propagation Rate of Evoked Epileptiform Activity is Faster Near the Malformation .....	146
4.7	Density of vGlut2 Immunohistochemical Staining is Higher in PMR Cortex than in Control for Middle and Deep Layers .....	148

### List of Abbreviations

°C	degrees Celsius
aCSF	artificial cerebral spinal fluid
AED	anti-epilepsy drug
AD	anno domini
AIDA	1-amino-2,3-dihydro-1H-indene-1,5-dicarboxylic acid
AMPA	alpha-amino-3-hydroxy-5-methyl-4-isoxazolepropionic acid
APV	D,L-2-amino-5-phosphonopentanoic acid ATP adenosine 5'-triphosphate
BC	before christ
BCNU	1,2-bis-chloroethyl-nitrosourea
CGE	caudal ganglionic eminence
CNS	central nervous system
CO	cytochrome oxidase
Cp	cortical plate
CRI	continuous repetitive ictal-like activity
DHPG	S-3,5-dihydroxyphenylglycine hydrate
DNQX	dinitroquinoxaline [(6,7)],2,3(1H,4H)-dione
e-	evoked
E-	embryonic day
EEG	Electroencephalography



EPSC	excitatory postsynaptic current
FDA	Food and drug administration
FS	fast-spiking
GABA	$\gamma$ -aminobutyric acid
HCN	the hyperpolarization-activated non-specific cation
Hz	hertz
II	interictal
IZ	intermediate zone
IPSC	inhibitory postsynaptic current
LFP	local field potential
LGE	lateral ganglionic eminence
Low Mg <sup>2+</sup>	low magnesium artificial cerebral spinal fluid
LRFP	late rectified field potential
LTP	long term potentiation
LTS	low threshold spiking
m-	miniature
MAM	methylazoxymethanol
MEG	Magnetoencephalography
MG	microgyrial area
MGE	medial ganglionic eminence
mGluR	metabotropic glutamate receptor
MGN	medial geniculate nucleus
Mins	minutes

mM	millimolar
mOsm	milliosmolar
MPEP	6-methyl-2-(phenylethynyl) pyridine hydrochloride
mRNA	messenger ribonucleic acid
msec	millisecond
MUA	multi-unit activity
mV	millivolt
mz	marginal zone
NMDA	N-methyl-D-aspartate
O <sub>2</sub>	oxygen
P	postnatal day
PMG	polymicrogyria
PMR	paramicrogyral region
RS	repetitive spike ictal event
s-	spontaneous
SLE	seizure-like events
sp	subplate
spont	spontaneous
SS	single-spike ictal event
SZ	subventricular zone
TISH	telencephalic internal structure heterotopia
VB	ventrobasal
vGlut2	vesicular glutamate transporter 2

VIP	vasoactive intestinal peptide
VSD	voltage sensitive dye imaging
Vz	ventricular zone
$\mu\text{m}$	micrometer
$\mu\text{M}$	micromolar

## **Abstract**

### **AGE DEPENDENT SPATIAL CHARACTERISTICS OF EPILEPTIFORM ACTIVITY IN MALFORMED CORTEX**

by L. Andrew Bell

A dissertation submitted in partial fulfillment of the requirements for the degree of Doctor of Philosophy at Virginia Commonwealth University.

Virginia Commonwealth University, 2011

Director: Kimberle Jacobs, Ph.D.  
Associate Professor, Department of Anatomy and Neurobiology

Developmental cortical malformations are a major cause of intractable seizures. Determining the location and timing of susceptibility for epileptiform activity is critical to identifying what mechanisms contribute to epileptogenesis in any model. Using the freeze lesion rat model of polymicrogyria, we have identified, in lesioned cortex, these two aspects of epileptogenesis.

Previous studies have demonstrated that epileptiform activity cannot be evoked prior to postnatal day (P) 12, but the malformed cortex is more susceptible to seizures as early as P10. An increase in excitatory afferents to the epileptogenic zone occurs before the onset of network epileptiform activity. Whether or not these afferents are a major contributor to the hyperexcitability of the malformed cortex can be investigated by determining if they specifically create a susceptibility for epileptiform activity. We have examined that here by measuring

whether that timing coincides with an increased susceptibility for evoked and spontaneous epileptiform activity. We report that the malformed cortex is more susceptible to evoked epileptiform activity than control cortex as early as P7 and as late as P36. Further, we also find that the form of spontaneous epileptiform activity in malformed cortex is altered as early as P7. The timing of these early disruptions of cortical function found here suggests additional epileptogenic mechanisms exist prior to the reported increase in excitatory afferents at P10.

Determining the location of the seizure initiation is an essential part of epilepsy research. Some patients with developmental cortical malformations have seizures initiated within the malformation, while others have seizures generated by the surrounding cortex. Previous data in the freeze lesion model of microgyria suggests that the timing of freeze lesion (from P0 to P1) can shift the epileptogenic focus from the malformation to the paramicrogyrial region (PMR). We report that both the timing of the freeze lesion and the survival age of the animal can alter the epileptogenic circuitry of the malformation and surrounding tissue. These findings provide new insight to the timeline of hyperexcitability in malformed cortex and will possibly lead to greater surgical success for patients with intractable epilepsy.

## Chapter 1

### Introduction to Epilepsy and the Timeline of Seizure Susceptibility

#### 1.1 Introductory Statement

Epilepsy is a chronic and sometimes debilitating neurological condition that is difficult to control in part because there are multiple disease forms with distinct underlying mechanisms. Most important to investigate with animal models are the forms of epilepsy with intractable seizures. The fact that the seizures are intractable demonstrates that we currently have no effective treatments. A significant portion of these types of epilepsy come from cortical maldevelopment that produces structural malformations (322). There are a variety of malformations induced with different timing and quality of insults, including genetic mutation (148). In these studies we focus on the malformation of microgyria, one of the most common forms, that can produce a severe seizure condition (24).

Our ultimate goal is to identify treatments and preventions that target the underlying neurological mechanisms. Critical to identifying what mechanisms contribute to epileptogenesis in any model is determining the location and timing of susceptibility for epileptiform activity. Experiments here examine these two aspects of epileptogenesis.

Previous work in the animal model used here, the freeze lesion-induced microgyria, shows that an increase in excitatory afferents to the epileptogenic zone occurs before the onset of network epileptiform activity (320). Whether or not these afferents are a major contributor to the hyperexcitability of this cortex can be investigated by determining if they specifically create a

susceptibility for epileptiform activity. We have examined that here by determining if that timing coincides with an increased susceptibility for epileptiform activity.

Often the approach to identifying the neurological mechanisms of epileptogenesis is to list the abnormalities that occur after onset. However, in order to identify the epileptogenic mechanisms, the initiating region must be first identified. This issue is of particular clinical importance in cortices with malformations. Studies of the effect of resection have already repeatedly demonstrated the usefulness of including cortex adjacent to the malformation in resection for best outcome (267) (highest percentage of seizure reduction). In addition, there appear to be two distinct clinical populations, one that shows clear seizure initiation from within the malformed region as identified on imaging (156), and a separate population in which seizure initiation is also dependent on adjacent cortex (50). Here we have examined whether the timing of the insult might account for these differences in the location of seizure initiation relative to the site of malformation.

## **1.2 Epilepsy**

### ***Introduction***

Epilepsy is a collection of complex disorders of the brain, which involve a wide range of manifestations and which are due to a variety of causes. The defining feature of epilepsy is the occurrence of recurrent epileptic seizures (more than one). There are many definitions of an epileptic seizure, the International Bureau for Epilepsy (IBE) proposed the definition of an epileptic seizure to be: “A transient occurrence of sign and/or symptoms due to abnormal excessive or synchronous neuronal activity in the brain” (93).

### ***History***

The word “epilepsy” derives from the Greek verb “epilambvanein,” meaning “to be seized, to be overwhelmed by surprise.” Some of the first written accounts about the basic medical concepts of epilepsy appear in ancient Indian medicine of the Vedic period of 4500-1500 BC (70), but for most of human history the disorder has been associated with the supernatural and considered demonic, magical, and/or contagious.

A real advance in Western medicine’s understanding of epilepsy came from Hippocrates (460-370 BC) in ancient Greece. In his famous treatise “On the Sacred Disease”, Hippocrates declared that epilepsy was just a natural disease of the brain no more divine and no more sacred than other diseases. The idea that seizures could originate outside of the brain had been a prevailing thought for centuries. Galen of Pergamon (200 AD) believed that seizures could arise from within the brain but also from other organs acting upon the brain. He believed that there was a continuous sensory system that connected all limbs and organs and that any one of them could set off an “ascending sensory *aura*”. Unfortunately, Hippocrates and Galen’s beliefs weren’t universally held for most of the last two millennia, and instead misunderstanding and misdiagnosis of people with epilepsy continued to be the norm in some underdeveloped countries.

The groundbreaking development in the modern understanding of epilepsy, or of seizures more specifically, came with the implementation of electroencephalogram (EEG) recordings in epilepsy research by Gibbs, Davis, and Lennox in 1935 (for review see Bladin (43)). With EEG recordings, researchers and clinicians could recognize and study the electrical correlates of various types of seizures, which has led to enormous advances in understanding and managing the disorder.



### ***Classification of Seizures***

Like any medical disorder with unknown mechanisms, classification of the epilepsy syndrome and, more specifically, seizures, into unique pathophysiologic phenomena has been challenging. Prior to 1981, characterization of seizures was phenomenologic. This was largely because at the time of conception there was insufficient knowledge of the underlying neuronal mechanisms and anatomic substrates of individual seizure types to permit a more scientific categorization based on natural classes (ILAE, 1981). This classification system has been revised twice since 1981 - in 1989 and again in 2010 (38), but the basic classification has remained: three main seizure types: generalized seizures (Tonic-clonic, absence, myoclonic, clonic, tonic, atonic), focal seizures, and unclassified epileptic seizures.

The International League Against Epilepsy and clinicians around the world are currently working to further enhance the classification system so that it allows for a flexible multidimensional approach, reflecting the discoveries of the last 20 years and providing clinicians with a classification system that will enable them to better serve their patients (39).

### ***Epidemiology***

Today, epilepsy itself is the most common serious brain disorder, affecting around 50 million people worldwide. As with many disorders, a country's socioeconomic status greatly affects the incidence and mortality rates of people with epilepsy. In developed countries, annual new cases are between 40 and 70 per 100,000 people in the general population. In developing countries, this figure is often close to double that due to the higher risk of experiencing conditions that can lead to permanent brain damage. In fact, close to 85% of epilepsy cases worldwide are found in developing regions (147, 227). The incidence of epilepsy cases is also

affected by the average age of the population. Data shows that the rates are much higher for newborns and elderly (215).

### ***Social and Economic Impact of Epilepsy***

Epilepsy can lead to many interacting medical, psychological, economic, and social repercussions, all of which need to be considered to fully understand the impact of the condition. Epilepsy has significant economic implications in terms of health care needs, premature death, and lost work productivity. The cost of epilepsy care depends on the country the patient lives in, but a study done in 2000 showed that the annual cost per patient with active seizures was \$4,559 in the US (\$802 for patients with inactive seizures) (31). For the developing country of India, it was estimated in 2007 that the total cost per epilepsy case was \$344 per year (77% of the average per capita income), making the total cost for the estimated 5 million cases in India equivalent to 0.5% of their gross national product (71).

### ***Management of Epilepsies***

*Antiepileptic Drug (AED) Prophylactic Treatment:* The first effective medicinal treatment of seizures was with potassium bromide and was first used by Sir Charles Locock in 1857 (review (49)). Potassium bromide was the mainstay of epilepsy treatment for nearly 50 years until Hauptmann found that phenobarbitone, when used to sedate asylum patients, also controlled their epileptic seizures (49). Since the synthesis of Phenobarbital in 1912, more than 30 antiepileptic drugs have been developed and approved by the FDA. The mechanisms of action of these drugs are quite varied and in some cases may be complementary (49). A physician's decision on how to medicate an epileptic patient can be based on the patient's seizure type,

syndrome, tolerance, hepatic and renal function, other medications, comorbidities, and the antiepileptic drug's mechanism of action, pharmacokinetic and pharmacodynamic profile and cost (221). In general, about 50% of patients with newly diagnosed epilepsy achieve complete seizure control with the introduction of the first antiepileptic drug (30). An additional 20-30% enter seizure remission after one or more complementary treatments and/or treatment changes are introduced. While success rate with anti-epileptic drugs is high, many drugs carry with them possible psychological and behavioral effects that have a wide range of severity. For example, the FDA issued a warning in 2008 that there was an increased risk of suicidal thoughts and/or behavior with the use of anti-epileptic drugs by patients with epilepsy (32). While not ideal, current anti-epileptic drugs provide a means to treat the symptoms of seizures for many patients suffering with epilepsy. However, as new information about specific causes and mechanisms is discovered, the hope is that researchers and doctors will be able to better target the cause of seizure initiation rather than just treat the seizures themselves.

*Non-pharmacological Treatments:* While most patients with epilepsy have success with AEDs, there is still a large proportion of patients who do not respond to AEDs (roughly, 30% overall) (30). Surgery can be a viable option for many patients with intractable seizures, but successful surgeries depend on accurate assessment of the cortical zones associated with the epileptiform activity (175). The concept of dividing the cortex into zones serves as a model in the pre-surgical evaluation that provides surgeons with rough outlines of the most important zones. The epileptogenic zone is the area of the cortex that is indispensable for the generation of epileptic seizures (255) by being the site of highest epileptogenicity and most frequently producing spontaneous seizures. This zone is further broken down into smaller zones: the ictal

onset and irritative zones. These areas are found using a combination of behavioral tests and EEG, magnetencephalography (MEG), subdural electrode recordings and/or single photon emission computed tomography (SPECT). This seizure semiology provides information about the symptomatogenic zone and the functional deficit zone, which is the eloquent cortical area that is (in)activated by a seizure (255). The ability to accurately outline these zones plays a large role in the success of the surgery, but certain types of etiologies may be more viable candidates for successful surgery than others (221).

### **1.3 Cortical Development**

A cortical malformation is one of the most common causes of intractable epilepsy, particularly in children (322). The following section describes the way that the cortex normally develops. This is essential information for understanding the possible mechanisms associated with generating epileptogenic cortical malformations. This introduction section will focus on the mechanisms and timing of migration of newly born neurons to their laminar destinations.

#### ***Neurogenesis***

The basic principles of cortical neurogenesis are similar in all mammals (296). Most excitatory neurons and glia that will eventually form the cerebral cortex arise from a smooth sheet of neuroepithelium in the dorsal telencephalic proliferative zone. These multipotent cells migrate to the subventricular zone where they further differentiate and remain until migration into the intermediate zone. In rat, the neuroepithelium becomes apparent between E12 and E13, while the subventricular zone does not become apparent until E17. Quickly after the appearance of the subventricular zone, an intermediate zone appears. The function of the intermediate zone (IV) is not entirely clear, but it appears to be the site of continued mitotic and postmitotic activity

as well as a site of pre-cortical migration organization, eventually separating neurons in an intermediate zone\_Upper, \_Middle, and \_Lower by E21. For somatosensory cortex, most neurons are born in the neuroepithelium, subventricular zone, and/or intermediate zone between E13 and E21. Peak neurogenesis in rat for the following layers are: layer VI – E15, layer V – E16, layer IV – E17, layers II/III – between E18 and E19 (Fig. 1.1) (27).

Whereas most, if not all, excitatory neurons arise from the dorsal telencephalic proliferative zone, inhibitory (GABAergic) neurons arise from two cell masses in the ventral telencephalic proliferative zone, the medial and lateral ganglionic eminences (Fig. 1.3) for review (202)..

### ***Migration***

Neurons born in the neuroepithelium of the ventricular zone migrate to their final destination via a complex mechanism. Depending on the timing of neurogenesis, this migration can cover less than 100  $\mu\text{m}$  (early embryonic days  $\sim$ (E)13) but can exceed 3000  $\mu\text{m}$  (postnatal (P) days 1 and 2). This section will review the two main types of migration excitatory neurons and supportive cells undergo, as well as the tangential migration GABAergic neurons undergo.

*Somal Translocation:* Some of the first cells born in the ventricular zone are cells destined for the marginal zone (mz) or layer I include Cajal-Retzius and subplate neurons. Neurons migrating with this mode of locomotion are bipolar and attach the leading edge of the process to the pia. The soma is then transported to the pial surface by nucleokinesis which is a process by which a microtubule "cage" around the nucleus elongates and contracts in association with the centrosome to guide the nucleus to its final destination (257).

*Radial Migration:* In a series of experiments during the 1970s, Rakic's lab showed that most neurons migrated past the preplate and into the cortical plate by climbing radial glial cells that extend from pia to the ventricular zone. Waves of neurons migrate to their destinations this way – the deepest layers first. This inside-out development means that layer VI neurons are positioned first with subsequent layers migrating through existing migrated layers (Fig. 1.2A).

In the somatosensory cortex, the timing of the development of laminar architecture is difficult to study in rodents because the current methods of birthdating neurons have a large temporal window. Birthdating studies using bromodeoxyuridine (BRDU) injections, which label dividing cells during embryonic time points, have shown that layers in the cortical plate (future cortical layers 2–6) are established according to an inside-outside pattern, where the deeper layers contain cells that become postmitotic earlier than the cells in more superficial layers (Fig. 1.2B for the timing of laminar development) (10, 133, 236). Thus, neurons born simultaneously (in terms of cell-cycle sequence rather than time of neurogenesis *per se*) (279) migrate and stop migrating roughly at the same time, so they all occupy the same cortical layer. Although it has been shown that the laminar identity of cortical neurons is determined early in the cell cycle (97, 195), the nature of the factors that control the migration of cortical neurons to their appropriate layer is poorly understood.

A complex cocktail of transcription factors and secreted guidance molecules interact to help guide migrating neurons to their final cortical position (Fig. 1.2C).

*Reelin-Dab1:* Mutations of the reelin gene (69, 213) and DabI gene (109, 316) have revealed that there is an essential interaction between migrating neurons and Cajal-Retzius cells in the MZ. In *reeler* and *scrambler* mice, the first wave of migrating cells destined to form the

cortical plate fails to split the preplate. Subsequently, new waves of migrating neurons are unable to pass the previous ones and accumulate in progressively deeper positions. This creates a cortex in which layers 2–6 are roughly inverted. Interestingly, many neurons in these same *reeler* mice have correctly positioned neurons (56) suggesting multiple mechanisms at work.

**Cdk5 signaling pathway:** Mutations in the Cdk5 pathway have a similar inverted cortex phenotype as the *reeler* mutant. In these mutants, early-born neurons are not prevented from splitting the preplate into the MZ and subplate but late born neurons fail to migrate past the subplate (155, 197, 214). This dysfunctional migration alters the normal lamination of the cortex.

The precision in laminar architectural development is not fully understood at this point, but it is clear that excitatory neurons born near the same time become migrating partners and later laminar neighbors in the adult cortex. This process requires many intrinsic and environmental factors for the proper guidance of these neurons to their final cortical positions.

**Tangential Migration:** While radial migration is the primary system for excitatory neurons in the CNS to migrate, many cells, particularly GABAergic interneurons, migrate independent of the radial glial scaffold (9, 9, 202, 237), most predominately in rodents (144). In rodents, these interneurons (and oligodendrocytes) migrate ‘tangentially’ to the cortex from the medial ganglionic eminence (MGE) for most interneurons (167, 307) (Fig. 1.3C) and the entopeduncular area for oligodendrocytes (216).

Interneurons follow a precise route: they avoid entering the striatum (188) and superficially destined interneurons invade either the MZ or subplate of the cortex, avoiding the cortical plate itself (167). Deeper destined interneurons migrate through layer IV (74, 167) and later in development migrate through the subventricular zone (307). Eventually, interneurons

switch from tangential to radial migration to adopt their final laminar position in the cerebral cortex (229, 281).

Three different types of factors influence this tangential migration of interneurons (Fig. 1.3C): factors that stimulate movement, structural elements that constitute the substrate for their migration, and attractive/repulsive cues (Sema3A&F, Slit1/2) that direct the interneurons to their target.

Timing of tangential migration is not as extensively studied as radial migration. What is known is that some interneurons, particularly those born in the MGE, adopt the same cortical layer as pyramidal neurons born at the same time in the cortical ventricular zone (VZ) (126). Thus, coordinating the timing of different stages of interneuron migration may be key to determining the final position of the interneurons and their functional integration into cortical circuitry (126, 173, 178). The final migration from both subventricular zone and MZ pathways into the cortical plate appears to occur via a highly dynamic mechanism that occurs in the first postnatal week for rodents (202).

#### **1.4 Cortical Malformations Associated with Cortical Development**

Deviations from normal cortical development can lead to malformations. As previously noted, malformations are responsible for a large majority of cases of intractable epilepsy. This section will review the types of clinical cortical malformations associated with cortical development and the animals models used to study them.

##### ***Summary of Clinical Disorders***

*Inhibited Brain Growth:* Abnormal cell death and/or creation of too few cells during early central nervous system (CNS) development results in an underdeveloped brain that is



typically diagnosed as microcephaly. Patients with this condition have head circumferences that are smaller than average by more than two standard deviations (23). Many factors contribute to this underdeveloped brain including: vascular insult, intrauterine infection, maternal alcohol consumption and other teratogens (1).

*Excessive Brain Growth:* Whereas microcephaly is the result of inhibition of brain growth, increased proliferation and/or apoptotic failure can produce a number of pathologic conditions including but not limited to: neoplastic lesions; cortical dysplasia; and megalencephaly (23, 116). Megalencephaly is one of the most pronounced types of disorders stemming from excessive neuronal proliferation and/or errors in normal apoptosis. Patients with megalencephaly have few treatment options and typically will have large sections of brain resected to reduce the frequency of seizures.

*Improper Migration:* As previously stated, cortical development requires precise migration of both inhibitory and excitatory neurons, as well as non-neuronal cell types, into specific destinations. Errors in this migration can lead to many types of malformations, including, but not limited to: lissencephaly; heterotopia; and polymicrogyria.

Lissencephaly (smooth brain) is a condition in which the normal gyri of the cortical surface are absent or dramatically decreased in number. There are a number of genetic causes of lissencephalies, among them are point mutations or small deletions/duplications on the LIS1 gene (80% of patients) and the DCX gene (~17% of patients) (80, 170). Errors or deletions in the LIS1 and DCX genes both cause errors in migration of cortical neurons, but the exact role Lis1 and DCX signaling plays in nuclear positioning and cell migration is not clear (115).

A heterotopia is described by Foucault in the architectural context as ‘spaces of otherness’. In the context of neuroscience, a heterotopia is a cluster of neurons located in a wrong part of the brain. Heterotopias are typically the result of arrested migration of neurons to the cerebral cortex and thus are usually found at the site of neurogenesis (subventricular nodular heterotopia) and/or initiation of cortical migration (subcortical band heterotopia). Both types of heterotopia are seen most frequently in females, mostly because the genes that are associated with the disorders are x-linked genes: the lissencephaly gene, DCX and FLNA1, which encodes a protein important for cell morphology and migration (96). The severity of symptoms varies depending on the size and location of the heterotopia, but most patients suffer mild to moderate cognitive abnormalities and frequently have seizures (82, 112). This type of cortical malformation is widely studied in many animals models described later.

Schizencephly is another malformation caused by dysfunction of post-neurogenesis development, specifically, the result of an abnormal cleft in the brain that allows aCSF to flow directly from the ventricles through two cortical “lips” into the subarachnoid space(23, 115). Closed “lips” result in hemiparesis or motor delay, and the more common “open-lipped” schizencephaly results in epileptogenic hydrocephalus (171). De novo mutation of the EMX2 gene has been associated with several cases of schizencephaly, particularly those with severe clinical presentation (52). Almost always, one or more areas of polymicrogyria border the schizencephalic cleft. Polymicrogyria is a malformation that is characterized by an abundance of abnormally small gyri. It is the malformation most closely related to the experiments described here and will be discussed in detail in a later section.

### ***Animal Models of Cortical Malformation***

In order to study the cortical malformations described above, a number of techniques have been developed in rodents. These include, but are not limited to: genetic mutation; irradiation; exposure to methamphetamine or other chemicals *in utero*; injection of a toxin; direct mechanical damage to the cortex; and, as is used in these studies, ischemia secondary to freeze probe application. Similar to the clinical populations, the type and severity of the malformation generated depends on both the timing and nature of the insult (108). While some animal models replicate the disruptions associated with massive cortical malformations, i.e. micro- and megalencephaly, this review will focus on animal models of focal cortical malformations that produce spontaneous and/or *in vitro* hyperexcitability (205). Most of the following animal models have been investigated to understand the underlying mechanism of hyperexcitability and a comparison of these mechanisms is important for the justification of the experiments described within this dissertation.

As detailed in a previous section of this introduction, neurogenesis and the subsequent migration of cortical neurons in rodents begins *in utero* and completes within the first postnatal days. Animal models generating cortical malformations involve insults that disrupt normal cortical development during these critical time points.

The methods of inducing cortical malformations *in utero* are irradiation (248), 1,2-bis-chloroethyl-nitrosourea (BCNU) injection (35), and methylazoxymethanol acetate (MAM) exposure (21). Each of these methods reduces cortical thickness and some type of heterotopia is generated (Fig. 1.4).

X-irradiation of embryonic rat pups *in utero* leads to the development of various degrees of cortical malformations and architectural abnormalities in the neocortical areas that are similar to those seen in some forms of cortical dysplasia in humans (159, 248). Dyslamination and lack

of columnar organization are seen in multiple areas of the neocortex, as well as clustering of neurons in the molecular layer. Studies have also shown that the cortical malformations generated in these rats caused interictal epileptic discharges in a large number of these animals (150, 159). It has been suggested that reduced inhibition due to both decreased GABAergic neuronal populations and a reduced excitatory drive onto GABAergic cells is a major contributor to hyperexcitability seen in this model (232, 247).

Injection of MAM also results in a thinning of the cortex and, if injections are done early enough (E24 in ferret), disruption of radial glia (212). This model is characterized by an extensive area of cortical dysplasia (282), poor response to anti-epileptic drugs (271), increased sensitivity to various proconvulsant agents (60, 103) and heterotopia capable of independent burst generation *in vitro* (20). No clear epileptogenic mechanism has been found in this model, but excessive bursting behavior in pyramidal neurons within the cortical dysplasia have been shown and could play a role in promoting epileptiform activity (258). The pathohistological and physiological characteristics of the cortex in BCNU-exposed pups are similar to those in the MAM model, including disruption of radial glia and decreased GABAergic drive onto pyramidal neurons within dysplastic cortex (35).

As described previously, many cortical malformations are associated with gene mutations/deletions and there have been many animal models that have been utilized to study the effect of particular genetic manipulations. Two of the most studied genetic manipulations are the *TISH* (telencephalic internal structure heterotopia) mutant rat, which has a double cortex (band heterotopia), and the p35 knockout mouse, which has an inverted cortical lamination pattern (Fig. 1.4). Spontaneous seizures have been documented in both models (169, 304). Evidence

suggests that reduction of inhibition could contribute to the hyperexcitability in the *TISH* rat. A study has shown that there is a decrease of inhibitory synaptic transmission due, in part, to a decrease in the number of inhibitory afferents. This is because increasing the probability of release with a low  $Mg^{2+}$ /high  $Ca^{2+}$  solution fails to “rescue” the lost inhibitory function (293). A concomitant decrease in one specific GABAergic cell population is also seen in this model (293). Interestingly, in this model the epileptogenic activity is not apparent until two weeks after birth, highlighting a hallmark of most epileptiform activity associated with cortical malformations: a latent period between the malformation creation and the onset of seizures (293). This latent period will be the topic of further discussion in a subsequent section of this chapter. Many animal models utilizing genetic manipulation are used to create cortical malformations, but are beyond the scope of this dissertation.

The animal models described thus far have generated cortical dysplasias and heterotopias. The final cortical malformation modeled in the rat that will be discussed is microgyria. Microgyria can be modeled in a number of ways. A light mechanical disturbance of the exposed pial surface can cause a microgyral malformation (1, 2), as can exposure to methamphetamine *in utero* (67). Two of the more commonly used methods of inducing microgyria are ibotenate injection (190) and neonatal freeze lesion (86, 86, 137, 138). Injection of the glutamatergic agonist ibotenic acid shortly after birth causes the death of cells in layer V-VI of the developing rodent cortex (190). This manipulation produces a small sulcus in the brain, mimicking the human condition of polymicrogyria (114, 190). Hyperexcitability similar to that seen in the human condition is observed in cortical areas surrounding the lesion (243). The freeze lesion model creates a similar malformation and will be considered at length in the next section.

## 1.5 Polymicrogyria: Clinical Observations

### *What is Polymicrogyria?*

Polymicrogyria (PMG) is a specific developmental neurological disorder with characteristic histopathology: a four-layered or unlayered cortex that is characterized by an abnormal arrangement of the cell layers and intracortical fiber plexus, and by an excessive folding of the upper or all cellular layers under the continuous smooth molecular layer (115) (Fig. 1.5A). The four-layered cortex is composed of the molecular layer, an upper dense cell layer, a layer of low cellular density with horizontal myelinated fibers, and a deep cell layer (194) (Fig. 1.5D). The neurons can be small and some have described them as immature (98). The grey-white matter junction can be either sharp or histologically blurred by heterotopic neurons or nodules (273). The cortical plate is thinner than normal, especially in infants and newborns, but does appear thick in magnetic resonance scans because of excessive folding (23, 115) (Fig 1.5A).

### *Causes of Polymicrogyria*

There are many well-defined genetic PMG syndromes (24, 142), but the majority of PMG cases observed in the clinic are idiopathic. Further, although most PMG occurs as an isolated cortical malformation, it can be related to other brain malformations including agenesis of the corpus callosum, schizencephaly, microcephaly, or megalencephaly (142). While there appear to be many causes, brain pathology consistently demonstrates abnormal development or loss of neurons in middle and deep cortical layers (90).

*Extrinsic Factors Inducing Microgyria:* A hemodynamic mechanism is commonly proposed as a cause for the death of deep layer cortical neurons and subsequent formation of a microgyria. This is because PMG is typically located in the perisylvian region and because of many anecdotal reports of possible anoxic-ischemic injury in the second trimester (51). That said, cortical vascularization in humans is not present before week 22 and PMG can be seen as early as week 18. It has been proposed that PMG, from non-genetic causes, is the end result of many events occurring at any time during neuronal migration before 18 weeks (148). Events that have been associated with PMG include: Intrauterine cytomegalovirus infection; fetal cerebral ischemia from placental perfusion failure; twin-twin transfusion; loss of a twin *in utero*; and maternal drug ingestion.

*Genetic Factors:* Polymicrogyria has been associated with mutations of the SRPX2 (246), TBR2 (16), PAX6 (106), KIAA1279 (1), TUBB2B (141), GPR56 (228) , and RAB3GAP1 (6) genes. Developmental studies thus far have focused on the Pax6 pathway. The Pax6, TBR2, and TBR1 genes are sequentially expressed in radial glia (PAX6), intermediate progenitor cells (TBR2), and postmitotic neurons (TBR1). Disruption to this pathway leads to loss or altered fate of large cortical neurons (90) and is associated with larger spectrum PMG syndromes (269). Other chromosomal loci and genes have been identified in patients with different types of polymicrogyria as part of complex syndromes, but the proteins and pathways associated with those loci/genes have yet to be identified (81, 246).

### ***Polymicrogyria and Epilepsy***

Up to 87% of patients with polymicrogyria have epilepsy (163) that typically develops between ages 4 and 12 (1), but the latent period to first seizure can be as long as 80 years (284). There is a broad spectrum of clinical manifestations associated with PMG. Some children have very severe encephalopathies with quadriparesis, profound mental retardation, and intractable epilepsy, while others with PMG are relatively ‘normal’ individuals with only selective impairment of higher order neurological function (100).

Current advances in medical imaging have helped to identify this malformation as one of the causative factors for epilepsies previously classified as idiopathic (22, 174). However, the epileptogenic zone of this malformation is not always confined to the area of the visible anatomical lesion. Hyperexcitable portions of cortex surround the lesion as well, making it difficult to definitively assign boundaries to the “damaged” tissue (58). The extent of polymicrogyria and the amount of cortex involved can vary greatly between individuals, but there is usually a correlation between the size of the lesion and the severity of clinical signs and EEG findings (283). This inability to locate the epileptogenic focus will be the focus of chapter 4 of this dissertation.

### ***Introduction to the Freeze Lesion Model of Microgyria***

First introduced in the late 1970s by Dvorak and Feit, the freeze lesion model of microgyria mimics human four-layered histopathology (86, 87, 87). Their freeze lesion protocol involves placing a freezing probe ( $-50^{\circ}\text{C}$ ) on a portion of the skull overlying the somatosensory cortex in a neonatal rat pup (Fig. 1.5B and C). This creates an ischemic lesion that kills the neurons present in the cortical plate at the time of lesion. This can be, depending on the age of the animal, cells destined for the deep to middle layers (layers IV to VI) (252). Because neurons



destined for the superficial layer are not destroyed by the lesion, the superficial layer develops, but an invagination of the cortical surface develops around P5 (253). A microgyral region of laminated cortex containing four, instead of six, cortical layers (86, 87, 252) forms and is roughly as wide as the width of the freeze probe used (1 mm in most cases). The superficial layers of the malformed region are histologically similar to normal neocortical layer I and II/III. Under the superficial layers is a thin cell sparse layer that separates the superficial layers of the malformation (MG) from the 'deeper' layers of the MG and the normally six layered laminated cortex medial and lateral to the MG (131, 252). The 'deep' layer of the MG appears to be variable in size and presence and not well characterized, but in most cases is contiguous with layer VIb of normal cortex (Fig. 1.5C and E). This abnormal lamination is similar to the clinical microgyria previously described (194).

### ***Epileptogenicity of the Freeze Lesion-induced Malformation***

Studies published in the mid-1990s demonstrate that the resulting malformed cortex induced by freeze lesion is consistently epileptogenic in rats (137, 184). These studies showed that stimulation of the area of cortex adjacent to the malformation generates interictal-like activity (137, 184) that has similar incidence in rats as humans with polymicrogyria (24, 137). This area adjacent to the malformation is identified as the paramicrogyrial zone or region (PMR) and appears, histologically, to be normal, six-layered cortex with Nissl stains.

### ***Seizure Susceptibility***

Evidence suggests that rats with freeze lesion-induced microgyria do not have spontaneous seizures (129), but the malformation causes the rats to be more susceptible to

seizures (260). When challenged with hyperthermia, freeze-lesioned rats (at P10) developed seizures more quickly than control rats, and required a lower threshold temperature to achieve the most severe seizures stage (generalized convulsions) (260). Further, freeze-lesioned rats developed spontaneous seizures weeks after hyperthermia exposure, much earlier than control rats (259). Because seizures can alter many intrinsic neuronal properties, as well as connectivity of neuronal networks, this model serves as a helpful tool in determining the mechanisms of epileptogenesis without the confound of overt seizures. It also serves to help evaluate the propensity for seizures in the hyperexcitable brain.

It should be noted that not all kindling experiments demonstrate that the freeze-lesioned brain is more susceptible to seizures. Inducing seizures by injecting bicuculline (antagonist for inhibitory transmission), Kellinghaus, et al found control and freeze-lesioned rats had similar thresholds for epileptiform activity (151). This suggests that the intrinsic excitability of the malformed cortex was not increased. The conflicting results of the Kellinghaus and Scantlebury studies highlight the importance of differentiating between kindling techniques and the timing of the induction of the freeze lesion, the latter of which will be discussed at greater length below.

The cortical architecture, epileptogenicity, and seizure susceptibility outlined above suggest that the freeze lesion model of microgyria is a useful model to study the human disorder, polymicrogyria. In order to gain an understanding of the mechanisms proposed to be associated with the development of epileptogenicity and increase seizure susceptibility, a review of the cellular and subcellular alterations found in and around the microgyrus will be reviewed in the section below.

### ***Cellular Characteristics***

*Origin and Classification of Cells within Malformed cortex:* The cell dense, superficial layer of the MG contains neurons generated on embryonic day 20, as well as those generated on E17 (the date most neurons of the superficial layers are born)(253). This birth dating study utilizing BrdU injections (labeling dividing, new born cells) at both pre- and postnatal ages demonstrates three important aspects of the freeze lesion model. First, the freeze lesion does not induce massive neuronal differentiation or proliferation. Secondly, the neurons that form the malformation must either migrate through or around the lesioned area. Finally, the neurons of the malformation are cells born after E15, consistent with the mechanism of selective cell death of neurons in the cortical at the time of lesioning (those destined for deep layers). They also confirmed that horizontal migration of deep layer neurons of adjacent normal cortex do not invade the MG (253). There does appear to be some proliferative response to the injury, but the newly-generated cells also stain for glial fibrillary acidic protein and thus are likely astrocytes (131, 265).

*Astrocytes:* Astrocytes were found in and around the malformation in some of the earliest publications utilizing this freeze lesion model (131). Reactive gliosis is the process by which astrocytes show profound morphological and biochemical alterations in response to various pathological conditions within the brain, for review see Pekney (226) and, not surprisingly, reactive gliosis has been noticed in the malformation (45, 131). These astrocytes show signs of having an altered potassium buffering capacity that may contribute to abnormal electrical behavior in and around the malformation (45). Because astrocytes play a vital role of *in vivo* ionic concentrations, it is logical to think that alterations to astrocytic function near and around the malformation could play a role in the malformation's hyperexcitability. Altered potassium

buffering has also been demonstrated in astrocytes of brains associated with epilepsy-related tuberous sclerosis in mouse (142). In this paradigm, astrocytes have a decreased inward rectifying  $K_{(ir)}$  current, suggesting poor potassium uptake that is likely secondary to a reduction in mRNA and  $K_{ir}$  channel subunit protein (142). The resulting excess extracellular potassium may contribute to hyperexcitability by reducing the potassium gradient by preventing cells from hyperpolarizing, thereby increasing their resting membrane potential.

*Microglia:* Like astrocytes, microglia respond to pathological conditions with proliferation and ramification. Again, not surprisingly, activated microglia have also been observed in cases of intractable epilepsy in humans, likely due to excitotoxic damage caused by seizures (11, 44). Microglia activation can be a mechanism of the development and perpetuation of hyperexcitability (321), in part due to inflammatory cytokine secretion (299, 300). To date, the role of reactive microglia in the development of the hyperexcitability seen in the freeze lesion model has not been studied directly, although the recruitment of these cells in early response to the lesion has been noted (45).

*Developmental delay and persistent presence of migration-essential non-neuronal cells:* There are number of alteration in cell types, particularly those associated with neuronal migration, that suggest a developmental delay occurs in the freeze lesion model. Radial glia that provide the scaffold for most neuronal migration during the perinatal days typically either die or differentiate into other non-neuronal cell types by P12 (209), but are observed in lesioned cortex up to the fifth postnatal week (252). The signals associated with the differentiation of radial glial cells are thought to be important for the maturation of the cortex (189), and thus the presence of

radial glial cells suggests the persistence of an immature state. In addition to the persistence of radial glia, the normally transient Cajal-Retzius cells also persist in the malformed brain. These cells have been shown to, in part, provide signaling cues for proper laminar organization and connectivity (113) and are still present in the PMR cortex at P12 (277).

For these reasons, delayed maturity has emerged as a theme in the freeze lesion model, as well as for focal cortical dysplasia in humans. In fact, what is known as the “dysmature hypothesis” of cerebral development suggests that the abnormal characteristics of dysplastic cortex bear some similarity to a normal prenatal time point, providing some idea of when appropriate development deviated from the typical timeline (57). One prominent, if not characteristic, feature of focal cortical dysplasia in humans is the presence of morphologically abnormal cells, the large, aspiny balloon cells and cytomegalic neurons (57). Their similarity to neurons that populate the preplate suggests that incomplete development has allowed them to persist, even in mature cortex. These cell types, characteristic of human focal cortical dysplasia, are not observed in the freeze lesion model, although some subtle alterations in cell structure are seen. The superficial layers of the MG and PMR have pyramidal cells with simpler basal dendrites than those seen in control animals (104). In contrast to that simplicity, layer V pyramidal neurons of the PMR have apical dendrites that are longer than those found in control cortex (79). These structural results suggest that the structural alterations to neuronal dendrites depend on cell location and subtype. In addition to the idea that functional and anatomical changes in malformed cortex can be dependent on the neuronal location and subtype, the following section about the subcellular alterations found in neurons near the malformation introduces how time can also play an integral role in the developmental of the physiological characteristics of the malformed network.

### ***Subcellular Alterations in the Malformation***

In addition to the alteration of specific cellular expression and structural characteristics, the subcellular characteristics within neurons in and around the malformation are also altered by freeze lesion. Receptors and ion channels are made up of specific subunits that can be developmentally regulated and, depending on the subunit composition, can alter the intrinsic properties of the neuron in which the receptors and ion channels are expressed. Errors in the programmed receptor subunit composition development have been shown to increase cortical excitability by either decreasing the inhibitory drive via altered GABA<sub>A</sub> receptor composition or increasing the excitatory drive via glutamatergic receptor composition (28, 143). This section will review the literature in the freeze lesion model that explores alterations to subcellular composition of neurons within and adjacent to the malformation.

*GABA<sub>A</sub> receptor composition:* Redecker et al. has analyzed the optical density of immunohistochemical staining for individual GABA<sub>A</sub> receptor subunits and shown a decrease in all subunits, except the  $\alpha 3$  subunit, in the malformed cortex (242). During normal development, both the  $\alpha 3$  and  $\alpha 2$  subunits decrease their expression by the second postnatal week and are replaced by the  $\alpha 1$  or  $\alpha 4$  subunit (166). Supporting Redecker's observation, Defazio et al.'s physiological experiments suggested that a persistent expression of  $\alpha 2$  or  $\alpha 3$  subunit is found in the lesioned cortex, at the expense of  $\alpha 1$  expression (75). In contrast to Redecker's imaging study, Defazio derived his conclusions from indirect evidence in malformed cortex showing decreased sensitivity to application of zolpidem, a type-1 GABA<sub>A</sub> receptor agonist in an *in vitro* slice preparation. Type-1 GABA<sub>A</sub> receptors express the  $\alpha 1$  subunit, so a decreased sensitivity to

Type-1 receptors suggests that the  $\alpha 2$  or  $\alpha 3$ , but not  $\alpha 1$ , subunit were present in the recorded cells (75). Autoradiography has also demonstrated decreased binding to GABA<sub>A</sub> receptors (all subunits included) in the perilesional area, whereas normal binding levels are seen in the surrounding cortex (319). These three studies suggest that the decreased expression of  $\alpha 3$  and/or  $\alpha 2$  and increased expression of  $\alpha 1$  and/or  $\alpha 4$  is delayed while there may be an overall decrease in the expression of GABAergic receptors around the MG.

*Glutamate Receptor Composition:* In addition to GABA<sub>A</sub> receptor composition alteration, the composition of glutamate receptors is altered in the freeze lesion model. Specifically, it has been shown that there is an increase in AMPA and kainite receptor binding (319), as well as enhanced function of NR2B-containing NMDA receptors (76). Normally in development, NMDA receptor composition undergoes a shift from only NR2B in the embryonic brain to a combination of NR2B, NR2A, and NR2C by the end of the first postnatal week. A selective increase in immunoreactivity for NR2B has also been shown in animals with *in utero* freeze lesions(280). Additionally, electrical stimulation kindling exposure further increased the NR2B expression. This data is consistent with tissue taken from patients with epilepsy secondary to focal cortical dysplasia, who also showed increased levels of NR2B expression (92). In normal tissue, the developmental shift from NR2B to NR2A/C has been suggested to decrease the excitability associated with the NMDA receptor (315), consistent with the end of the critical period of plasticity for cortical information processing (123). A persistent expression of NR2B-containing NMDA receptors in lesioned cortex not only provides further support for the maintenance of immature cortex theory, but could also play a role in the hyperexcitability of the malformed cortex. Neurons within periventricular nodular and subcortical band heterotopias also

have downregulated NR2B expression (92). Additional and more targeted experiments (specific laminar and cell type comparisons as well as additional time points) are needed to determine the role that glutamate receptor expression and composition plays in the development of hyperexcitability, but evidence suggests that expression and composition of both NMDA and AMPA receptors can be altered due to cortical malformations.

### ***Subcellular Composition Changes in PMR Contribute to Intrinsic Properties Changes***

Many ionic transporters and channels determine the intrinsic properties of neurons within the cortex. Alteration of these proteins can have a drastic effect on the intrinsic properties of neurons and such alterations have been linked to a number of different epilepsies (29, 55). This section will describe the studies examining the expression of some of these proteins in malformed cortex and whether the intrinsic properties of neurons within the malformed cortex are altered as a result.

The cation-Cl<sup>-</sup> cotransporters, NKCC1 and KCC2, which are essential for proper GABAergic responses in the mature cortex, are expressed differently within but not outside of the cortical malformation during the first postnatal week (265). Another ionic transporter, Na/K ATPase plays a critical role in maintaining the normal resting potential of cells by actively transporting Na<sup>+</sup> out and K<sup>+</sup> into the cell. Layer V pyramidal neurons near the malformation (<360 from microgyral edge) show a decrease in the expression of the  $\alpha 3$  isoform of the Na/K ATPase at from P14 to P28. Another molecule important to the intrinsic properties of neurons is the hyperpolarization-activated non-specific cation (HCN) channel that plays an important role in the hyperpolarizing activated current I<sub>h</sub>. This current is important in modulating action potential frequency (204) and dysfunction of this current has been linked to a number of hyperexcitable



models (146, 231), including the freeze lesion model (5). This alteration is suggested to contribute to hyperpolarized resting membrane potentials and increased input resistances in layer V pyramidal neurons of the PMR (5). In addition to the intrinsic properties of pyramidal neurons of the malformed cortex, both FS and LTS interneurons of the malformed cortex also appear to have altered intrinsic properties (102), but a subcellular mechanisms for this alteration is not yet known.

These changes to neuronal neurotransmitter receptor subunit composition and intrinsic properties in malformed cortex highlight the importance of the developmental timing in studying alterations within the malformed cortex. Correlating the timing of alterations found in malformed cortex with the timing of seizure susceptibility is important for understanding the mechanisms associated with hyperexcitability and is a continuous theme in this dissertation.

### ***Anatomical and Functional Connectivity Changes in Malformed Cortex***

The malformation induced by freeze lesion has been shown to disrupt the normal anatomical connections to and from the malformed cortex, surrounding areas, and projectional structures like the thalamus. These studies utilize dye injection (typically dextran), which retrogradely labels cells connected to the site of injection. These studies show that thalamocortical fibers, commissural fibers, and afferents from local pyramidal cells demonstrate abnormal organization in and around the microgyrus.

*Commissural Fibers:* Injection into the site of the lesion caused retrograde labeling of cell bodies of the contralateral *infragranular* cortex, whereas injection into homotopic areas in control produced labeling of the contralateral *supragranular* cortex (105). This finding suggests

that the interhemispheric projections into perilesional regions come from deeper layers than they do normally. Interestingly, when injections were made in the hemisphere without lesion, the retrogradely labeled neurons were found in the deep layers of the contralateral cortex instead of the normal labeling of superficial layers (104). These two studies suggest that there is a shift toward the deeper layers of cortex for both the origin and targets of commissural fibers. Callosal efferents from the lesioned area also showed an increase in the density of their projection to heterotopic areas of cortex, as well as (in a few cases) decreases in some homotopic projections (250). This study also found that projections from homotopic regions in the hemisphere opposite to the malformation terminated most often in the medial portions of the microgyrus or avoided it entirely (250). Other studies have looked specifically at the size of the corpus callosum and found that bilateral lesions reduce corpus callosum size, particularly when lesions are done on P1, not P3 or P5 (288). This finding suggests that interhemispheric connections can be decreased, particularly when lesions are made perinatally. All these commissural fiber studies suggest that the anatomical connectivity between hemispheres is altered in the freeze lesion model. The functional significance is not well understood, though one study found that inhibition, as measured by paired pulse inhibition, is reduced in the contralateral cortex, perhaps because of a reduction in excitatory commissural afferents onto inhibitory neurons (263).

*Thalamic projections/afferents:* Neurons from the ventrobasal (VB) nuclei of the thalamus carries somatosensory information into somatosensory barrel cortex and thus is a major source of afferents. Many studies in the freeze lesion have looked at alterations in anatomical connections between the lesioned cortex and the thalamus and found them to be changed. Rosen, et al. (250) noted that there are not many connections between the VB and MG, but the area

adjacent to the MG has a dense plexus of thalamocortical fibers at the border between the malformed and normal cortex. Barrel cortex is characterized by a 'barrel' wall of high cellular density with a high fiber density center that responds to a specific whisker on the rat. This barrel (or barreloids, barrelettes in subcortical structures) organization is maintained throughout the entire somatosensory pathway. Placement of a freeze lesion into the barrel field causes changes to the architecture of the barrel field, as well as to the contralateral barrel field (254). This distortion consists of a near absence of barrels as denoted by CO activity in the superficial layers of the microgyrus and dense areas of continuous, as opposed to punctate, CO activity in tissue adjacent to the microgyrus (254). In addition to a disruption in CO staining, Jacobs, et al., also reported an increase in CO staining in the cortex surrounding the MG (139).

*Other anatomical alterations:* The distribution of neuronal size in the MGN is altered in male rats, resulting in more small neurons and fewer large neurons. This effect is not seen in females, but can be induced in females by injecting testosterone from E16 to P5 (124).

*Functional alterations in malformed cortex:* Clearly the cortical malformation induced by freeze lesion creates functional changes in the neuronal networks near and adjacent to the malformation, as evidenced by the presence of evoked epileptiform activity. What functional change(s) are responsible for this hyperexcitability is not clearly understood, but, in addition to the previously described cellular and subcellular changes, alterations to the functional connectivity of inhibitory and excitatory circuits have been demonstrated, as well as changes to plasticity mechanisms.

*LTP*: Two methods for generating long-term potentiation in the cortex are: (1) high frequency stimulation of layer IV; and (2) high frequency stimulation of layer VI in the presence of low concentrations of bicuculline (GABA<sub>A</sub> antagonist). Interestingly, LTP is differentially altered in the freeze lesion model such that layer IV LTP cannot be obtained at all, while a NMDA-dependent LTP can be generated in layer VI without the presence of disinhibition (1). These results suggest that functional afferent reorganization occurs in this model and it may be layer dependent.

*Enhanced Excitatory Connectivity*: Local excitatory circuitry can be enhanced if there is an increase in excitatory afferents onto excitatory neurons. In the PMR cortex, increased miniature excitatory postsynaptic current (mEPSC) activity is seen compared to control. This suggests that excitatory afferents are functionally increased (140). This increase occurs between the first and second postnatal week when one sees an increase in both miniature and spontaneous(s) EPSC frequency from P7 to P11(320). This is prior to the onset of epileptiform activity at P12 (138) and suggests that this increase in excitation may contribute to the onset of epileptogenesis. While the increase in mEPSC frequency suggests that there may be an increase in excitatory afferents to the PMR, there is also the possibility that there is an increased release probability (320). Evoked EPSCs are also multi-peaked and have larger amplitude and greater area in PMR, which provides further support of the idea of increased excitatory input to this area of cortex (320).

*Excitatory Connectivity and the Spatial Extent of Activation*: Stimulation of the cortex adjacent to the malformation (~0.5-2.5mm from the MG but not within it) can evoke local field

potential epileptiform activity. This activity can spread across the cortex many millimeters. However, stimulation at distant sites from the MG (+3 mm away) does not evoke epileptiform activity, suggesting that there is a specific portion of cortex that is hyperexcitable. The spatiotemporal dynamics of evoked epileptiform in this model is a focal point of this dissertation and greater discussion will take place in a subsequent section, but it is also interesting to note that the malformation itself is not necessary for epileptiform activity to be elicited (138). Voltage sensitive dye experiments have shown that stimulation of cortex adjacent to the malformation elicits a response that extends to a larger horizontal area and that the increased excitatory response is due, in part, to the proposed persistent expression of NMDA receptors containing NR2B (19). This is because NR2B antagonism restricts the spatiotemporal spread of activity in the PMR.

*Inhibitory Circuitry:* Inhibitory circuitry surrounding the malformation caused by freeze lesion is also altered. However, there is conflicting data on whether inhibition is impaired or enhanced. Luhmann, et al has shown a decrease in GABA<sub>A</sub> receptor mediated inhibitory transmission in layer II/III pyramidal neurons of the PMR cortex, possibly due to weaker inhibitory input onto the GABAergic cells (181), whereas another study showed that, for a subset of pyramidal neurons in layer V of lesioned cortex, evoked IPSCs were actually enhanced (140). When glutamate transmission was blocked in this latter study, the eIPSCs returned to control levels, suggesting that the increase in eIPSC was due to increased excitatory input of inhibitory cells. Additionally, mIPSC frequency in layer V neurons of PMR cortex is not altered, suggesting that if release probability at those terminals is maintained, there is not an alteration in the overall number of inhibitory synapses (140). The role of this altered inhibitory circuitry in

generating the hyperexcitable PMR cortex is not clearly understood, but selective loss of inhibition from FS cells has been implicated in the longer duration / larger spread of multi-unit activity (MUA) in layer IV caused by stimulation of the VB in thalamocortical slices (276). These differing results suggest that inhibitory circuitry alterations in malformed cortex might be dependent on the cell type and location (near or far from malformation as well as laminar position).

*Glial Function:* Glia, particularly astrocytes, play an essential role in neuronal health and neuronal circuit maturation (7). As stated before, both the proliferation and activation of astrocytes appear to be altered in the freeze lesion model. In addition to those changes, there is evidence that suggests the functional properties of astrocytes may be altered. It has been shown that preventing glutamate transport, particularly in glial cells, enhances excitability in lesioned animals (53). This finding suggests chronic deficits in glutamate transport, potentially in astrocytes, can contribute to hyperexcitability of the PMR. More results are needed to know how, when, and where astrocytic function is altered in order to fully understand the role that astrocytes play in the maturation of the hyperexcitable, malformed cortex.

### ***Behavioral Effects***

The previous section has outlined the cellular, subcellular, and connectivity alterations found in and around the freeze lesion-induced microgyria. This section will describe some of the behavioral changes that are associated with polymicrogyria and presumably related to the alterations just described. Polymicrogyria has been associated with a number of behavioral deficits including dyslexia (100). To explore the role that the freeze lesion-induced malformation

plays in auditory processing, the Rosen lab has done many behavioral studies in freeze-lesioned rats (124, 224, 225, 286, 287). In the first of these studies, they found that the freeze-lesioned rats had fast auditory processing impairment. They came to this conclusion because their ability to distinguish small silent gaps in a background of white noise was diminished (124). They have also found that as the severity of the malformation increases, the auditory deficits increase (225) and that the most severe auditory deficits occur from perinatal lesions instead of lesions after P3 (286). Subsequently, they have shown that early acoustic discrimination experience ameliorates the auditory processing deficits caused by the malformations (285). Another lab has also shown that lesioned animals show mild spatial memory cognitive deficits compared to unlesioned rats via their performance in the Morris Water Maze (259). Luhmann, et al. has assessed somatosensory function by looking at thigmotaxis (whisking) of the contralateral (from malformation) whiskers (180). Mice lesioned during adulthood showed increased scanning of the whiskers that were represented in the lesioned barrel field, suggesting that it may be indicative of increased excitation in the damaged cortex or a compensatory response to decreased cortical activity. This increased thigmotaxis resolved within one week of lesioning and other assays, such as location and exploration of a novel environment, showed no difference (180). Rats with lesions to the temporal associational cortex at P4 had visual discrimination deficits that were more severe than those with lesions induced at P10 (158).

*Sex Differences in Behavioral Deficits:* An interesting caveat to the auditory deficits found in the Rosen studies is that there is a sex bias, such that males exhibit the auditory deficits but females do not (94). There is no baseline bias, as male and female sham rats perform the task equally well (94). To assess whether hormonal differences provided the female rats with an

advantage, male rats were injected with estrous, but the deficits persisted (225, 251).

Testosterone administration in the female rats, however, did appear to contribute to differential cellular effects, but did not have behavioral effects (251). These results suggest that there may be a sex bias in certain behavioral deficits associated with the freeze-lesioned rat but the role that hormones play in this bias is unclear.

## **1.6 Postnatal Maldevelopment: Timeline of Hyperexcitability**

### ***Introduction***

Most literature about the freeze lesion model is on the adult or late adolescent rat, thus most of the knowledge gained from those studies is important for the understanding of the mechanisms of innate hyperexcitability, but not as useful for understanding the mechanisms of the *development* of hyperexcitability. Because most seizures resulting from cortical malformations are intractable and there is a latent period until seizures become evident, this model is perhaps best utilized by examining how and when hyperexcitability evolves. With imaging techniques becoming more sophisticated (148), clinicians may have the ability to identify patients with malformations prior to the development of hyperexcitability and thus prevent seizures and the possibility of life altering resection surgeries.

### ***The Latent Period***

The latent period between the insult to the brain and the onset of epileptiform activity has been described in many epilepsy models, including kindling and developmental cortical malformation models (64, 138, 293, 317). The length of the latent period can depend on many factors, including the location, timing, and severity of injury (68, 125, 309), but the identification of the latent period is dependent on the ability to accurately detect epileptiform activity. These



measurements are restrained by both the recording method and the amount of seizure monitoring (83).

Persistent temporal lobe epilepsy is modeled in animals by kindling the animals by a number of different methods, including pilocarpine injections and high frequency stimulation. These models display a latent period between the kindling and the onset of persistent motor seizures that ranges from several days to months (40, 41, 46, 110, 121, 122, 193) . There are two prevailing hypotheses associated with the latent period of temporal lobe epilepsy models: the traditional view is that seizures arise suddenly after a period of time, whereas the more modern view is that seizures frequently arise gradually at first, then more rapidly <sup>for review see</sup> (83). It is known that interictal epileptiform activity cannot be evoked in the microgyria model until P12 (138) but whether there is a gradual and sudden development of hyperexcitability is not known.

Epilepsy associated with human cortical malformations is also sometimes delayed in onset (4, 26, 157, 222, 284) and animal models replicating the human malformations have also shown a latent period between time of insult and epileptiform activity onset: undercut model (15-33 days) (128); freeze lesion model (12 days) (139); and TISH mutant (30 days) (293). With the exception of the undercut model, the latent periods are from the date of birth until the first epileptiform event. This means that in each of these models, maladaptive plasticity occurs during a critical period of cortical development that involves both the migration of cells and synaptogenesis. Understanding the mechanisms and timing of maladaptive plasticity is then key to helping prevent the onset of seizures in newborn and children with developmental cortical malformations.

### ***Critical Mechanisms During First Two Postnatal Weeks of Cortical Development***

As previously noted, the latent period between insult and epileptogenicity is 12 days in the rat freeze lesion model of microgyria. This section will isolate several important developmental steps during those first two postnatal weeks that evidence suggests are erroneously affected by the freeze lesion and can help explain the development epileptogenicity.

*GABA<sub>A</sub>-mediated Depolarization in Early Cortical Development:* GABA<sub>A</sub> depolarizes and excites immature neurons in many mammalian species because the concentration of intracellular chloride is higher relative to mature neurons (33) and activation of the GABA<sub>A</sub> receptor causes an outward (instead of inward) flow of chloride ions. The developmental shift from an outward to an inward current is dependent on the expression levels of the chloride cotransporters NKCC1 and KCC2 (for review see Ben-Ari (34)). KCC2 is rarely expressed in the immature neuron but is gradually upregulated starting around ~P10 (89). NKCC1 expression spikes in the first postnatal week and is followed by a gradual decrease in adolescent neurons (89). It is thought that GABAergic membrane depolarization is a key regulator of several features of early circuit development (3). This notion comes from studies that manipulated the expression of KCC2 and NKCC1. Early expression of KCC2 in the *Xenopus* tadpole retinotectal system prevented the normal maturation of glutamatergic synapses and caused an increase in the expression of inhibitory synapses (62). Knocking down expression of NKCC1 in hippocampal neurons severely impaired the synaptic and morphological development of the immature neurons (101). In the freeze lesion model, the expression of cation-Cl<sup>-</sup> cotransporters, NKCC1 (upregulated) and NCC2 (downregulated) has been shown to be altered within the first week post lesion, suggesting the transition from excitatory to inhibitory of GABAergic neurons could be affected prior to the onset of epileptiform activity at P12 (265). It should be noted that NKCC1

and NCC2 expression returns to normal levels later in development in the malformed cortex but the functional role the altered expression in immature plays is unknown.

*NMDA receptor subunit transition:* As previously described, it is well established that a switch from predominately NR2B-containing to NR2A-containing synaptic NMDARs normally occurs in the somatosensory cortex in response to experience during the first two weeks of postnatal development (25, 297). Delayed conversion from NR2B- to NR2A-containing NMDARs have been implicated in a number of models of cortical malformation associated with hyperexcitability (92) including the freeze lesion model (18). However, the time course of NR2B expression in and around the microgyrus before epileptogenesis is not known. Additionally, the role that the delayed conversion from NR2A to NR2B plays in seizure susceptibility is not known.

*Synaptogenesis and Dendritic Arborization:* During the end of neuronal migration and early postnatal development, neurons rapidly make functional connections with synaptic partners via experience-dependent plasticity mechanisms (91), (8, 36, 59). This process causes the rapid development of receptive fields (275) through many developmental steps, including: extension of axonal afferents; dendritic morphology development; spinogenesis; and unsilencing of functional synapses (12, 73, 179, 305). In the anatomical connectivity of the malformed cortex section, the abnormal connectivity of both the afferents and efferents to and from the malformed cortex was outlined. The timing of the development of these abnormal anatomical connections and how they contribute to seizure susceptibility is not known.

### ***The Latent Period and the Freeze lesion Model of Microgyria***

The latent period of the freeze lesion model is known to be 12 days, but an understanding of the mechanism(s) that develop(s) between the induction of the malformation after birth and the onset of epileptiform activity on P12 is unknown. The introductory sections in this dissertation about the microgyria demonstrate that very little research has been conducted on the freeze-lesioned cortex during the first two postnatal weeks. The following paragraph will organize the previously presented information to highlight what is known about alterations in malformed cortex prior to P12.

Epileptiform activity cannot be elicited in malformed cortex until P12 (138), but susceptibility to hyperthermia-induced seizures increases as soon as P10 (260). It is known that the frequency of mEPSCs increases abruptly between P9 and P10 in layer V pyramidal neurons in the PMR (320), which suggests a rapid increase in functional excitatory afferents at that age. The ionic gradient within cells is set in part by the  $\text{Na}^+/\text{K}^+$  ATPase. Disruptions to this protein can contribute to epileptogenesis and changes to the  $\text{Na}^+/\text{K}^+$  ATPase have been shown in the malformed cortex but only after P14 and not between P7 and P14. The final study that examines possible mechanisms of epileptogenesis during the first two postnatal weeks is the  $\text{Cl}^-$  cotransporter study, which shows a misregulation of both  $\text{Cl}^-$  cotransporters. From these three studies we can conclude that prior to the onset of epileptogenesis: (1) excitatory afferents increase abruptly between P9 and P10 (320); (2) intrinsic ionic homeostatic mechanisms do not appear to be altered (until after P14) (61); and (3) the regulation of cation- $\text{Cl}^-$  cotransporters appears to be altered as early as P7, particularly in the abnormal lamination within the malformation (265). What is not understood is whether these mechanisms and other unknown

mechanisms occurring during this period affect the susceptibility to and/or characteristic seizure-like activity or prior to P12.

The first two chapters of this dissertation will specifically address the following questions:

- 1) Does the immature, malformed cortex have a greater susceptibility for seizure-like events during the latent period between malformation creation and epileptiform activity onset? And if so, does the timing of acquired susceptibility correlate with the timing of known altered properties in the malformed cortex?
- 2) What role does development play in the characteristics of seizure-like events in both the malformed and control cortex?

### ***Epileptogenic Focus in the Cortical Malformation of Microgyria***

In the new definitions for the classifications of seizures, Berg, et al. defined focal epileptic seizures as

...conceptualized as originating within networks limited to one hemisphere. They may be discretely localized or more widely distributed. For each seizure type, ictal onset is consistent from one seizure to another, with preferential propagation patterns. (38)

There have been documented cases of patients with focal seizures consistently originating from specific brain locations (i.e. somatosensory, auditory, visual, and associational cortices) which cause specific functional disruptions (tingling (256), auditory(63), and visual hallucinations (42)). Many of these types of focal seizures are associated with focal, developmental cortical malformations such as heterotopias and polymicrogyria (24). However, not all focal seizures associated with developmental cortical malformations are initiated within the malformation. The fundamental question is what

are the differences between a malformation that is the epileptogenic focus and one that is not.

Understanding the differences between an epileptogenic and non-epileptogenic initiating malformation is essential for the treatment of patients suffering from intractable seizures (219, 241). For many of these patients, surgical resection is the only hope of becoming seizure free but the volume of tissue resected must be restricted to prevent behavioral or cognitive deficits. Imaging technology has allowed for greater resolution of malformations associated with seizures (24, 148), but our current understanding of how the malformation characteristics (time of creation, size, location) affect the epileptogenic focus is minimal.

### ***Polymicrogyria and Uncertainty of the Epileptogenic Focus***

Studies examining the efficacy of surgical resection for patients with polymicrogyria appear to identify multiple populations: some that respond to surgical resection of the malformation (156), others that do not and only have their seizures abated by resection of a much larger area (50) (270). In the freeze lesion model, multiple populations might also exist – one population of animals with a epileptogenic focal region adjacent to malformed cortex (138) and one population with a highly focal epileptogenic malformation (244). The main difference between these populations is the timing of the freeze lesion. The hyperexcitable PMR arises from lesions on P1 and the hyperexcitable malformation arises from lesions on P0 (102).

In clinical populations, the timing of brain lesions can have a drastic affect on the severity of functional deficits (223). There are critical periods for topographical specificity and if lesions occur before these periods, cortical representations can primarily develop in brain regions

different from the usual adult topography. That said, evidence suggests that these plasticity mechanisms are dependent on the timing of the insult, as well as the affected brain region or functional system (145, 162).

The timing of the freeze lesion has been shown to affect the histopathology and epileptogenicity of the malformed cortex and also alter behavioral deficits in malformed animals. There appears to be a window of time in which a freeze lesion will produce a four-layered microgyrus with pronounced reductions in brain weight and corpus callosum volume. Freeze lesion *in utero* does not produce the characteristic four-layered microgyrus, but does produce an epileptogenic cortex with cellular abnormalities consistent with human focal cortical dysplasia (1). Freeze lesion after P3 (P5 specifically) also does not produce the characteristic four-layered microgyrus (286,288), nor does it reduce brain weight and corpus callosum volume. The behavioral deficits associated with the four-layered microgyrus are also seen in animals with P5 freeze lesions, but they do not persist in adulthood as they do in P1 freeze-lesioned animals (286).

P0 to P3 freeze lesion does produce the characteristic four-layered microgyrus (87, 252, 288) but whether subcellular, network, and/or epileptogenicity characteristics are different depending on the timing of the freeze lesion within that three day period is not known. Considering there are differences at P0 and P1 in the presence of excitatory neurons (133) and could be differences in the presence of different subtypes of inhibitory neurons (54, 202, 203), functional differences should be expected to be seen between the P0 and P1 induced malformation. Most studies either freeze lesion on P0 or P1 but disagreement on the definition of a postnatal day makes understanding what day freeze lesions were done difficult. In some studies (76, 77), the first day of life is considered postnatal day 1 or P1, while most, including this study,

considers the first day of life postnatal day 0 or P0. Some studies don't differentiate between P0 and P1 but rather state freeze lesions were done within 48 hours (140, 276).

Due to the lack of specificity and variability in reporting of freeze lesion date, developing conclusions on whether the P0 and P1 lesion alters the subcellular, network, and epileptogenicity characteristics is difficult. However, two studies examining the susceptibility to seizures may provide preliminary evidence that the P0 and P1 lesioned cortex varies in susceptibility to seizures. One group has shown that P0 lesioned animals are not more susceptible to bicuculline induced seizures (151), whereas another group has shown that P1 lesioned animals are more susceptible to hyperthermia induced seizures (260). The possibility exists that the different results could be explained by their methods of inducing seizures, but it does provide evidence that functional differences may exist between P0 and P1 lesioned cortices. As previously stated, the epileptogenic focus or initiating site may be different depending on the age of freeze lesion. Studies utilizing P1 freeze lesion find that the site of epileptiform event initiation is the cortex adjacent to the malformation and epileptiform activity can be initiated even when the malformation is mechanically separated (138). In contrast to that study, a study utilizing P0 freeze lesion found that nearly 100% of evoked and spontaneous generated epileptiform events originated within the malformation itself (245). Considering more than 60 studies have used the perinatal freeze lesion to study epileptiform activity associated with a developmental cortical malformation and the model continues to be an important model to study polymicrogyria, more needs to be understood about the differences between the P0 and P1-induced malformation.

The third chapter of this dissertation will specifically address the following question:



- 1) Are network and epileptiform activity characteristics, i.e. site of epileptogenesis and propagation rate of epileptiform events, different in the P0- and P1-lesioned cortex and if so, what possible mechanisms could explain the differences?

## 1.7 General Methods

### *Freeze Lesion Protocol*

On postnatal day (P) one (Chapters 2, 3, and 4) and/or postnatal day zero (Chapter 4), Sprague Dawley rat pups were anesthetized in ice for ~4 minutes. When movement and response to tail pinch ceased, an incision was made through the scalp. With the skull exposed, a freezing (-50° C) rectangular probe (tip size = 2 X 5 mm) was placed over the somatosensory cortex for five seconds. The scalp was then sutured and the pup was placed under a heat lamp to warm, and ~10 minutes later returned to the dam. For a detailed description of procedure see Jacobs, 1996 (137).

### *Brain Extraction and Slice Preparation*

Between P7 and P38, rats were anesthetized with pentobarbital (55 mg/kg i.p.) or isoflurane exposure and decapitated for brain removal. Once the brain was removed it was immediately chilled in sucrose-modified artificial cerebral spinal fluid (aCSF) containing: (in mM) 2.5 KCl, 10MgSO<sub>4</sub>, 3.4 CaCl<sub>2</sub>, 1.25 NaH<sub>2</sub>PO<sub>4</sub>, 234 sucrose, 11 glucose, and 26 NaHCO<sub>3</sub>. Coronal 400 μm thick slices were cut in modified aCSF with a 1000plus vibratome. Once cut, the slices were placed in an oxygenated *normal* aCSF containing: (in mM) 126 NaCl, 3 KCl, 2 MgCl<sub>2</sub>, 2 CaCl<sub>2</sub>, 1.25 NaH<sub>2</sub>PO<sub>4</sub>, 10 glucose, and 26 NaHCO<sub>3</sub>. The slices remained in this

solution at 34° C for 30-45 minutes and at room temperature thereafter until placed in the recording chamber.

### *Electrophysiological Recordings*

Slices were placed in an oxygenated interface chamber with 34° C normal aCSF flowing over the slice. In order to observe the activity of many cortical neurons in both control and malformed cortex, field potential recordings were used in the studies contained in this dissertation. They were made using glass micropipettes (2-8 M $\Omega$ , 1 M NaCl), placed within superficial layers (II/III) ~1 mm lateral to the microsulcus in PMR or in homotopic control (unlesioned) cortex. For extracellular stimulation, a concentric bipolar electrode was placed at the interface of white and gray matter directly beneath the recording site, such that these two electrodes were in a plane orthogonal to the pia. A normal cortical response can be seen in figure 1.6A. In this local field potential trace, a stimulus artifact is followed by a short latency response that is reflective of activity of many excitatory cortical neurons.

Both spontaneous and evoked epileptiform activity were generated in malformed and control cortex using low magnesium aCSF. Low threshold stimulation of epileptiform activity was utilized in the experiments contained in both chapters 2 and 4 to initiate epileptiform activity. This extracellular stimulation elicited two types of evoked epileptiform activity: interictal (Fig. 1.6B) and ictal-like (Fig. 1.6C,D) activity. Interictal-like activity was characterized by a slow, large all or none depolarization shift (Fig. 1.6B). In contrast, ictal-like activity was faster (Fig. 1.6C) and at times repetitive (Fig. 1.6D). Local field potential recordings of spontaneous epileptiform activity were used in chapters 3 (Fig. 1.6E) and 4 (Fig. 1.6H). Two distinctive spontaneous epileptiform events could be distinguished using continuous local field

potential recordings: seizure-like events (Fig. 1.6F) and continuous repetitive ictal-like activity (Fig. 1.6G). Because of dye bleaching and toxicity, long recordings of spontaneous epileptiform activity was not possible in chapter 4 but constant monitoring of the field potential allowed for identification of when epileptiform activity began and ended. This meant we were able to use spontaneous epileptiform events that were always the initial event of a seizure-like event (Fig. 1.6H).

### *Voltage Sensitive Dye Imaging*

Voltage sensitive dye imaging was used in chapter 4 to visualize cortical activity over a large spatial area. We used the absorption dye RH-765 which is a lipophilic dye that embeds itself in the membrane of neurons and changes its spectral properties when membrane potential changes. For absorbance measurements, slices were illuminated with a tungsten-halogen 100-w lamp passed through a band-pass filter (705 +/- 30 nm, Chroma Technology). The transmitted light was passed through a 4X objective and collected with a Wutech H-469IV photodiode array that is part of the Redshirtimaging integrated Neuroplex II imaging system (176  $\mu$ m resolution between diodes). The data were acquired and analyzed using variable normalization with Neuroplex software and epileptiform activity was confirmed by a simultaneously record field potential (Fig. 1.6H – dotted line = LFP, solid line = optical trace). The optical responses for each diode were converted into a heat-mapped image that had a scale from blue to red which corresponded to 0% to 100% of the maximal response at each individual diode.

**Figure 1.1** Timing of Neurogenesis in Rat: **A)** Low power images of the developing neural tube at E12 to the emergence of the cortical layers at E21 **B)** The separation of the subplate (SP), cortical plate (CP), intermediate zone (iz), and subventricular zone (sv) and eventual thickening of the cortical plate from E14 to E20. **C)** The day of origin for neurons destined for the five major cortical layers. Vertical axis = the percentage of total neurons destined for each designated layer. All figures taken from Bayer & Altman, 1991.

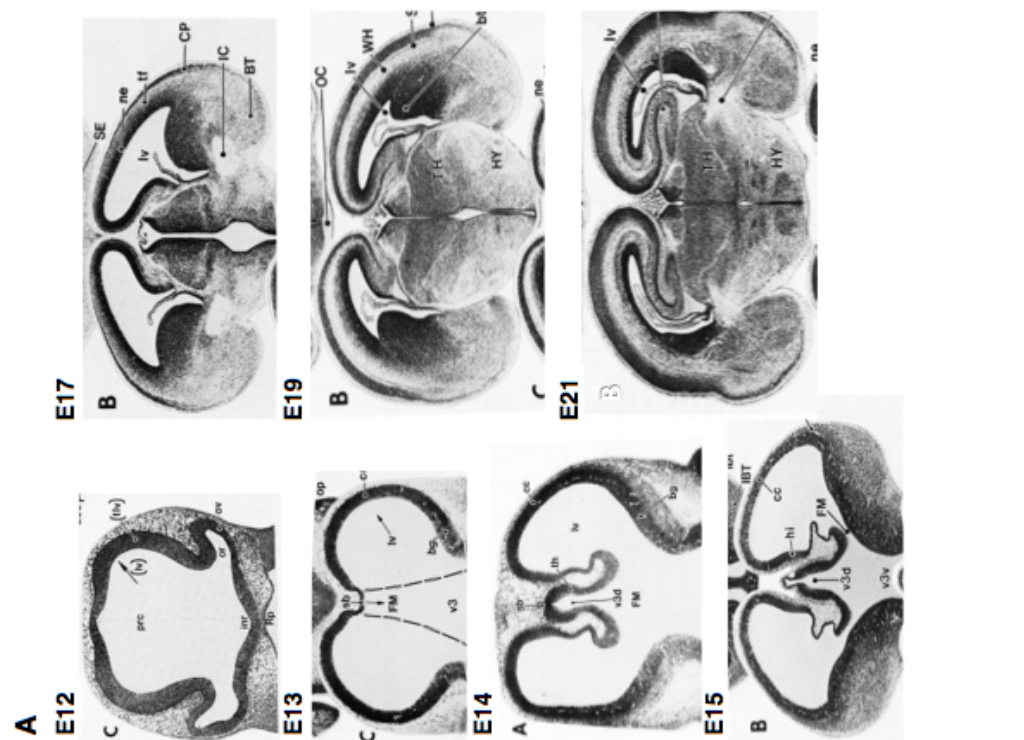
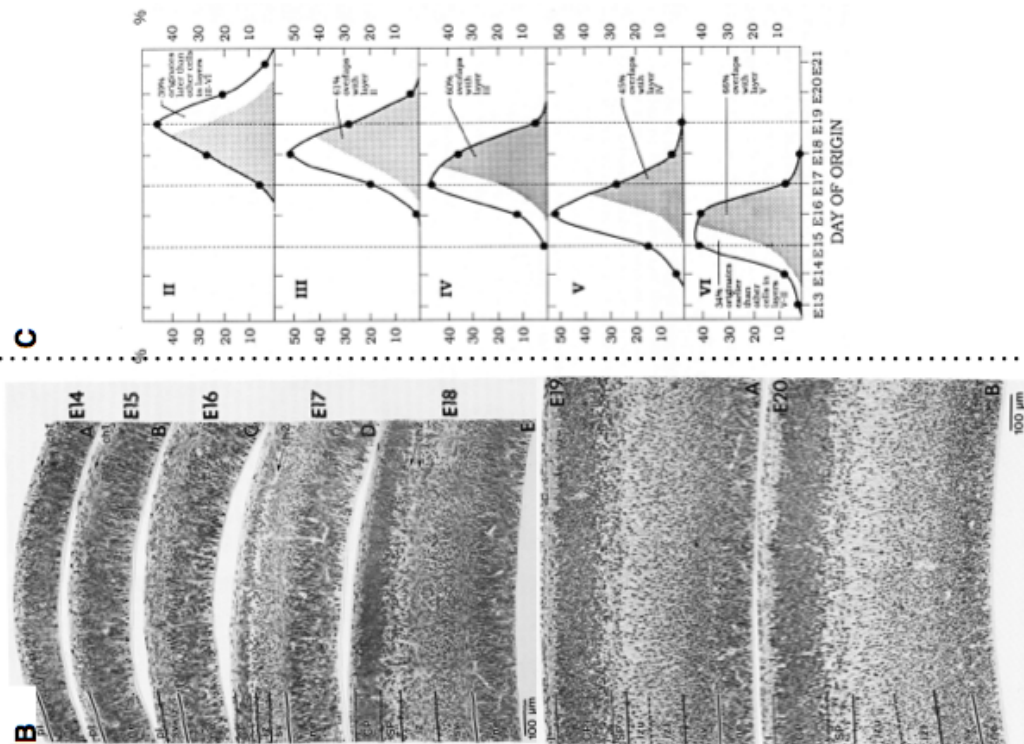


**Figure 1.2** Cortical Radial Migration: **A)** Cartoon sketch of typical radial migration of newly born neurons from the subventricular zone to the cortical plate (taken from Nadarajah, 2002). **B)** A summary of the identified molecules associated with different aspects of proper radial migration (taken from Marin, 2003). **C)** The cell location of E14 to E19 BrdU stained neurons at P0, P1, and P6 (taken from Ignacio, 1995).

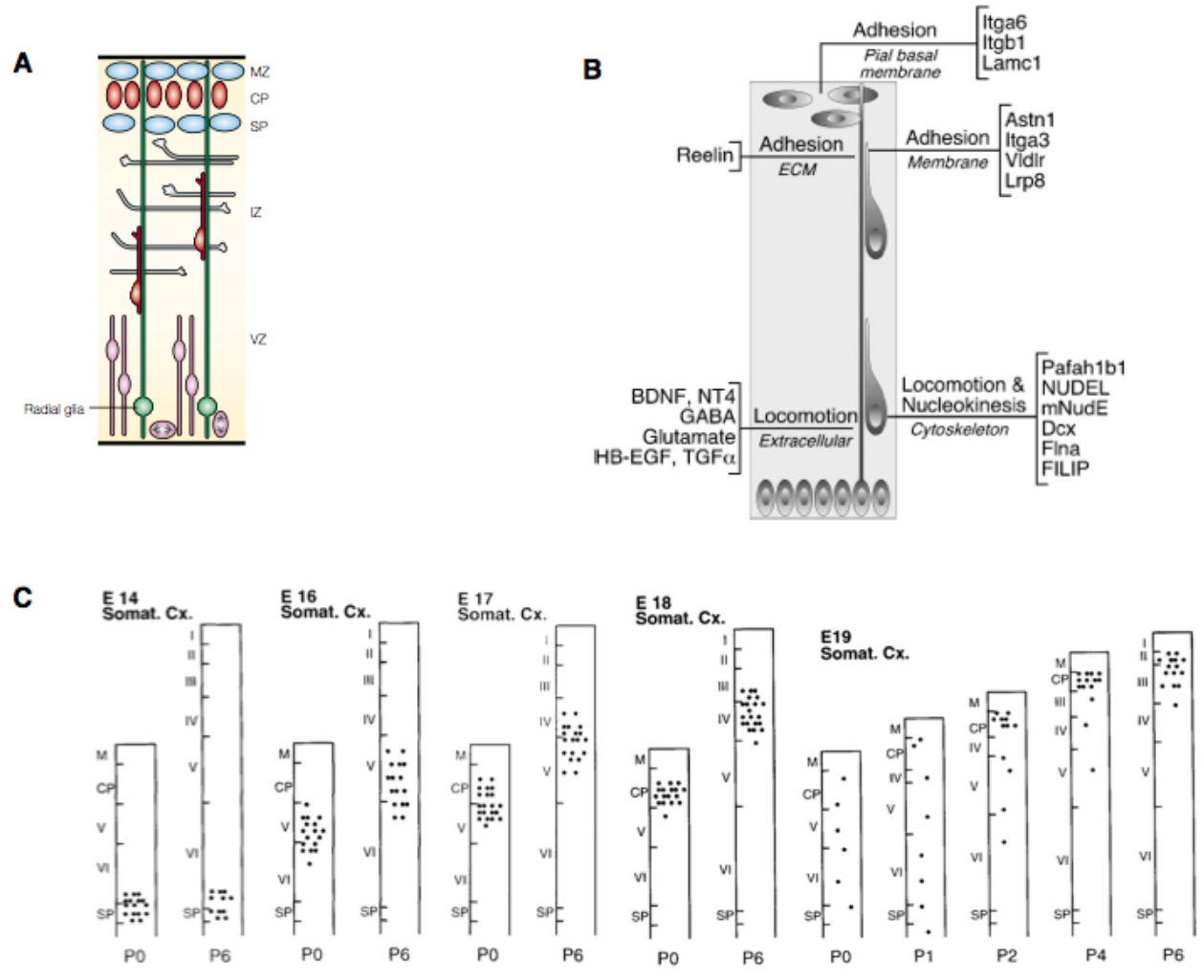


**Figure 1.3** Interneuron Neurogenesis and Tangential Migration: **A)** A basic cartoon of interneuron neurogenesis and migration with the guidance molecules that are associated with proper tangential migration (taken from Powell, 2004). **B)** The birthdays and final destinations of interneuron populations originating from the two main sites of interneuron neurogenesis: medial ganglion eminence (MGE) and caudal ganglion eminence (CGE). **C)** The laminar position of interneurons stained with BrdU at E12.5 and E16.5 at P1, P3, P5, P7, and adult ages (B and C taken from Miyoshi, 2011).



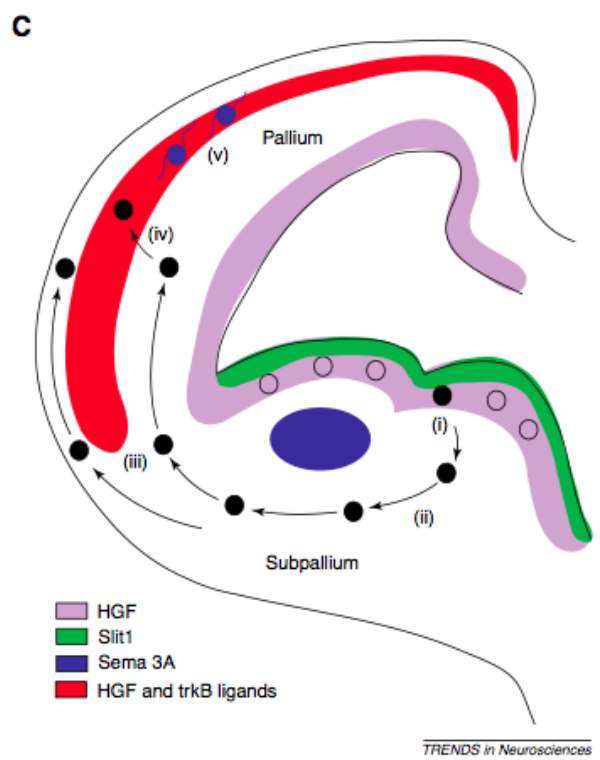
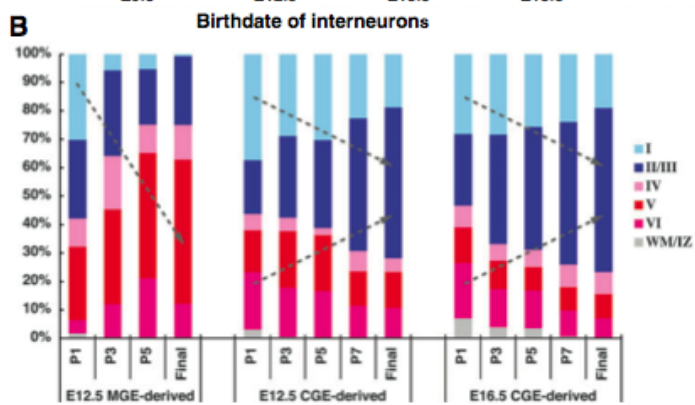
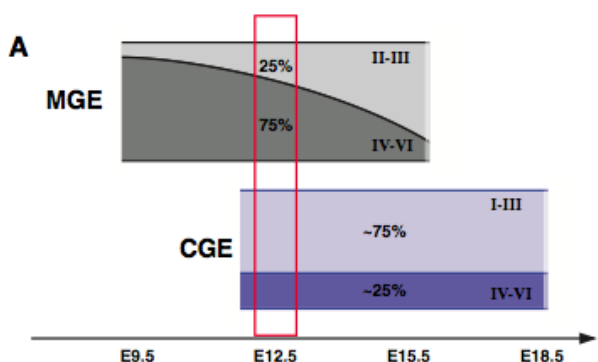


**Figure 1.4** Five Types of Developmental Cortical Malformations: **A)** Perinatal insults to the developing cortex, BCNU and MAM injections as well as perinatal irradiation, create heterotopic lamination. **B)** Genetic knockout of *TISH* and *p35* genes create a band heterotopia (*TISH*) and inverted cortical lamination (*p35*) malformations (taken from Benardete, 2002; Baraban, 2001).

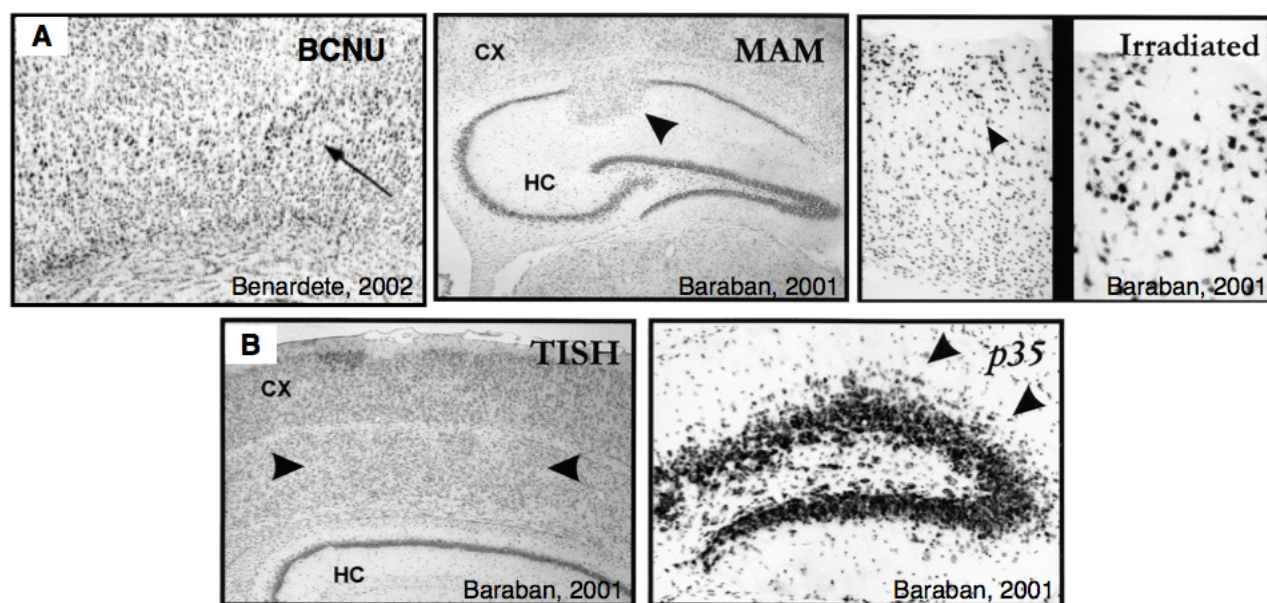
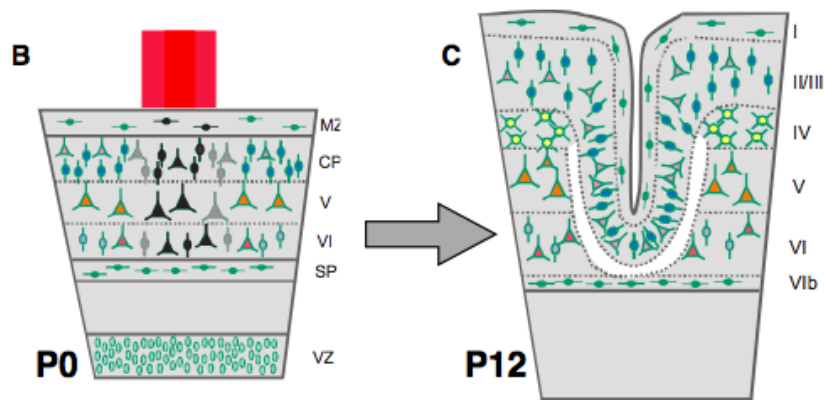
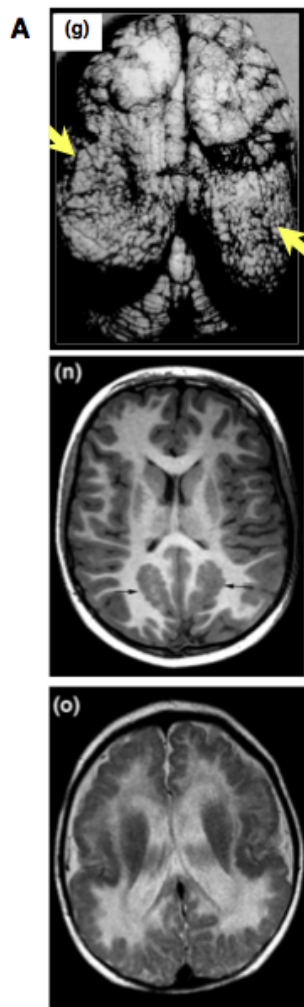
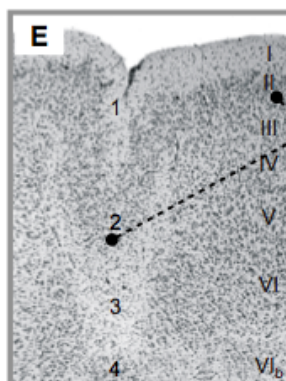


**Figure 1.5** Human Polymicrogyria and Freeze Lesion Model of Microgyria: **A)** Clinical examples of polymicrogyria: (g) surface of gross brain illustrating the multiple, abnormal gyriations (taken from Barkovich, 2001), (n) MRI localization of polymicrogyria, and (o) global example of polymicrogyria (n and o taken from Guerrini, 2008) **B and C)** Illustration of the freeze lesion method that kills neurons present at the cortical plate (B) followed by superficial layer migration to create a malformed invagination (C). **D and E)** The resulting four-layered malformed cortex (E) is histopathological similar to the microgyrus seen in patients with polymicrogyria (D, taken from Robain, 1996). **F)** Stimulation of the area adjacent to (but not within) the sulcus has been shown to be capable of evoking epileptiform events after P12



Human Microgyrus



Rat Microgyrus

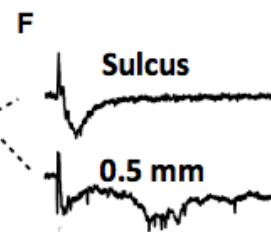
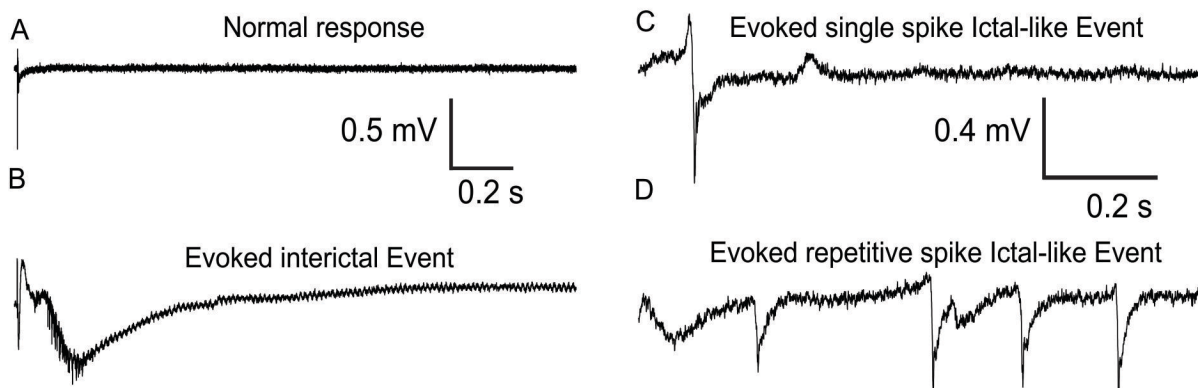


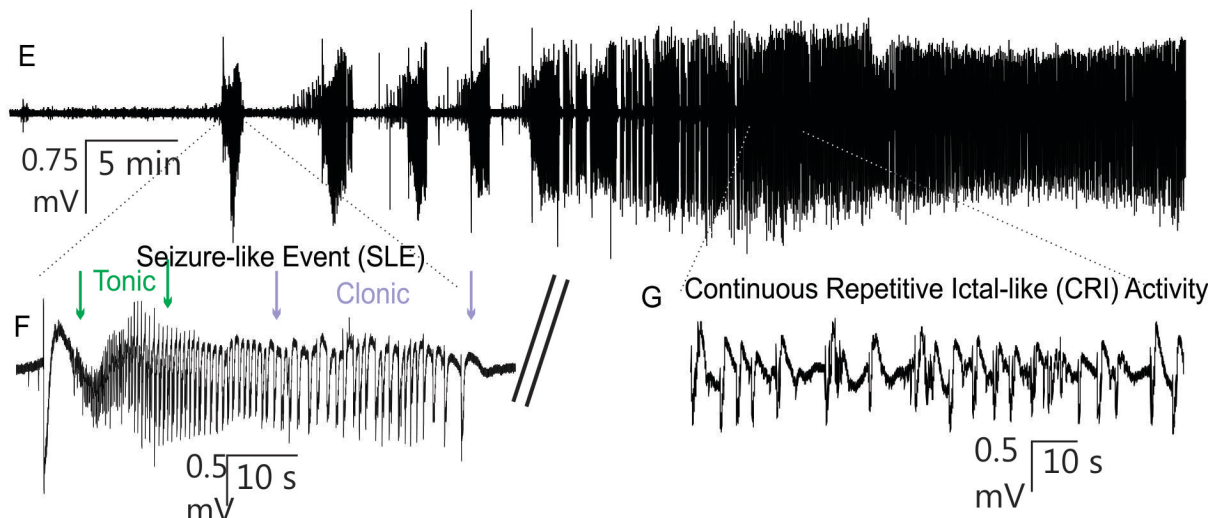
**Figure 1.6** Types of Epileptiform Activity in Low Magnesium aCSF Recorded for Dissertation

**A-D)** Examples of evoked cortical responses - **(A)** Normal evoked response: a stimulus artifact is followed by a short latency response that reflects the activity of pyramidal neurons **(B)** Interictal-like event: a slow but large, all or none epileptiform event **(C-D)** Ictal-like events: fast and at times repetitive **(D)** epileptiform events **E-G)** Examples of spontaneous epileptiform events - **(E)** A 100 minute field potential recording of the development of spontaneous epileptiform activity in control P12 cortex. Two distinct types of epileptiform activity can be generated: seizure-like events (SLEs) **(F)** that can be divided into tonic (green arrows) and clonic phases (purple arrows) and continuous repetitive ictal-like (CRI) activity **(G)**. **H-J)** Visualization of the spatial-temporal characteristics of epileptiform activity with voltage sensitive dye imaging – **(H)** Epileptiform activity confirmed with field potential recording (dotted line) is recorded by a large diode array **(I)**. The optical traces can be converted into a heat mapped image which represents depolarized states in reds and oranges and hyperpolarized or resting potential states as greens and blues **(J)**.

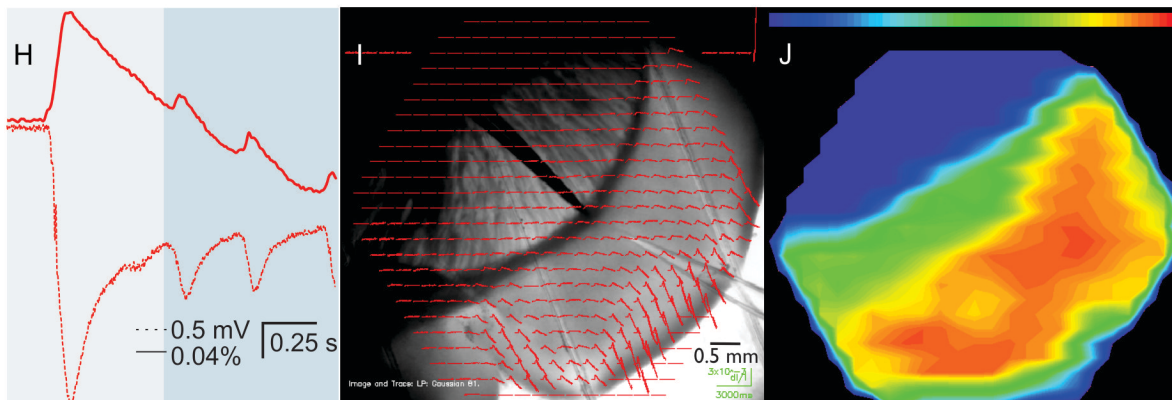
### Field Potential Recording of Evoked Epileptiform Activity



### Field Potential Recording of Spontaneous Epileptiform Activity



### Voltage Sensitive Dye Imaging of Evoked Epileptiform Activity



## Chapter 2

### Early Susceptibility for Epileptiform Activity in Malformed Cortex

#### Abstract

Despite early disruption of developmental processes, hyperexcitability is often delayed after the induction of cortical malformations. In the freeze lesion model of microgyria, interictal activity cannot be evoked in vitro until postnatal day (P)12, despite the increased excitatory afferent input to the epileptogenic region by P10. In order to determine the most critical time period for assessment of epileptogenic mechanisms, here we have used low-Mg<sup>2+</sup> aCSF as a second hit after the neonatal freeze lesion to examine whether there is an increased *susceptibility* prior to the overt expression of epileptiform activity. This two-hit model produced increased interictal activity in freeze-lesioned relative to control cortex. We quantified this with measures of incidence by sweep, time to first epileptiform event, and magnitude of late activity. The increase was present even in the P7-9 survival group, before increased excitatory afferents invade, as well as in the P10-11 and P12-15 groups. In our young adult group (P28-36), the amount of interictal activity did not differ, but only the lesioned cortices produced ictal activity. We conclude that epileptogenic processes begin early and continue beyond the expression of interictal activity, with different time courses for susceptibility for interictal and ictal activity.



## Introduction

Cortical malformations, induced by errors in developmental steps or loss of neurons during the formation of the cortical plate, necessarily affect the subsequent course of maturation (1). Interestingly, despite this early disruption of cellular processes and connections, hyperexcitability is often delayed in both experimental epilepsy models (64, 138, 293, 317) and the clinical population (26, 157, 222, 235, 283, 284, 289, 308). A waiting or latent period suggests that epileptogenic mechanisms are developing but not yet capable of producing epileptiform activity. This then makes the latent period a critical time for identification of epileptogenic mechanisms, particularly since seizures themselves can alter physiological processes (191) and exacerbate hyperexcitability (136).

The rodent neonatal freeze lesion model of microgyria replicates the histopathological features of human 4-layered polymicrogyria (86, 87, 137), with a focal four-layered malformed region missing deep layers present by P7 (252). We have previously suggested that the absence of layer IV within the microgyrus triggers reorganization of afferent inputs, particularly thalamocortical ones that find the appropriate laminar targets in the cortex surrounding the malformation, the paramicrogyral region (PMR). This was subsequently supported by anatomical studies showing that afferents avoid the microgyrus and accumulate in the PMR. The physiological evidence of increased excitatory input to this region further suggested that this remapping of afferents might contribute to the expression of epileptiform activity that occurs with an abrupt onset on P12. To confirm that excitatory hyperinnervation could be a cause rather than a result of hyperexcitability, we have previously examined whether it occurred prior to or after the onset of network hyperexcitability at P12. We found that there was an abrupt and

consistent increase in the frequency of mEPSCs in PMR pyramidal neurons on P10. When neonatally freeze-lesioned animals are given a second hit via hyperthermia on P10, they develop spontaneous seizures as adults (259). Since many alterations of microgyral and PMR cortex other than the increased excitatory afferents are known, it is important to determine if it is indeed the presence of this increased afferent input that initiates the epileptogenesis.

To examine this we have asked if there is an increased susceptibility for epileptiform activity during the latent period, particularly coinciding with the hyperinnervation on P10. We have tested this in vitro with a two-hit model of neonatal freeze lesion followed 6 or more days later by the presence low-Mg<sup>2+</sup> aCSF. Low-Mg<sup>2+</sup> aCSF has commonly been used to test for hyperexcitability and models a general overall increase in cortical excitability.

## **Methods**

### *Freeze Lesion*

On postnatal day (P) one, Sprague Dawley rat pups were anesthetized in ice for ~4 minutes. When movement and response to tail pinch ceased, an incision was made through the scalp. With the skull exposed, a freezing (-50° C) rectangular probe (tip size = 2 X 5 mm) was placed over the somatosensory cortex for five seconds. The scalp was then sutured and the pup was placed under a heat lamp to warm, and ~10 minutes later returned to the dam. For a detailed description of procedure see Jacobs, 1996 (137).

### *Brain Extraction and Slice Preparation*

Between P7 and P38, rats were anesthetized with pentobarbital (55 mg/kg i.p.) or isoflurane exposure and decapitated for brain removal. Once the brain was removed it was immediately chilled in sucrose-modified artificial cerebral spinal fluid (aCSF) containing: (in mM) 2.5 KCl, 10MgSO<sub>4</sub>, 3.4 CaCl<sub>2</sub>, 1.25 NaH<sub>2</sub>PO<sub>4</sub>, 234 sucrose, 11 glucose, and 26 NaHCO<sub>3</sub>. Coronal 400 μm thick slices were cut in modified aCSF with a 1000plus vibratome. Once cut, the slices were placed in an oxygenated *normal* aCSF containing: (in mM) 126 NaCl, 3 KCl, 2 MgCl<sub>2</sub>, 2 CaCl<sub>2</sub>, 1.25 NaH<sub>2</sub>PO<sub>4</sub>, 10 glucose, and 26 NaHCO<sub>3</sub>. The slices remained in this solution at 34° C for 30-45 minutes and at room temperature thereafter until placed in the recording chamber.

### *Electrophysiological Recordings*

Slices were placed in an oxygenated interface chamber with 34° C normal aCSF flowing over the slice. Field potential recordings were made using glass micropipettes (2-8 MΩ, 1 M NaCl), placed within superficial layers (II/III) ~1 mm lateral to the microsulcus in PMR or in homotopic control (unlesioned) cortex. We have previously demonstrated that the PMR is the most sensitive region for epileptiform activity (138). For extracellular stimulation, a concentric bipolar electrode was placed at the interface of white and gray matter directly beneath the recording site, such that these two electrodes were in a plane orthogonal to the pia. A single current pulse (20 μsec long) of varying current intensity (0.30-10 mA, defined as threshold current) was applied to generate a short latency field potential with a peak negativity of 200 μV. To further assess slice health and to estimate intrinsic cortical excitability, a series of increasing stimuli (stimulus intensity protocol) were applied by successively increasing the duration of the pulse (1X, 2X, 4X, 8X, and 16X). Slices were deemed viable if they met two criteria: 1) the

short latency response increased in a fashion that was graded with stimulus intensity; and 2) at a stimulus intensity of 16X threshold, the field potential negativity had a peak of at least 0.6 mV. Field potentials were amplified 1000x (AxoClamp 2B, Axon Instruments and FLA-01 amplifier, Cygnus Technologies) and digitized at 5-10 kHz with a Digidata 1322a (Axon Instruments) and recorded to hard drive with Clampex software (Axon Instruments). In order to test the susceptibility to epileptiform activity, before and after low-Mg<sup>2+</sup> aCSF, two sec of response to threshold current stimulation was recorded once a minute. After 10 minutes of recordings in normal aCSF, low-Mg<sup>2+</sup> aCSF (normal aCSF without the MgCl<sub>2</sub> added) was applied for the remainder of the experiment (100 minutes). With our chamber, the solution required five minutes to reach the chamber.

### *Data Analysis*

Measures of the peak, area, and time to peak were made on three sweep averages of the short latency field potential negativity in response to the stimulus intensity protocol using IGOR software (Wavemetrics). Prior to measurement calculation, the responses were zeroed based on the time from zero to nine msec, with the stimulus occurring 10 msec into the sweep. Examination of the peak and area of responses began just after the stimulus artifact. Differences between control and PMR cortex were analyzed using 2-way ANOVAs (intensity versus experimental group). Differences within experimental group between age groups were also tested using 2-way ANOVAs. Epileptiform activity was detected and sorted into interictal and ictal-like (hereafter called ictal) activity by an automated epileptiform detection module written in IGOR by Jeremy Bergsman. Interictal events were detected as peaks occurring after the short latency response that were 2-3X the baseline voltage of the Gaussian filtered (70 Hz) raw field

potential trace (see Fig. 2.2D). Ictal events were detected as peaks that were 2-3X the baseline of the derivative of the filtered trace (see Fig. 2.2F, H). Sweeps with two or more ictal events were considered repetitive ictal. The area of the rectified late (490 to 1990 msec) activity was measured with Clampfit software (Axon Instruments). Because comparisons between control and PMR cortex were truly independent for each age group, Bonferroni adjusted t-tests were used to detect significant differences ( $p < 0.05$ ) for measures of amount of epileptiform activity. For the measure of time to first epileptiform sweep, age appeared to be a factor for the PMR group, thus we used a 2-way ANOVA to determine if there were differences between PMR and control responses as well as differences among age groups.

Spectrograms were created by importing event driven data collected with Clampfit 8.2 (Axon) as gap free data in Matlab (7.9.0, 2009b) using a custom m-file. The initial 400  $\mu$ s of each sweep was eliminated to reduce the effect of the stimulus artifact on the generated spectrogram. For this study, spectrograms with a 0.5 Hz frequency resolution were plotted from 0.0 to 15 Hz.

## Results

In order to understand the onset of excitability changes in malformed cortex, responses from four age groups were characterized: a) P7-9; b) P10-11; c) P12-15; and d) P28-36. The first group, P7-9, reflects a time prior to the increase in excitatory afferent input to layer V pyramidal neurons reported in this malformation model (320). The second group, P10-11, reflects an age when these excitatory afferents are increased, yet field potential epileptiform activity cannot be evoked under conditions of normal aCSF. In the third age group, P12-15, epileptiform activity is

readily and consistently evoked from the PMR (138), although control cortex also shows an increase in excitability at these ages (182, 183). In the final, adult age group, the PMR continues to show epileptiform activity while control cortex is at its lowest level as measured by evoked field potentials.

### *Intrinsic excitability*

Although there is no epileptiform activity evoked within the PMR at P10-11 in normal aCSF, we reasoned that the increase in excitatory afferents observed at these ages (320) might be reflected within the peak or area of the short latency evoked response in normal aCSF. To test this, an extracellular stimulus was applied to deep layers while recording the network response as field potentials from the overlying superficial layers. The current required to evoke the threshold response was not different between control and PMR for any age group (t-tests,  $p < 0.05$ , N.S.). A series of increasingly intense stimuli was applied (see Methods) and the area of the short latency field potential negativity examined. As expected, control and PMR short latency responses did not vary for the P7-9 age group (Fig. 2.1A). Surprisingly, there was also no difference between control and PMR groups at ages P10-11 (Fig. 2.1B). In contrast, for the P12-15 age group, the PMR cortex had responses more than twice as large for stimulus intensities of 4X and greater (Fig. 2.1C, 2-way ANOVA,  $p < 0.001$ ). In the adult age group, the PMR responses were also significantly larger than control (Fig. 2.1D, 2-way ANOVA,  $p < 0.05$ ). The PMR responses at P12-15 were larger than any other responses at any other time. In all cases, the same result was obtained with the measure of peak field negativity (not shown).

### *Effect of 2<sup>nd</sup> Hit*

We sought to determine whether there was an underlying *susceptibility* to epileptiform activity at the ages corresponding to the increase in excitatory afferents (P9-10). To investigate this, we employed a two-hit model, using low-Mg<sup>2+</sup> aCSF to increase overall cortical excitability. The PMR and homotopic control cortex were stimulated once a minute at the threshold current. After 10 minutes of normal aCSF, the bathing solution was switched to low-Mg<sup>2+</sup> aCSF and the responses followed for another 100 min. An automated system was used to detect evoked epileptiform events and to characterize them as interictal or ictal (Fig. 2.2, also see Methods). Events characterized as interictal were slower, particularly in time to peak, and typically larger in amplitude and duration as compared to ictal events. In addition, ictal events often occurred repeatedly within the same sweep (2 sec post-stimulus period, Fig. 2.2D).

Low-Mg<sup>2+</sup> aCSF produced epileptiform activity in all slices from both control and PMR cortex. The changes in field potential activity occurring over the course of an individual experiment were easily visualized in spectrograms displaying power versus frequency over experiment time (Fig. 2.3A). While the short latency activity produced high power at low frequencies (0-1.5 Hz), epileptiform activity produced increased power at frequencies above 1 Hz. Over the course of an experiment, the epileptiform activity typically evolved from slower, interictal events to fast and ultimately repetitive ictal activity (Fig. 2.3B). This pattern was similar in both control and PMR cortex, but typically occurred earlier for PMR than controls.

#### *Effect of Age on Epileptiform Activity Incidence*

In order to examine changes in susceptibility for epileptiform activity, three aspects were analyzed: incidence of events (interictal and ictal), time to first epileptiform event, and magnitude of the late field potential activity. Confirming previous descriptions of increased

excitability in the second to third postnatal week in rodents (Jensen et al., 1991; Luhmann and Prince, 1990), our results show that for control cortex, the P12-15 age group was the most excitable, with significantly more total epileptiform sweeps (Fig. 2.4A-D, I, 1-way ANOVA,  $p < 0.005$ , LSD posthoc) and significantly more single spike ictal than other age groups (Fig. 2.4E-H, 1-way ANOVA,  $p < 0.05$ , LSD posthoc). The adult age group in controls had the fewest sweeps with epileptiform activity, including no ictal activity (Fig. 2.4H). The PMR cortex showed similar trends with age, however there was not a significant effect of age with either total epileptiform activity or ictal incidence (1-way ANOVAs, N.S.). Both control and PMR also showed a significant positive correlation between incidence of ictal activity and age for ages up to P15 ( $R = 0.62$  for control, and  $0.39$  for PMR).

#### *Incidence of epileptiform events in PMR versus Control*

In PMR compared to control cortex, epileptiform activity not only occurred earlier within individual experiments, but also more often and with greater severity than in control cortex from the same age groups (Figs. 2.3-5). For all age groups, there was an increased incidence of epileptiform activity in PMR relative to control cortex (Fig. 2.4). In the P7-9 age group, the majority of the epileptiform events were in the form of interictal activity for both control and PMR cortex (Fig. 4E). In this age group, the increase in epileptiform activity within PMR cortex was due specifically to an increase in interictal events (Fig. 2.4E). In the P10-11 age group, the contribution of ictal sweeps to the total number of epileptiform sweeps was significantly larger relative to that for the P7-9 age group in control cortex:  $28 \pm 8$  versus  $55 \pm 13\%$  of epileptiform sweeps showed ictal activity for 11 and 8 control slices in the P7-9 and P10-11 age groups, respectively (t-test,  $p < 0.05$ ). The same was true for PMR cortex:  $21 \pm 8$  versus  $57 \pm 10\%$  of



epileptiform sweeps showed ictal activity for 12 and 10 slices in the P7-9 and P10-11 age groups, respectively (t-test,  $p < 0.005$ ). Comparing PMR to control within the P10-11 age group, PMR cortex had significantly more epileptiform activity due to a greater percentage of interictal sweeps (Fig. 2.4B, F). In the P12-15 age group one of seven (14%) control slices had interictal epileptiform prior to application of low-Mg<sup>2+</sup> aCSF, while this was true for three of seven (43%) PMR slices. In no case was ictal activity ever observed prior to application of low-Mg<sup>2+</sup> aCSF. Similar to the younger age groups, for P12-15, the increase in percentage of epileptiform sweeps for PMR compared to control cortex was due to an increase in interictal activity (25 ± 0 versus 52 ± 0% of sweeps contained interictal activity for control and PMR respectively,  $P, 0.05$ , t-test, Fig. 2.4C, G). Even when the sweeps prior to application of low-Mg<sup>2+</sup> aCSF were excluded, the PMR still had a significantly larger percent of epileptiform sweeps compared to control (65 ± 0 versus 82 ± 0 % epileptiform sweeps for 7 control and 7 PMR slices, respectively, t-test,  $p < 0.05$ ). In this age group, the proportion of epileptiform sweeps that contained ictal activity was similar for control and PMR cortex (59 ± 8 and 42 ± 12 % of epileptiform sweeps for control and PMR, respectively). In the adult age group, none of the control, but all of the PMR slices exhibited ictal activity (Fig. 2.4H). Thus, only in this age group was the increase in epileptiform sweeps for PMR compared to control cortex due to ictal and not interictal activity. The proportion of PMR ictal sweeps for this age group was similar to that for the previous two age groups (52 ± 20% of epileptiform sweeps).

#### *Threshold for epileptiform activity*

The time to the first epileptiform activity after application of low-Mg<sup>2+</sup> aCSF is another measure of susceptibility to hyperexcitability, but more specifically measures the threshold for

epileptiform events. In PMR slices, the mean time to first epileptiform sweep was less than 10 minutes after low-Mg<sup>2+</sup> aCSF application, for all age groups (Fig. 2.5). The results of the 2-way ANOVA show that the threshold for epileptiform activity is less in the PMR than in control cortex ( $p < 0.05$ ). There was no effect of age nor was there a significant interaction between age and experimental condition.

### *Magnitude of late activity*

The magnitude of field potential activity, particularly at the site of the largest current sink (2), is a reflection of the size of the population EPSC (200), and the number of cells participating when the presynaptic neurons are within the same structure. To determine if malformed cortex had a larger network participating in the generation of epileptiform events in PMR cortex, we analyzed the rectified area of the field potential response occurring after the short latency event ended (500 – 2000 msec, late rectified field potential, LRFP, Fig. 2.6A). Rectification was necessary since epileptiform events often cross the baseline. Each age group showed a distinct pattern in this measure over the course of the experiment (Fig. 2.6C-F). For the P7-9 age group, the PMR cortex showed a significant increase relative to control cortex in the LRFP (Fig. 2.6C, 2-way ANOVA,  $P < 0.001$ ). This increase was most pronounced just after application of the low-Mg<sup>2+</sup> aCSF (Fig. 2.6G, adjusted Bonferroni t-test,  $P < 0.01$ ). The responses from both control and PMR however reached a similar maximum by 50 min after the solution change (Fig. 2.6C, G). For the P10-11 age group, the LRFP was increased in the PMR (Fig. 2.6D, 2-way ANOVA,  $P < 0.05$ ). This age group was the only one that showed an increase in LRFP *prior* to application of the low-Mg<sup>2+</sup> aCSF for PMR relative to control cortex (Fig. 2.6H, adjusted Bonferroni t-test,  $P < 0.01$ ). This increase in LRFP for PMR cortex persisted for the duration of the experiment (Fig.

2.6D, H). In the P12-15 group, there was no difference between PMR and control cortex until ~60 min after onset of low-Mg<sup>2+</sup> aCSF (Fig. 2.6E, 2-way ANOVA,  $p < 0.05$ ). Ultimately, control cortex obtained a larger maximum LRFP than did the PMR (Fig. 6I, adjusted Bonferroni t-test,  $p < 0.01$ ). In the adult age group, the control cortex failed to show an increase in LRFP after low-Mg<sup>2+</sup> aCSF application. (Fig. 2.6F, J). In PMR cortex the LRFP increased at a slower rate than at younger ages, but reached a level near to that obtained for PMR in the P12-15 age group (Fig. 6I, J), and was significantly greater than control (Fig 2.6F, 2-way ANOVA,  $p < 0.05$ ), specifically during the last two time points, (Fig. 2.6J, adjusted Bonferroni t-test,  $p < 0.01$ ).

## Discussion

Here we have demonstrated an early susceptibility for increased levels of hyperexcitability in the freeze lesion model of microgyria. Surprisingly, the age of onset for increased susceptibility does not match the timing of one of the previously identified potential epileptogenic mechanisms, that of increased excitatory afferents to layer V pyramidal neurons (320). We have also suggested that alterations occur in specific interneuron subtypes (102), and some effects on interneurons suggest anti-epileptogenic effects (48, 140). Yet to be determined is the onset timing for these pro and anti-epileptogenic interneuron effects. Early susceptibility followed by delayed onset of epileptiform activity in normal aCSF also suggests that network expression may require maturation of particular cellular properties in the presence of previously occurring abnormalities.

### *Developmental Changes in Excitability*

A number of previous findings in malformation models suggested that early insults may ‘freeze’ the cortex in an immature state or at least delay maturation. In rodent and cat models of microgyria, these included a maintenance of radial glia into adulthood (249), increased duration of the action potential (181), a maintenance of normally pruned connections from auditory to visual cortex (134), enhanced functional response to an immature form of both the GABA<sub>A</sub> and the NMDA receptors (19, 76) and a delayed transition from NKCC1 to KCC2 (265). These effects largely occurred within the malformed region rather than the adjacent area of hyperexcitability. Our current results suggest that hyperexcitability does not arise as a result of a simple maintenance of an earlier hyperexcitable state. This is true since the most excitable age for controls was P12-15, yet the increased level of epileptiform activity was already present prior to this age. The increase in ictal events does not occur until the adult age group, suggesting that there is a continued development of epileptogenic processes, rather than a static mechanistic abnormality, but also that a chronic state of hyperexcitability is ultimately induced in this model. Previous studies have suggested that in fact ictal and interictal mechanisms may develop independently (13, 14, 72). Our data suggest further that independent latent periods exist for expression of interictal activity without a second hit, and susceptibility to ictal activity. Although for some models the malformation is induced in utero, expression of hyperexcitability is delayed to weeks postnatally (64, 293, 317). Changes in susceptibility over development have not been well-studied in malformation models and as shown here, could occur substantially earlier than when seizures or in vitro hyperexcitability is present as has been shown recently for a non-malformation model (240).

#### *Latent Period*

Recent studies have suggested that development of convulsive seizures occurs gradually, rather than suddenly after a latent period (47, 84). For at least some epilepsy models, non-convulsive seizures precede convulsive ones, suggesting an increasing severity (310). Here we find that susceptibility for increased interictal activity is present long before the expression of such activity under conditions of normal aCSF (at P12). This could result from a progressive nature of the interictal activity, although our data do not support this idea. The measures of percentage of epileptiform activity, time to first epileptiform sweep and even magnitude of late activity do not get progressively worse from P7 to P12. Although the P12-15 group was the most hyperexcitable in PMR as well as control cortex, the difference between the excitability for PMR relative to control was actually lowest for this age group (see Fig. 2.4I). A second explanation for the delayed expression in the presence of susceptibility is that a normal maturational process may be necessary for this expression. Previous explanations for the normal increased excitability seen at 2-3 weeks postnatally in control rats include changes in both NMDA and GABA receptor development (182, 183, 298). In adult freeze-lesioned rats, NMDA receptor binding is increased while that of GABA<sub>A</sub> is decreased over control levels (319). These effects are most prominent within the malformed region, but also present in the surround. The onset timing of these effects are unknown, however if they alone created the hyperexcitability, the malformed region would be expected to be the most excitable region in this model, however it is less excitable than the PMR (138). Thus changes in NMDA and/or GABA<sub>A</sub> receptors are unlikely to create the hyperexcitability, however they may influence the expression of it based on developmental changes, including increased expression of NMDA in superficial layers.

The decrease in excitability in mature animals compared to the 2<sup>nd</sup>-3<sup>rd</sup> postnatal week has also been proposed to be due to an increased postictal refractoriness based on kindling

experiments (298). The difference in ictal activity that we found between control and PMR may reflect a lack of development of this refractoriness or the increased NMDA receptors responding to the lack of  $Mg^{2+}$  block.

### *Conclusions*

We have found an early susceptibility for interictal activity in malformed brain, as well as a chronic susceptibility for ictal activity. Once established, there appears to be a maintained rather than progressive effect of the susceptibility for interictal activity. We conclude from this that the delay between this susceptibility and the expression of increased interictal activity without the second hit may be due to normal maturation of characteristics that increase excitability even in control brains combined with the abnormalities such as the previously demonstrated increased excitatory afferents. The separate time course for susceptibility to increased levels of ictal activity suggests that this may arise from separate mechanisms. This study highlights the importance of determining the timing of susceptibility for epileptiform activity in order to identify the underlying mechanisms.

**Figure 2.1** Intrinsic Excitability Changes in Normal aCSF During Development: Stimulus intensity series profiles for immature (**A**: P7-9; **B**: P10-11; **C**: P12-15) and adult (**D**: P28-36) age groups, for control (gray) and PMR (black) cortex. Typical responses from each experimental group are shown in inset, for control (left), and PMR (right), with stimulus artifact masked. For control and PMR respectively, n = 15 and 17 (P7-9); 13 and 10 (P10-11); 28 and 40 (P12-15); 6 and 7 (P28-36) slices. \* = significant difference, 2-way ANOVA,  $p < 0.05$ .

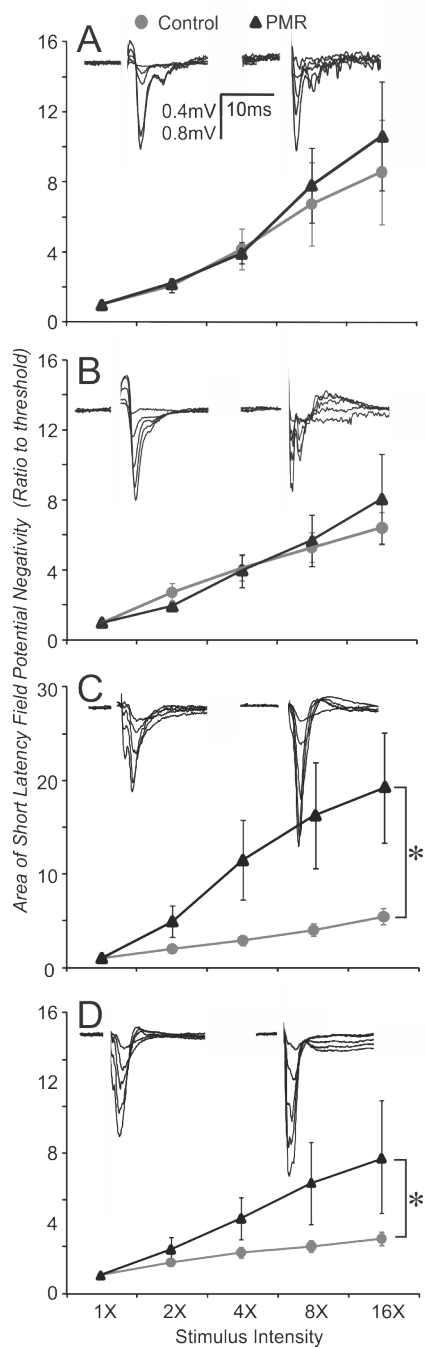




**Figure 2.2** Example of Automated Epileptiform Activity Detection. *Left:* Raw sweep examples of: short latency activity only (**A**); interictal (**C**); single spike ictal (**E**); and repetitive spike ictal activity (**G**). *Right:* Preparation of trace on left for detection of a particular type of epileptiform activity. Traces were filtered at 70 Hz to detect interictal activity (**B**, **D**). The derivative of the filtered trace was used to detect ictal events (**F**, **H**). Dashed lines above traces depict detection threshold, which was set to 2-3 times baseline of the prepared wave. Solid lines above traces indicate location of detected peak. Although here only one example of the prepared wave is shown, each sweep was processed for all three types of epileptiform activity with ictal detection overriding interictal and repetitive ictal overriding single spike ictal. Detection began after the end of the stimulus artifact.

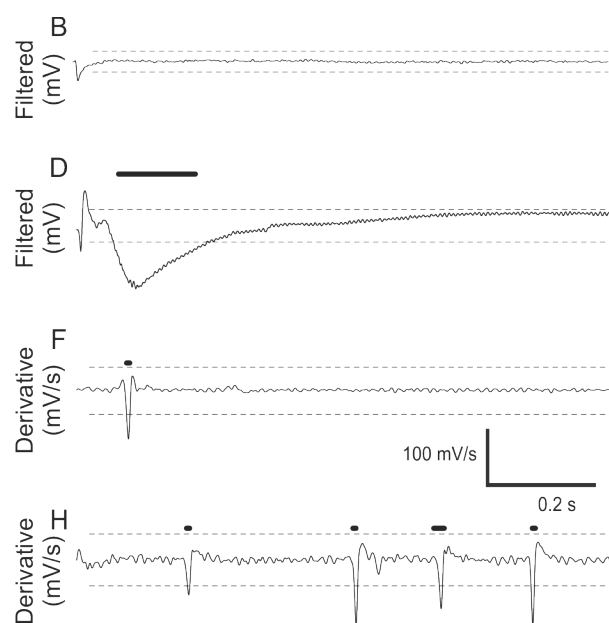
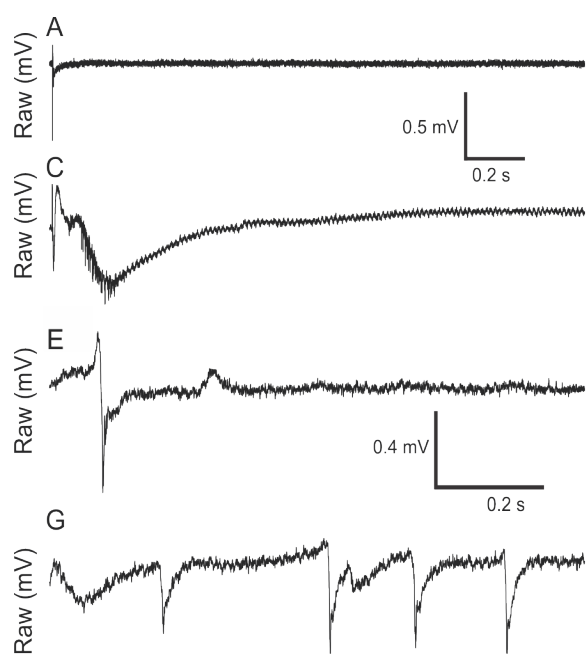


**Figure 2.3** Threshold for Evoked Epileptiform Activity Visualized by Spectrogram: After application of low-Mg<sup>2+</sup> aCSF at time 0, epileptiform activity occurred earlier and more frequently in PMR cortex compared to controls. **(A)** Spectrograms of field potential responses to threshold stimulus given to deep layers below recording. Activity occurring in between stimulus presentations (58 sec) is not shown. The x-axis plots the time over the course of individual experiments for control (top panel) and PMR (bottom panel). ‘Hot’ colors indicate higher power field potential activity (mV/ms<sup>2</sup>). Black arrows point to the first epileptiform sweep. Blue arrows point to the traces shown in B (sweeps 5, 20, 66, and 98). **(B)** Examples of the progression of epileptiform activity through an individual experiment in control (top) and PMR (bottom) cortex. Epileptiform activity begins as slow, large amplitude events and evolves into repetitive sharp ‘spikes’.

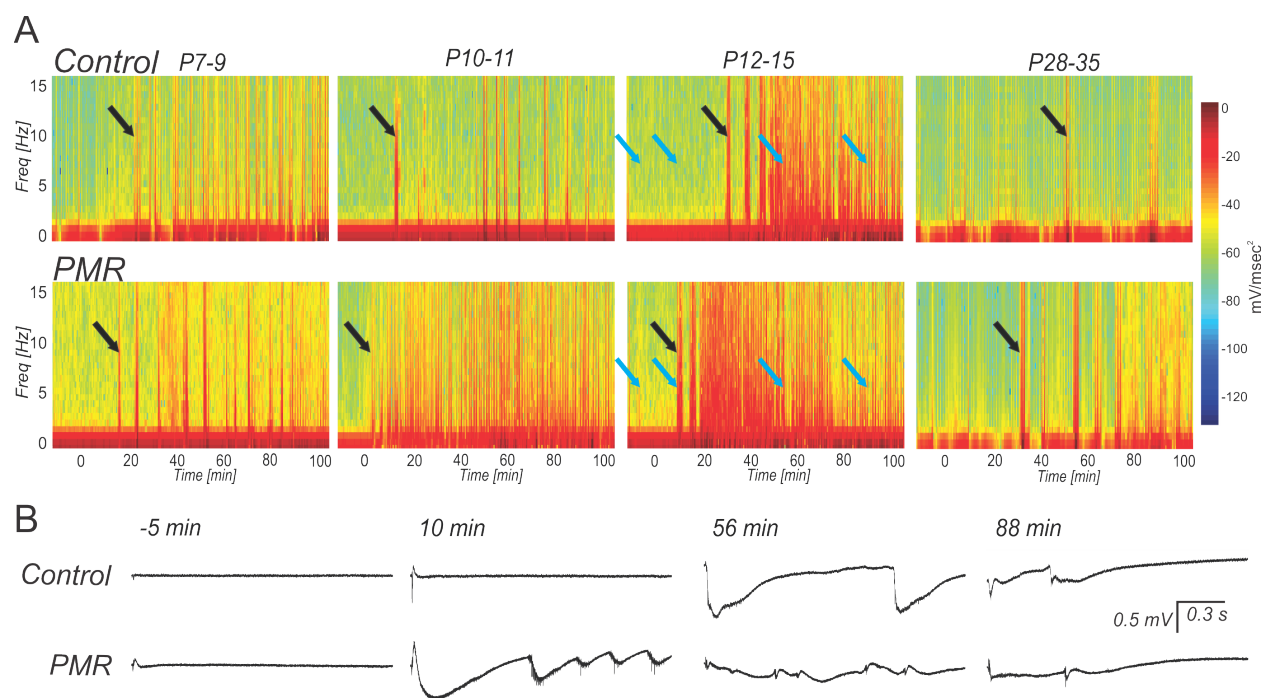


**Figure 2.4** Increased Incidence of Epileptiform Sweeps in PMR Cortex. **(A-D)** Percentage of sweeps with evoked epileptiform activity for age groups (control, PMR slices): P7-9 (**A**, 11, 12 slices); P10-11 (**B**, 8, 10 slices); P12-15 (**C** 7, 7 slices); and P28-40 (**D** 4, 4 slices). \* = significant difference between control and PMR (t-tests,  $p < 0.05$ ). **(E-H)** Distribution of the type of epileptiform activity observed for each group: Interictal, light gray; Single spike (SS) ictal, dark gray; and Repetitive spike (RS) ictal, black. The following symbols represent significant differences between control and PMR: # = interictal, % = SS ictal, and \* = RS ictal (t-tests,  $p < 0.05$ ). **(I)** Percentage of evoked epileptiform activity relative to the average amount observed in control P28-36 (100%) for control groups (gray filled symbols with black outlines) and PMR groups (black filled symbols with gray outlines), for P7-9 (diamonds), P10-11 (triangles), P12-15 (circles), and P28-36 (squares).

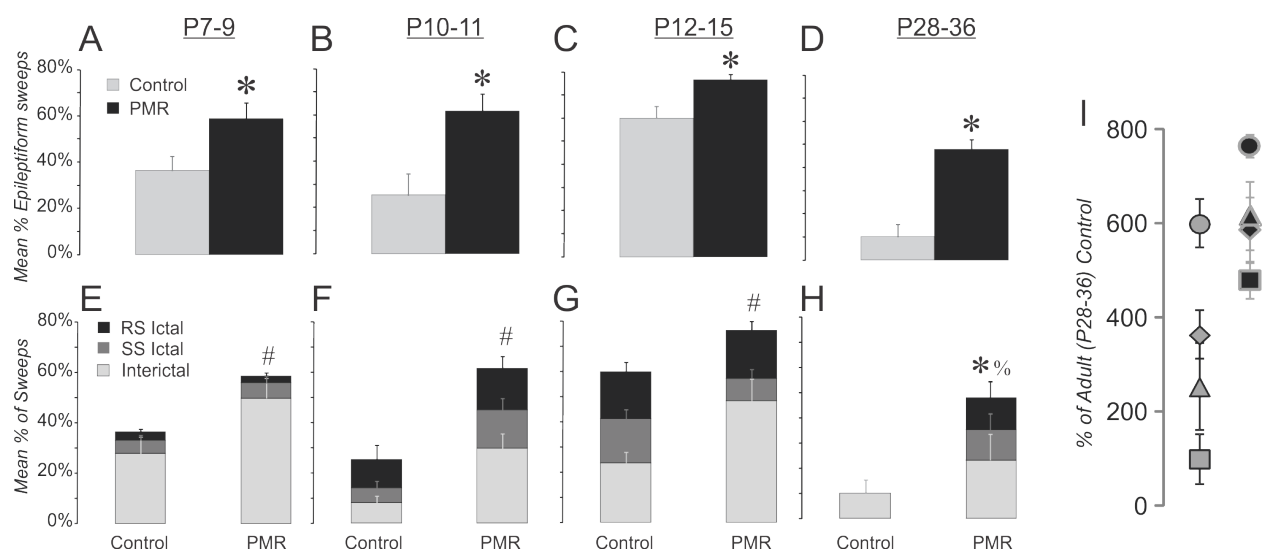


**Figure 2.5** Time (mins) to First Epileptiform Sweep After Low-Mg<sup>2+</sup> Application: Control on left, PMR age groups on right. N = 12, 10, 7, and 4 control slices and 11, 8, 7, and 4 PMR slices for age groups P7-9, P10-11, P12-15, and P28-36, respectively. \* = p<0.05, 2-way ANOVA.

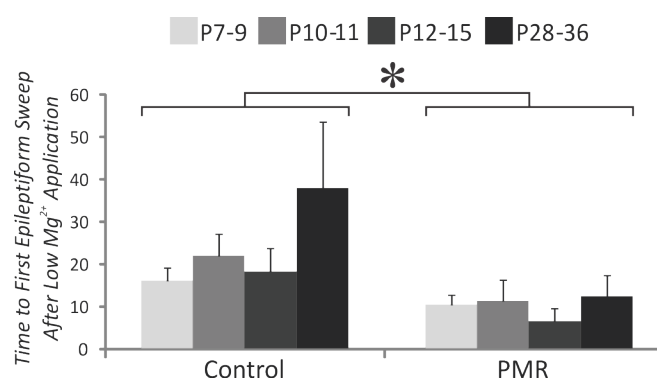
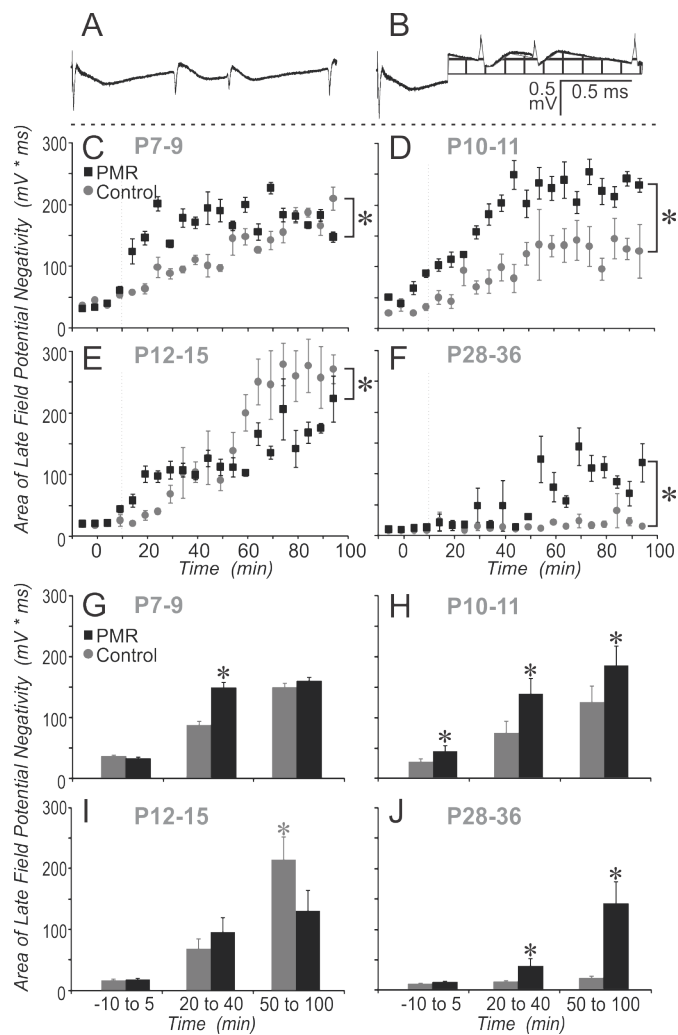




**Figure 2.6** Magnitude of Late Field Potential Activity: (A) Typical raw field potential sweep. (B) Same sweep as in A, with late activity (490 – 1990 msec) rectified. (C-F) Plots of the area of the rectified late field potential activity before (0-9.99 min) and after (10-100 min) low-Mg<sup>2+</sup> application, for control (gray circles) and PMR (black squares). Age group indicated at top of plot. Activity was averaged over 5 min (5 stimulus presentations) before averaging across subjects within group. Error bars indicate SEM. Vertical dashed line indicates when low-Mg<sup>2+</sup> aCSF reached chamber. (G-J) Bar graphs comparing control (gray) to PMR (black) for data shown above, but averaged within three time periods: Early (sweeps 1-15), before low-Mg<sup>2+</sup> reaches the slice; Middle (sweeps 30-50), after effect of low-Mg<sup>2+</sup> is apparent; and Late (sweeps 50-110) when maximum effect has stabilized. \* = p<0.05, 2-way ANOVA.



### Chapter 3

#### Developmental Alterations of Spontaneous Low $Mg^{2+}$ Induced Epileptiform Activity in Malformed Cortex

##### Abstract

A wide range of data supports a role of developmental cortical malformations in hyperexcitability, but the factors that shape ictal-like epileptiform events in developmental cortical malformations have not been as thoroughly addressed. We report the developmental characteristics of spontaneous ictal-like activity generated the freeze lesion model of polymicrogyria using low- $Mg^{2+}$  aCSF. We find that NMDA and AMPA receptor dependent continuous repetitive ictal-like (CRI) activity emerges after a series of seizure-like events (SLEs) in both malformed and control cortex at P12. However, the proportion of slices capable of generating CRI activity in malformed cortex (67%) is much greater than in control cortex (10%) in the P7 to P11 cortex. Pharmacological manipulation of CRI activity in malformed cortex at these ages suggests that the persistence of CRI activity does not depend on group I mGluRs, NKCC1 cation/ $Cl^-$  cotransporter, or NR2B specific NMDA receptors. Inhibition of AMPA receptor desensitization causes CRI activity to emerge in control P9 tissue and enhancement of AMPA receptor desensitization causes CRI activity to cease in malformed P9 tissue. These results demonstrate a possible role that altered AMPA receptor kinetics may play in the characteristics of spontaneous epileptiform activity in the P7 to P11 malformed cortex.

## Introduction

Epidemiological studies show that the propensity of the young brain to develop seizures is much greater than that of the adult brain (119, 120). This higher propensity for seizures in the immature brain is further exacerbated by genetic and extrinsic factors involving congenital cerebral malformations (261). Since the immature brain has a number of structural and functional properties that are fundamentally different from the adult brain (i.e. excitatory action of GABA (34); subunit composition of NMDA receptor (315)) the mechanisms of epileptogenesis during early development are best studied in the immature brain. Polymicrogyria is an epileptogenic developmental cortical malformation that is characterized by an abundance of microsulci on the surface of the cortex (24). The four-layered version of this malformation can be modeled in the rodent using a postnatal transcranial freeze lesion that kills the cortical plate neurons present at the time of lesioning (deep cortical layers). The resulting malformed cortex has an invagination of the superficial layers (86, 87, 252). Evoked epileptiform activity can be generated in cortical areas adjacent to the malformation (PMR) as early as postnatal day (P) 12 (137, 138). As early as P10, rats with this malformation are more susceptible to hyperthermic seizures (259, 260). However, it is unknown how the malformation modulates the form of induced spontaneous epileptiform activity in either the immature or mature cortex. Further, we also do not know the age of greatest susceptibility to spontaneous epileptiform activity in either the immature or mature PMR cortex.

Low-Mg<sup>2+</sup> aCSF can be used to generate epileptiform events in the hippocampus, neocortex, and olfactory bulb (15, 132, 291). The use of Low-Mg<sup>2+</sup> aCSF to generate

epileptiform events in the immature cortex has also been shown as early as P0 in hippocampus (206) and P2 in the neocortex (301). Developmental studies examining epileptiform activity induced by low-Mg<sup>2+</sup> suggest the lowest threshold for epileptogenesis is around the second postnatal week (301). The threshold for ictal-like events, also called seizure-like events (SLE), decreases from P2 to P15 and increases in the adult cortex (301). One study even suggests that low Mg<sup>2+</sup> aCSF-induced epileptiform events cannot be generated in the P4-7 cortex at all (311). In the intact cortico-hippocampal formation, the duration of SLE increases from P2 to P11 and, after P7, persistent epileptiform discharges emerge after an hour of low Mg<sup>2+</sup> perfusion (233). The timing of the emergence of persistent epileptiform discharges in the neocortex has not been studied from a development perspective in either control or malformed cortex. Understanding the characteristics of seizure-like activity in the malformed, immature cortex is essential to developing therapies to treat children with developmental cortical malformations who are suffering from seizures.

In this study, low Mg<sup>2+</sup> induced spontaneous epileptiform activity is examined for four age groups: P7-9, P10-11, P12-15 and P30-35. We examined whether the threshold for spontaneous generation of epileptiform activity was altered through development in both the malformed and control cortex. SLE characteristics and the timing of the onset of continuous repetitive ictal-like epileptiform activity (CRI) were also studied.

## **Methods**

### *Freeze Lesion*

On P1, Sprague Dawley rat pups were anesthetized in ice for approximately four minutes. When movement and response to tail pinch ceased, an incision was made through the scalp. With the skull exposed, a freezing ( $-50^{\circ}\text{C}$ ) rectangular probe (tip size =  $2 \times 5\text{ mm}$ ) was placed over the somatosensory cortex for five seconds. The scalp was then sutured and the pup was placed under a heat lamp to warm, and  $\sim 10$  minutes later returned to the dam. For a detailed description of procedure see Jacobs, 1996 (137).

#### *Brain Extraction and Slice Preparation*

Rats aged P7-38 were anesthetized with pentobarbital (55 mg/kg i.p.) or isoflurane exposure and decapitated for brain removal. Once the brain was removed, it was immediately chilled in sucrose-modified artificial cerebral spinal fluid (aCSF) containing: (in mM) 2.5 KCl, 10  $\text{MgSO}_4$ , 3.4  $\text{CaCl}_2$ , 1.25  $\text{NaH}_2\text{PO}_4$ , 234 sucrose, 10 glucose, and 26  $\text{NaHCO}_3$ . Coronal 400  $\mu\text{m}$  thick slices were cut in modified aCSF with a 1000plus vibratome. Once cut, the slices were placed in an oxygenated *normal* aCSF containing: (in mM) 126 NaCl, 3 KCl, 2  $\text{MgCl}_2$ , 2  $\text{CaCl}_2$ , 1.25  $\text{NaH}_2\text{PO}_4$ , 10 glucose, and 26  $\text{NaHCO}_3$ . The slices remained in this solution at  $34^{\circ}\text{C}$  for 30 to 45 minutes and at room temperature thereafter until placed in the recording chamber.

#### *Electrophysiological Recordings*

Slices were placed in an oxygenated interface chamber with  $34^{\circ}\text{C}$  normal aCSF flowing over the slice. Field potential recordings were made using glass micropipettes (2-8  $\text{M}\Omega$ , 1 M NaCl), placed within superficial layers (II/III)  $\sim 1\text{ mm}$  lateral to the microsulcus in PMR or in homotopic control (unlesioned) cortex. We have previously demonstrated that the PMR is the most sensitive region for epileptiform activity in P1-lesioned cortex (Jacobs et al., 1999). For

extracellular stimulation, a concentric bipolar electrode was placed at the interface of white and gray matter directly beneath the recording site, such that these two electrodes were in a plane orthogonal to the pia. A single current pulse (20  $\mu$ sec long) of varying current intensity (0.30-10 mA, defined as threshold current or 1X) was applied to generate a short latency field potential with a peak negativity of 200  $\mu$ V. To further assess slice health and to estimate intrinsic cortical excitability, a series of increasing stimuli (stimulus intensity protocol) were applied by successively increasing the duration of the pulse (1X, 2X, 4X, 8X, and 16X). Slices were deemed viable if they met two criteria: 1) the short latency response increased in a fashion that was graded with stimulus intensity; and 2) at a stimulus intensity of 16X threshold, the field potential negativity had a peak of at least 0.6 mV. Field potentials were amplified 1000x (AxoClamp 2B, Axon Instruments and FLA-01 amplifier, Cygnus Technologies) and digitized at 5-10 kHz with a Digidata 1322a (Axon Instruments) and recorded to hard drive with Clampex software (Axon Instruments). After five minutes of recordings in normal aCSF, low-Mg<sup>2+</sup> aCSF (normal aCSF without the MgCl<sub>2</sub> added) was applied for the remainder of the experiment (from 80 to 150 minutes). For pharmacological studies in P7-9, malformed and control slices were used. To study the pharmacological mechanism of CRI activity in malformed cortex, drugs were applied three minutes after onset of CRI and washed out after 10 minutes. To study the SLE dynamics in control cortex, cyclothiazide was applied after the fourth SLE burst and washed out after 10 minutes. With our chamber, the solution required 2.5 minutes to reach the slice.

### *Data Analysis*

Spectrograms were created by importing data collected with Clampfit 8.2 (Axon) as gap free data in Matlab (7.9.0, 2009b), using a custom m-file. For this study, spectrograms with a 0.5

Hz frequency resolution were plotted from 0.0 to 25 Hz. Power spectra were generated in Clampfit 8.2 (Axon) for three distinct SLE time periods: the entire SLE (80 secs), the SLE tonic phase (first 10 secs), and the SLE clonic phase (last 20 secs). The spectral properties of CRI activity were sampled (100 secs) at three distinct time points: ‘early’ CRI activity (after first two minutes of continuous activity), pharmacological CRI (after eight minutes into drug application), and ‘late’ CRI activity (after 30 minutes of continuous activity). The duration of SLEs was calculated using the time of the initial large depolarization as the onset and the final clonic burst as the end (noted as not being preceded by another event for 15 seconds).

## Results

### *Characterization of Low-Mg<sup>2+</sup> aCSF-Induced Activity in P12 Cortex*

In agreement with previous observations in cortico-hippocampal slices from newborn rodents (207, 233, 234), low-Mg<sup>2+</sup> aCSF induced spontaneous epileptiform activity in immature neocortex (Fig. 3.1). At P12 in both control (Fig. 3.1A) and PMR (Fig. 3.1B) cortex, the initial form of this activity was discontinuous bursts of seizure-like events (SLEs) (Fig. 3.1C and E), followed by continuous repetitive ictal-like or CRI activity (Fig. 3.1D and F).

The SLE consisted of an initial large amplitude event, followed by a tonic phase (Fig. 1C and E, green arrows) that subsequently evolved into a clonic phase (Fig. 3.1C and E, purple arrows). Frequency analysis of these two components in malformed and control cortex determined that the malformed cortex did not generate a different oscillatory pattern (or power) of either the tonic (Fig. 3.1K) or clonic (Fig. 3.1L) phase compared to control. Power spectrum analysis of the entire SLE event also revealed no differences in the oscillatory pattern (or power)



between control and malformed cortex (Fig. 3.1M). The SLE in both control and malformed cortex had large peaks at ( $\sim 0.1$  Hz).

Spectrograms of SLE and CRI activity in PMR (Fig. 3.1I and J) and control cortex (Fig. 3.1G and H) further demonstrate that the two types of epileptiform-like events were distinctly different in both control and PMR cortex. Spectrograms confirm that SLEs were characterized by continuous bursting, beginning with a large depolarization followed by a high frequency (4 to 10 Hz) tonic (green arrows) phases followed by a low frequency clonic (purple arrows) phase (Fig. 3.1G and I). In contrast, CRI was characterized by periodic activity (Fig. 3.1H and J). At P12, CRI evolved in both control and malformed cortex and consisted of either a single or multiphasic depolarization event that occurred over a range of frequencies 0.1 to 1.5 Hz (Fig. 3.1N). No differences were found between control and malformed P12 cortex in the oscillatory patterns of CRI activity (Fig. 3.1N).

#### *SLE dynamics and the Emergence of CRI in P7-11 Malformed Cortex*

The spectral properties of SLEs generated in malformed and control cortex at P7-11 (data not shown) were not different from events produced in P12-15 cortex, but the percentage of slices generating CRI activity was much less in control cortex (Fig. 3.2H). In the P7-9 malformed cortex, CRI typically emerged after the fifth SLE or  $26.32 \pm 2.87$  minutes (Fig. 3.2G) during low  $Mg^{2+}$  perfusion in 67% of the slices examined (Fig. 2H); whereas only one (out of 28) control slices had CRI emerge (Fig. 3.2H) after the fifth burst or 26.71 minutes.

The proportion of P10-11 malformed animals expressing CRI, 67% ( $n = 9$  slices), remained constant from the P7-9 age group (Fig. 3.2H). Only one slice from the control P10-11 animals exhibited CRI ( $n = 10$  slices). For both P7-9 and P10-11, there were a significantly

higher percentage of slices expressing CRI in the malformed animals than in the control animals (z-test,  $p < 0.01$ ). While the P7-11 PMR cortex was more likely to generate CRI activity, the threshold for SLE generation was not significantly greater in PMR cortex compared to control cortex at either P7-9 or P10-11 (Fig. 3.2G, ns, two-way ANOVA). Additionally, the threshold for SLE generation in both control and PMR cortex did not change from P7-9 to P10-11 (Fig. 3.2G, ns, one-way ANOVA).

The SLE duration has been shown to play a role in the development of persistent epileptiform activity (165). In these studies, the average first SLE duration did not change with age nor were there differences between control and PMR (Fig. 3.3C, ns, two-way ANOVA) cortex. Over the course of an experiment, the SLE duration changed for only the P7 control group (increased) and the P12 PMR group (decreased) (Fig. 3.3D,  $P < 0.05$ , one-way ANOVA). To test whether an increased or decreased SLE duration was predictive of the emergence of CRI in the P7-11 PMR cortex, the SLE durations during experiments with and without CRI were compared (Fig. 3.3G). The mean percent change of SLE duration throughout experiments with and without CRI did not differ significantly (Fig. 3.3G).

The interval between SLE was also measured to test whether the interval between SLEs was predictive of the emergence of CRI. The interval between the first and second SLE did not change with age or between control and PMR cortex (Fig. 3.3E, ns, two-way ANOVA). The interval between SLEs throughout the experiment did not change except for groups PMR P10 and P12 (Fig. 3.3F,  $P < 0.05$ , one-way ANOVA). To determine whether SLE interval predicted the emergence of CRI activity in the P7-11 PMR cortex, the CRI and non-CRI populations were compared (Fig. 3.3H). The change in interval between SLEs was not significantly different between the CRI and Non-CRI P7-11 PMR cortex at any interval examined (Fig. 3.3H).

### *Age Effects on SLE dynamics*

For both malformed and control cortex, the threshold for spontaneous SLEs, but not CRI, increased with age (Fig. 3.2G and I,  $P < 0.05$ , two-way ANOVA). The average time to onset of spontaneous epileptiform activity at P12-15 was  $12.81 \pm 1.08$  minutes and  $11.05 \pm 1.32$  minutes for control and malformed cortex respectively. This was a significantly lower threshold for SLE generation than the threshold for SLE generation in the adult control and malformed cortex (Fig. 3.2G,  $P < 0.05$ , one-way ANOVA). Interestingly, the threshold for SLE generation for both malformed and control cortex at P12-15 was not lower than the threshold at P7-9 or P10-11 (Fig. 3.2G, ns, one-way ANOVA). Threshold for CRI was not different between control and malformed cortex, and did not change with age in either experimental group (Fig. 3.2I, two-way ANOVA). Across all age groups, the average threshold for CRI was  $26.55 \pm 1.51$  minutes and  $26.15 \pm 1.64$  minutes for control and malformed cortex.

The form of spontaneous epileptiform activity in the mature cortex was much different than the form found in immature cortex. As mentioned previously, the threshold for SLE generation was much greater in the mature cortex than the immature cortex. The number of SLE bursts prior to the emergence of CRI activity was also significantly less than in immature cortex (data not shown). Because there were so few SLE bursts and CRI activity emerged in all control and malformed mature tissue, the immature cortex was the focus of the remaining portions of this study.

### *Desensitization of the AMPA receptor contributes to the generation of CRI in P7-11 Malformed Cortex*

In order to determine the role that glutamate receptors play in the generation of CRI in the P9 malformed, but not control, cortex, a number of pharmacological experiments were undertaken. Bath application of pharmacological agents was added to the slice preparation after three minutes of CRI activity. Bath application of the NMDA receptor antagonist APV (50  $\mu$ M) caused a reversible block of the CRI ( $n = 5$  slices), but did not block all spontaneous activity (Fig. 4A). In four of the five slices, SLEs emerged after discontinuing APV application and within three SLEs, CRI reemerged (Fig. 4A). Bath application of the AMPA receptor antagonist DNQX (20  $\mu$ M) caused an irreversible block of CRI in all slices ( $n = 5$  slices), but in all cases SLEs emerged after CRI was ceased (Fig. 3.4B). In three cases, only a single shortened SLE (see insert, Fig. 3.4B) emerged after CRI was ceased. After DNQX was removed from the bath, discrete SLE bursting reemerged, but in all cases CRI did not return within 60 minutes of the washout.

To further explain the role of AMPA receptors in the generation of CRI, cyclothiazide, a pharmacological agent that promotes AMPA receptor desensitization, was bath applied to the P10 control cortex during CRI (Fig. 3.4D). In a previous study, cyclothiazide was shown to increase the duration of the tonic phase of the SLE and, in some cases, induce activity similar to CRI in the hippocampus (165). Bath application of cyclothiazide (100  $\mu$ M) in control cortex after 80 minutes of discrete SLEs induced CRI within five minutes of application in all slices (five of five). To test whether inhibition of AMPA receptor desensitization could prevent generation of CRI in P10 malformed cortex, hypoxic conditions were applied to the slice preparation (a method used to reduce pH to 6.0). These conditions have been shown to (in addition to other effects) inhibit AMPA receptor desensitization (Ihle, 2000). CRI was always (five of five) irreversibly discontinued in hypoxic conditions in malformed cortex (Fig. 3.4C).

### *NKCC1 role in the initiation and persistence of CRI activity in P9 cortex*

During the first postnatal week, cation/Cl<sup>-</sup> cotransporter NKCC1 expression is upregulated and KCC1 is not expressed causing GABAergic responses to be depolarizing (34). Tetanus-evoked SLEs in hippocampal slices bathed in low-Mg<sup>2+</sup> are contingent on GABA<sub>A</sub> receptor-dependent depolarization (99, 161), and excitatory responses to GABA may also play a role in high-K<sup>+</sup> seizure models, at least in immature animals (88, 89, 135, 152). It has been previously shown that NKCC1 expression is prolonged in malformed cortex (265) and the possibility exists that this abnormal expression contributes to the high prevalence of CRI activity in the P9 malformed cortex. To test whether altered Cl<sup>-</sup> transport contributed to the generation of CRI in P7-9 malformed cortex, NKCC1 was blocked with bumetanide (10 μM). Bumetanide has been shown to alter the kinetics of SLEs, but the role it plays in CRI kinetics is unclear (Kilb, 2007). In all slices (four of four) bumetanide had little effect on the presence or frequency of CRI (Fig. 3.5E and 6A) and bumetanide did not induce CRI in P9 control cortex (three of three, data not shown).

### *Group I Metabotropic Glutamate Receptor Role in the Initiation and Persistence of CRI Activity in P9 Cortex*

Epileptiform activity increases the extracellular glutamate concentration (85, 168), which increases the likelihood of extrasynaptic group I mGluR contributing to the shape of epileptiform events. It has already been shown in hippocampal slices that activation of group I mGluRs can prolong SLE burst duration *in vitro* (168, 199) and antagonism of group I mGluRs can decrease the duration of SLEs *in vitro* (168), as well as *in vivo* (176). To test whether group I

metabotropic glutamate receptors played a role in the presence of CRI activity in the P9 malformed cortex, we applied 10  $\mu\text{M}$  MPEP (mGluR5 antagonist) alone and with 300  $\mu\text{M}$  AIDA (mGluR1 antagonist) to CRI activity in P9 malformed cortex (Fig. 3.5C-D). In each case, blocking mGluR5 (Fig. 3.5C) and mGluR1 and 5 (Fig. 3.5D) did not cause CRI activity to cease, nor did it affect the spectral properties of the epileptiform events (Fig. 3.6A). To test whether group I metabotropic glutamate receptors could initiate CRI activity in the P9 control cortex, 10  $\mu\text{M}$  DHPG (group I mGluR agonist) was applied to the bathing solution after the fourth SLE burst. In all experiments (four of four), DHPG did not initiate CRI activity (data not shown).

#### *NR2B-containing NMDA Receptor Role in the Persistence of CRI activity in P9 cortex*

During normal postnatal development, the composition of the NMDA receptor changes from a predominately NR2B subtype expression to a NR2A/NR2B subtype expression. A selective increase in expression of NR2B subunit in dysplastic (but not in non-dysplastic) cortex has been demonstrated in tissue taken from patients with intractable epilepsy (208, 306) and may play a role in hyperexcitable tissue. To test whether the NR2B-containing NMDA receptor specifically plays a role in the persistence of CRI activity in P9 cortex, 10 RO-25-6981 (a selective NR2B-containing NMDA antagonist) was applied to bathing solution (Fig. 3.5F). In contrast to the nonselective NMDA antagonist, APV, that ceased both CRI and SLE activity, RO-25-6981 did not cease CRI activity, nor alter its spectral properties (Fig. 3.5F and 3.6A).

## **Discussion**

We have reported that perfusion with aCSF containing low-Mg<sup>2+</sup> induces epileptiform activity in both control and malformed neocortex at both immature and mature time points. Two distinct types of hypersynchronous activity could be distinguished: 1) Seizure-like events (SLE) occurring in all slices at every age group and 2) continuous repetitive ictal-like (CRI) activity that emerged on P7 in malformed cortex, but not until P12 in control cortex. We have characterized the basic pharmacology of the CRI activity in the P9 malformed cortex and found its presence and spectral properties not to be critically dependent on NKCC1 cation/Cl<sup>-</sup> cotransporter, group I mGluRs, and the NR2B-containing NMDA receptor, but dependent on NMDA and AMPA receptors. The implications of these results for cortical development and epilepsy research will be discussed below.

#### *AMPA Desensitization, SLE Duration, and CRI Generation*

Previous experiments examining the role that inhibition of desensitization in hippocampal AMPA receptors plays in the generation of continuous activity showed that cyclothiazide increases the SLE duration (the tonic period, specifically) and can induce continuous activity (165). In the current study, we find that cyclothiazide induces CRI in immature (P9) control cortex that had been incapable of producing CRI. The effect of cyclothiazide on the duration of the SLE could not be assessed here because in four of the five experiments conducted, CRI begins immediately following the first and only SLE burst after cyclothiazide perfusion (Fig. 3.4D).

Our results suggest that SLE duration does not predict the generation of CRI activity. By examining the percentage change of the SLE duration throughout an experiment, our results demonstrate that neither an increase nor a decrease is predictive of whether CRI will emerge in a

slice. This suggests that the mechanism(s) involved in the perpetuation of SLEs might be separate from the mechanism involved in the generation of CRI activity. However, in this study, the duration of the tonic and clonic phases of the SLE were not examined because of technical difficulties in discerning the transition between the tonic and clonic phases. The possibility exists that the duration of either the clonic or the tonic phase could be predictive of the emergence of CRI activity, but the role they play in the observations made in this study is undetermined.

The role of AMPA receptor desensitization, a phenomenon that occurs within a subsecond range, in shaping epileptogenesis, perpetuation, and termination processes that can occur over tens of seconds, is not clearly understood (127, 217). The excessive high-frequency presynaptic activation during SLEs (164) may result in prolonged and increased extracellular [Glu] transients (168, 278) compared with basal activity. One hypothesis is that desensitization is induced by slowly increasing extracellular [Glu] during SLEs, which progressively decreases the population of functional AMPA receptors. Inhibition of this process may increase the number of functional AMPA receptors capable of participating in SLE burst, possibly aiding in the perpetuation of the SLE burst and contributing to the transition from SLE bursting to CRI. Our data suggests that there may be a greater number of functional AMPA receptors in immature, malformed cortex than in control cortex at P7-11. To date, no one has shown functional or expression alterations of the AMPA receptor in the immature malformed cortex, and previous studies examining the AMPA receptor expression in the adult PMR cortex provide conflicting results. A previous study using *in vitro* autoradiography showed an increase in AMPA receptor binding within and adjacent to the malformation in the adult malformed cortex (319), whereas another study using immunohistochemical staining for AMPA receptor subunits, GluR2 and GluR3, show that they are not changed in the adult malformed cortex (118). The unsilencing of



functional AMPA receptors is an important developmental step during the first postnatal week (12) and an acceleration of this step could contribute to maladaptive plasticity that helps promote the presence of CRI in malformed cortex prior to its presence in control cortex.

#### *P9 PMR Cortex CRI Activity Insensitivity to Pharmacological Manipulation*

Because seizure-like events (SLEs) and continuous repetitive ictal-like (CRI) activity have been shown to increase the extracellular glutamate concentration, extrasynaptic group I metabotropic receptors were expected to play a role in the presence or rhythmicity of CRI activity. Previous studies have shown that application of group I metabotropic glutamate receptor agonist can prolong SLE duration and antagonism of group I mGluRs shortens the duration of the SLE (168, 199). In this study we found that at P9, inhibiting group I mGluRs did not have a significant effect on the presence or spectral properties of CRI activity in PMR cortex, nor did activation of group I mGluRs generate CRI activity in control cortex. These results suggest that once CRI activity is initiated, mGluRs do not play a role in the persistence of CRI activity, but we cannot rule out the possibility that group I mGluRs may play a modulatory role in the generation of epileptiform activity (SLEs) prior to the onset of CRI activity.

#### *Threshold for Spontaneous SLEs and CRI*

In this study we replicated previous results showing that both SLE and CRI can be generated in the immature cortex (206, 234). We also replicated previous studies that show that the immature cortex is more susceptible to spontaneous SLEs than is the mature cortex (301). A surprising finding in this study is that the threshold for SLE generation is not lowest in the P12-15, whereas others have found that threshold to be lowest during the second postnatal week (301)

and some have even found spontaneous epileptiform activity difficult to generate in tissue less than P9 (107, 311). A possible explanation for this is the slight variation in the age groups examined by both Wong, et al. (P4-7 and P13-16) and Vilagi, et al. (P2-5, P8-10, and P15-17) compared to the age groups examined here (P7-9, P10-11, P12-15). The possibility exists that the pre-P7 cortex has a significantly increased threshold for SLE generation compared to older immature cortex. Another possible explanation for these differences is that the ionic concentrations of the aCSF used by Vilagi, et al. and Wong, et al. were different from those used in these experiments. In both previous studies, the KCl concentration was less (1.8 and 2.0 mM) than the concentration used in these experiments (2.5 mM). Additionally, we used a higher CaCl<sub>2</sub> concentration (2 mM) than previous studies (1.2 mM). The increased calcium concentration in our recording aCSF could contribute to an increased driving force of Ca<sup>2+</sup>, especially considering our method for developing seizure-like activity (low-Mg<sup>2+</sup>) increases the conductance of a Ca<sup>2+</sup>-permeable channel (the NMDA receptor).

#### *CRI Activity in the P7-11 PMR Cortex Represents an Accelerated Phenotype?*

In this study, CRI activity emerged in all cortical slices examined after P12 after an average of 28.23 +/-4.32 minutes. At younger time points, epileptiform activity in nearly all control slices from P7 to P11 exhibited SLE discrete bursting for as long as 2.5 hours (data not shown), whereas 67% of PMR slices were capable of generating CRI activity. This is the first finding in the freeze lesion-induced microgyria literature that demonstrates an acceleration of a developmental phenotype. There is extensive literature that demonstrates cellular and subcellular alterations in the malformed cortex that suggests there is a persistence of an immature state in the dysplastic cortex (57, 79, 104, 277). This study suggests a role for altered AMPA receptor

kinetics in P7-11 PMR cortex for the persistence of CRI activity, but this study does not rule out the possibility of other mechanisms associated with the transition for discrete SLE bursting to CRI activity.

Continuous repetitive ictal-like activity has been reported previously as interictal-like activity (or late recurrent interictal-like activity or discharges) (153, 154, 233, 318) in hippocampal, temporal cortex, and cortiohippocampal slices. This classification is misleading because interictal activity is characterized clinically as abnormal EEG events between seizures (274, 303). The CRI activity presented here and previously described in hippocampal slices, better reflect discharge patterns occurring late in status epilepticus than typical interictal activity (172, 177, 302). Traditionally, *in vitro* interictal-like activity is classified based upon the timing of the events, being between ictal-like events (called here: seizure-like events, SLEs). The activity described in this study represents a more rhythmic and persistent form of what is called interictal activity, but fires less frequently and without the characteristics of the tonic and clonic phases of ictal-like bursts. For these reasons, we characterize the late continuous repetitive activity as ictal-like activity.

### *Summary*

In this study we have found fundamental differences in the type of spontaneous epileptiform activity generated in control and malformed immature neocortex. Continuous repetitive ictal-like activity emerges in the malformed cortex as early as P7, but does not emerge in control until P12. We've shown that AMPA receptor kinetics, desensitization specifically,

could play a role in this difference and our results suggest that AMPA receptor function could be enhanced in the immature malformed cortex.

**Figure 3.1.** Type of Activity Induced by Low-Mg<sup>2+</sup> aCSF in P12 Neocortex: **A,B**) Shown is 60 min of a typical experiment from a control (**A**) and malformed (**B**) P12 slice in which the low-Mg<sup>2+</sup> aCSF reached the slice 5 min after the beginning of the trace. **C,E**) SLE bursting arises typically between 6.74 to 16.02 min after the low-Mg<sup>2+</sup> aCSF reaches the slice. **D,F**) CRI typically follows the SLE within 24.48 to 31.44 min. These two types of activity are non-overlapping and distinct from each other. **G-J**) Spectrograms showing change in frequencies over time for a typical experiment in a control (**G,H**) and PMR (**I,J**) slice. Note: The 10-4 Hz frequencies of the tonic phase (Green arrows) and the lower frequency events of the clonic phase (black arrows) and CRI. Mean power spectra occurring during the tonic (**K**) and clonic (**L**) phases of the SLE, the entire SLE (**M**), and CRI (**N**) for control (black) and PMR (red) slices from P12 to 15. Comparison of peaks via t-tests showed that there were no significant differences between control and PMR for the power spectra of these four forms of activity.

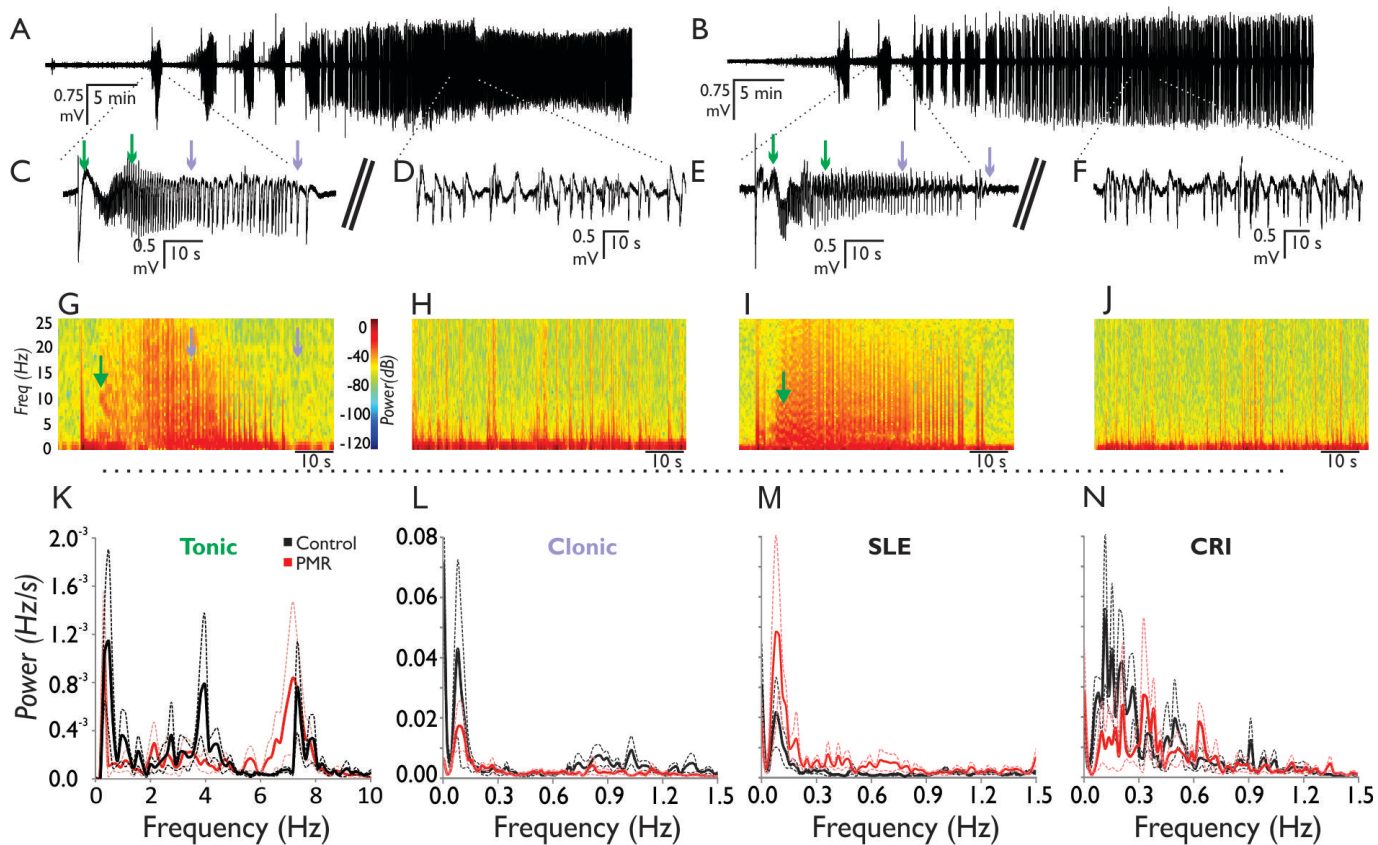


**Figure 3.2** Developmental Changes in Low-Mg<sup>2+</sup> aCSF-induced Epileptiform Activity: **A-F)** Continuous 60 min long field potential recording examples from control (**A-C**) and PMR cortex (**D-F**) at development ages P8, 15, and 30. **G)** The time to the first SLE was not different between control and PMR cortex for any of the age groups, but the time to first SLE did significantly increase with age in both control and PMR cortex (\* denotes significant increases from P7-9, p<0.05, two-way ANOVA). **H)** The percentage of experiments in which CRI emerges after SLE activity is significantly larger in PMR cortex for the P7-9 and P10-11 age groups (p<0.05, z-test). **I)** The time to the onset of CRI is not different between control and PMR cortex and does not change with development (two-way ANOVA, NS). Scale bar in A for A-E; scale bar in C for C & F.

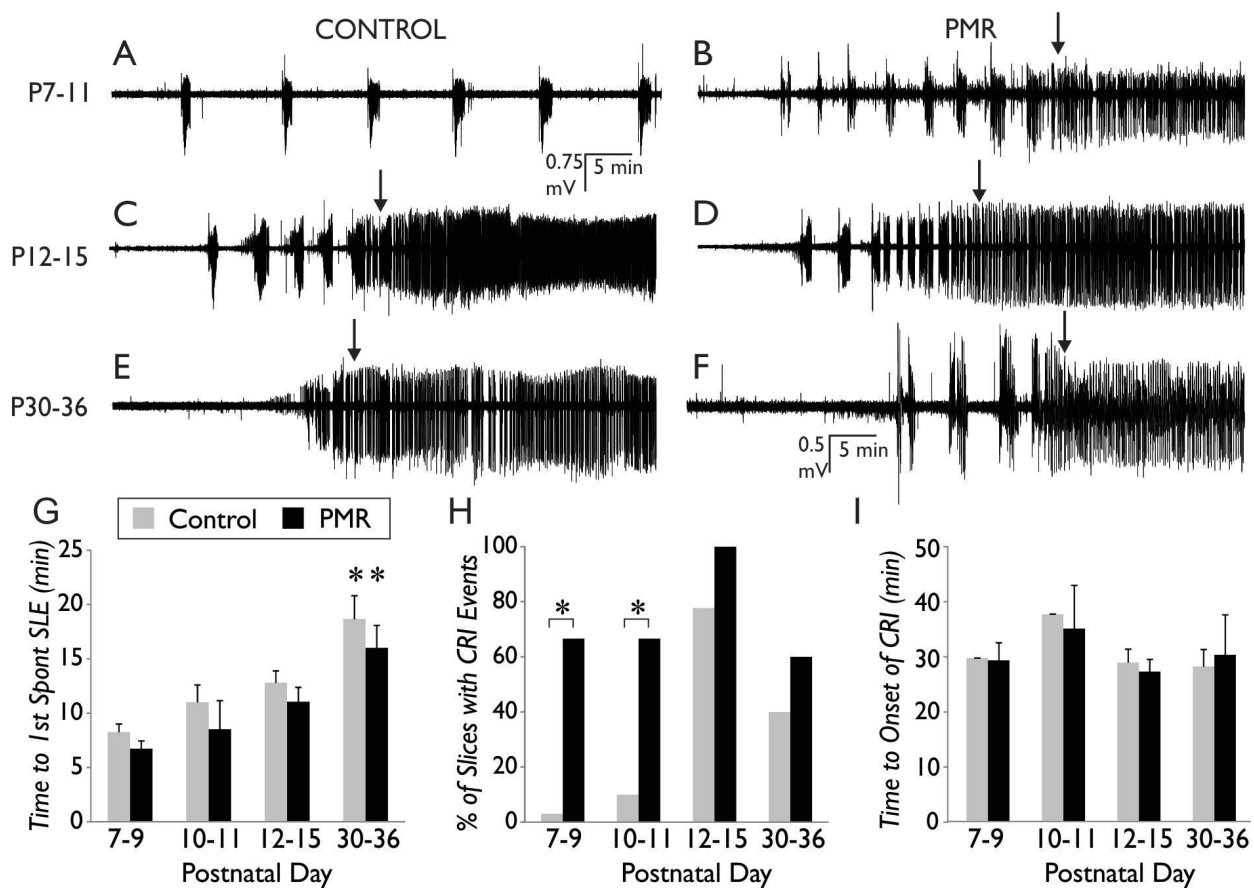




**Figure 3.3** Duration of SLE and Interval Between SLEs Does Not Predict Emergence of CRI: **A-B)** Shown are examples of typical SLE bursts from P10 control (**A**) and PMR (**B**) slices. **C)** The duration of the first spontaneously generated SLE did not vary with age nor were there significant differences between control and PMR. **D)** For all groups except control P7 and PMR P12, SLE duration did not change over the course of the experiment (one-way ANOVA,  $p < 0.05$ ). Note that in the PMR P12-15 group, there were only 4 SLEs that preceded the CRI. **E).** The interval between the first and second SLE did not vary with age nor were there significant differences between control and PMR. **F)** For all groups except PMR P10 & P12, the interval between SLEs did not significantly change over the course of the experiment (one-way ANOVA,  $p < 0.05$ ) **G and H)** Comparison of SLE characteristics in P7-11 PMR slices that generated CRI and did not generate CRI reveal no differences in either the SLE burst duration (**G**) or SLE interval (**H**)

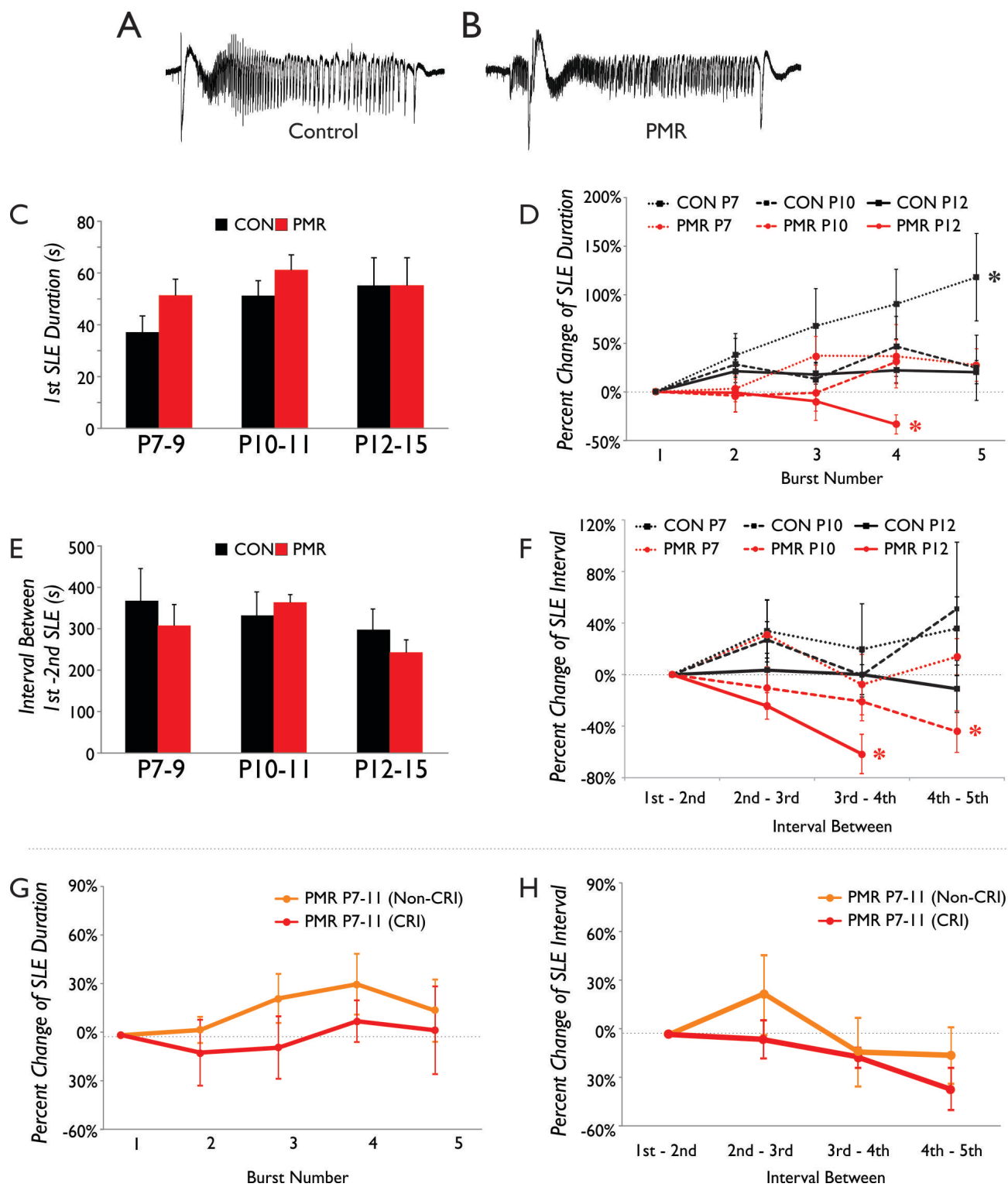


**Figure 3.4** Spontaneous Epileptiform Events in PMR P9 Cortex are Dependent on Glutamatergic Transmission: **A)** Both SLE and CRI were inhibited by 50  $\mu$ M APV. **B)** CRI was abolished, while SLE duration was reduced by 20  $\mu$ M DNQX (Green Arrow – Pre DNQX SLE and Orange Arrow – DNQX SLE). **C)** Low-pH aCSF inhibited CRI and caused reemergence of SLEs. **E)** CRI was induced within a P9 control slice with 100  $\mu$ M cyclothiazide. Time scale in A for A-C, and in D for D-E.

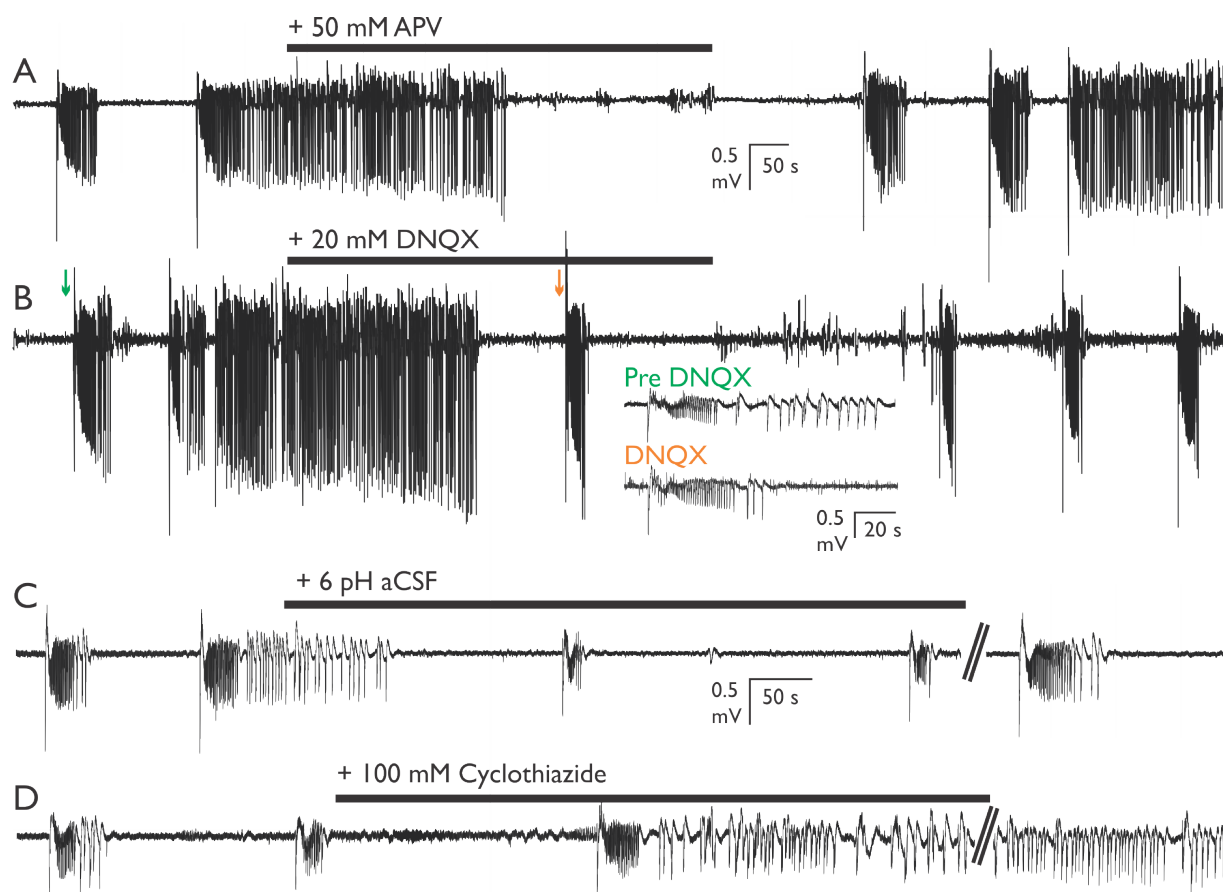


**Figure 3.5** Pharmacological Manipulation of CRI Persistence and Spectral Properties in P9 PMR Cortex: **A and D)** The spectral properties of CRI activity did not change from the onset (A) to the end of the experiment (C). **E and G)** Application of 10  $\mu$ M MPEP (E) as well as 10  $\mu$ M MPEP, 300  $\mu$ M AIDA (G) did not cease or alter the spectral properties of CRI activity. **I and K)** 20  $\mu$ M Bumetanide (I) and 10  $\mu$ M RO25-6981 (K) application also did not cease or alter the spectral properties of CRI activity. **M)** The CRI activity generated by 100  $\mu$ M cyclothiazide in control cortex had similar spectral properties as CRI activity generated in PMR cortex.

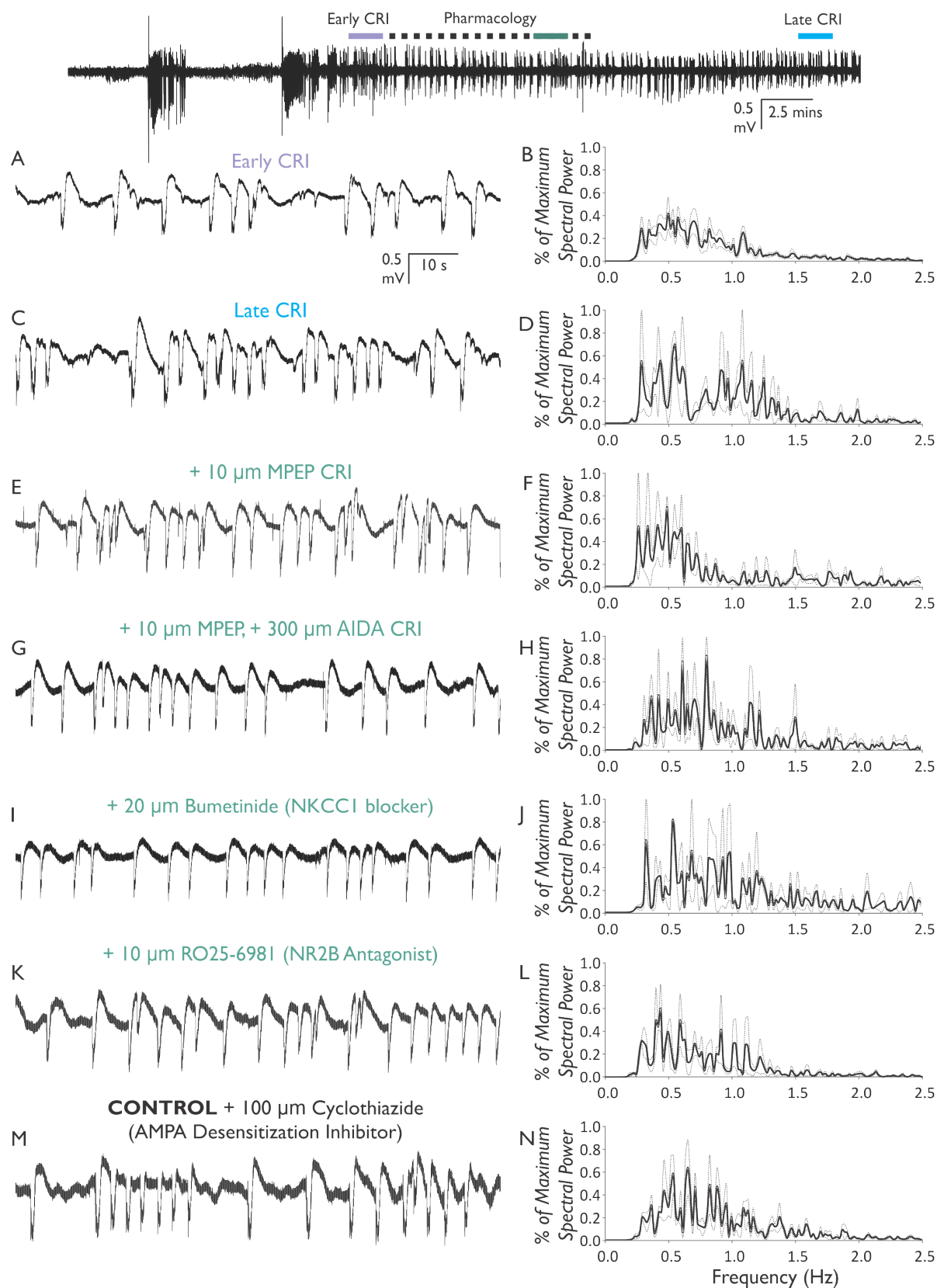
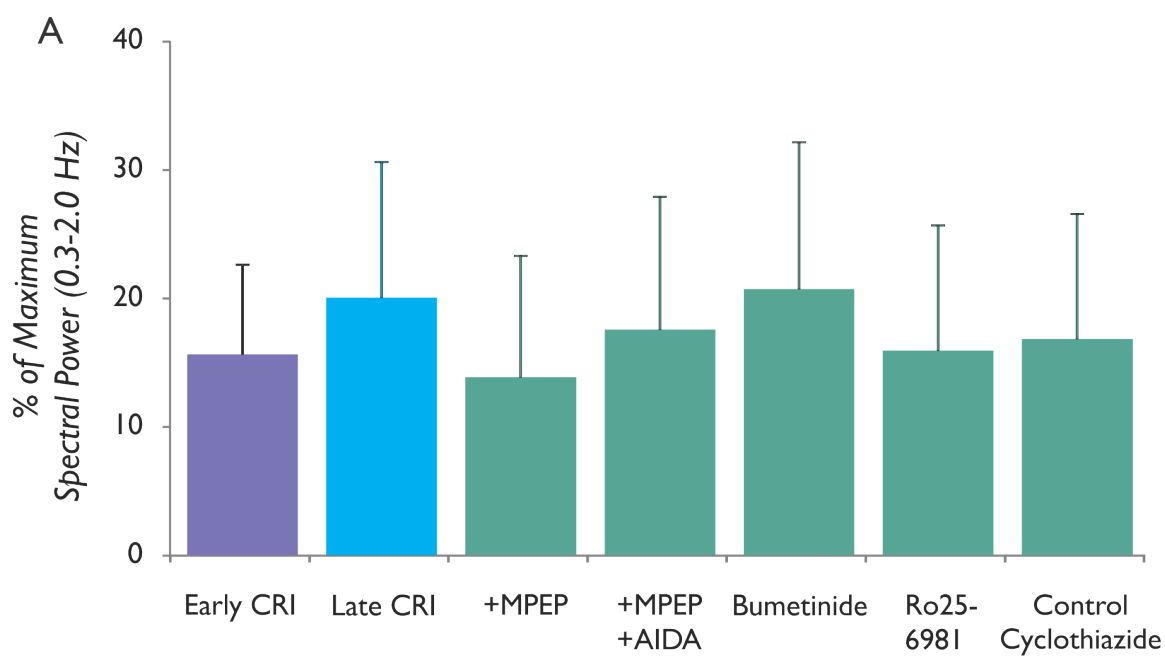
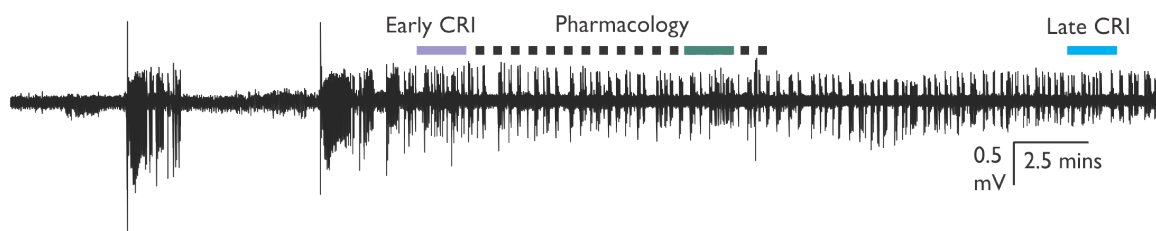


**Figure 3.6** CRI Rhythmicity After Pharmacological Manipulation Does Not Change: **A)** Averaging the spectral power between 0.3 and 2 Hz (characteristic of slow or delta oscillations) for CRI activity reveals no difference in the frequency of oscillations for any pharmacological manipulation done.





## Chapter 4

### Characterization of the Spatial Dynamics of Epileptiform Events in the Cortical Malformation of Microgyria

#### Abstract

Developmental cortical malformations are a major cause of intractable seizures. Some epilepsy patients have seizures initiated within the malformation while in others they are generated by the surrounding cortex. Data in the freeze lesion model of microgyria suggest that the timing of freeze lesion (from P0 to P1) can shift the epileptogenic focus from the malformation to the paramicrogyrial region (PMR). In this study, we investigate whether the timing of the freeze lesion can alter the epileptogenic circuitry of the malformation and surrounding tissue.

Here we use voltage sensitive dye imaging combined with local field potential recordings to identify the spatiotemporal characteristics of the initiation and propagation of epileptiform events generated using low magnesium (low-Mg<sup>2+</sup>) aCSF. We compare these characteristics in the P0-, P1-lesioned and control cortex at two age groups: immature (P9-12) and mature (P28-35).

We find that the epileptogenic focus in the malformed cortex can shift depending on the timing of the lesion, survival age of the cortex, and type of epileptiform event generated. Specifically, we find that the immature, P0-lesioned cortex has an evoked epileptogenic focus

near the malformation whereas the evoked epileptogenic focus in immature, P1-lesioned cortex is more distant from the malformation. In the adult cortex, the spontaneous epileptogenic focus shifts in P1-lesioned cortex to distances very far from the malformation. In addition to the epileptogenic focus, we find that the propagation rate of evoked epileptiform events is increased near the malformation compared to sites distant from the malformation in malformed cortex and sites analogous to the malformation in control cortex.

An essential component of relieving seizures in patients with intractable epilepsy is understanding of what tissue contributes to the epileptogenic focus. This study advances our understanding of how the timing of the creation of an epileptogenic malformation can alter the site of epileptogenesis and other key components of epileptiform activity.

## **Introduction**

Focal cortical malformations caused by erroneous cortical development have been linked to a high number of cases of intractable epilepsy (78, 157, 238). While surgery to remove seizure foci in non-development related epilepsy is typically quite successful, surgical resection of malformations have varying, but a lower rate of success (78, 157, 238). Studies of surgically removed brain tissue from these patients have shown intrinsic epileptogenicity in the dysplastic lesion and surrounding tissue (192, 220). Clinical studies clearly show two distinct populations: some patients that benefit from resection of just the malformation (156) and others that only benefit from resection of the combination of malformation and surrounding tissue (268). The reason for this disparity in surgical results with malformation-associated epilepsy is unknown.

but *in vitro* studies have shown that when malformed cortex is cut from adjacent cortex epileptiform activity persists (78, 157, 238), suggesting there is a type of malformation that can alter the circuitry of cortical areas surrounding the histopathological tissue. A greater understanding of the differences between these malformations is required to know when and how tissue outside the histopathological tissue is altered and how it contributes to hyperexcitability and seizures.

The microgyria produced by postnatal freeze lesioning of neurons at the cortical plate mimics the histopathology and epileptogenicity of a specific type of clinical cortical malformation, polymicrogyria (86, 87, 137, 184). Most investigations into this type of malformation have been conducted by lesioning the cortex on either postnatal (P) day 0 (<24 hours of birth) or P1 (between 24 and 48 hours). Freeze lesioning the cortex *in utero* generates an epileptogenic cortex but the abnormal lamination is absent (280). Freeze lesions after P2 do not replicate the abnormal lamination seen with P0-1 lesions and behavioral deficits associated with perinatal lesions are not present (286, 288). While the histopathology of the malformations created on P0 and P1 are similar, the difference in lesion date may explain conflicting results about the epileptogenicity of the malformation itself. The P1 lesion creates a hyperexcitable area adjacent to the malformation (138), whereas it has been reported that the P0 lesion creates a malformation that is much more hyperexcitable (245). To date there have not been any studies that directly address differences between the epileptogenicity of the P0- and P1- lesioned cortex.

The differences in cortical architecture at P0 and P1 are not entirely clear in rat. Neurons destined for deep layers (layer V and VI) have finished migrating into the cortical plate (CP) by P0 but layer IV neurons may or may not have migrated into the CP. Evidence suggests that in mice, neurons destined for layer IV are present (133) at P0 but there is a possibility that a

population of layer IV neurons are not yet in layer IV at P0 (27). While the exact timing of layer IV migration is not explicitly stated in previous literature, more is known about the thalamocortical innervation of the cortex. Thalamocortical axons begin to penetrate the cortical plate around E18 and are thought to influence migration of cortical plate neurons (160). Functional synapses become detectable around P4 and reliable communication between whiskers and layer IV neurons is present by P12 (266). The role that experience plays in the maturation of the developing cortex is not clearly understood but appears to play a large role in creating functional recurrent excitatory networks (12). Previous work has shown that alterations to layer IV can alter thalamocortical projections (218). Further, the areas adjacent to malformations induced at P1 show an increase in mEPSC frequency in areas adjacent to the malformation, suggesting an increase in excitatory inputs, perhaps from redirection of thalamocortical afferents intended for the lesioned cortex (140). Here we hypothesize that altering the timing of the creation of the malformation by one day could lead to differences in the immature and mature cortical networks within and/or adjacent to the malformation due in part to an alternation in the innervation patterns of thalamocortical afferents.

To test whether the pathophysiological cortical networks created by P0 and P1 lesions were different, optical imaging of neuronal activity using voltage-sensitive dye *in vitro* was used in combination with immunohistochemical analysis of thalamocortical innervation of the dysplastic and surrounding cortex. In order to induce evoked and spontaneous ictal- and interictal-like epileptiform activity, low  $Mg^{2+}$  was omitted from the perfused aCSF. From these studies we found that the site of epileptiform activity initiation and propagation properties depended on both the timing of the induction of the malformation, the survival age of the animal, and whether the event was evoked or spontaneously generated.

## Methods

### *In Vitro Slice Physiology*

Transcranial freeze lesions were made on either P0 (within 3 hours of birth) or P1 (between 30 & 40 hours after birth), above the somatosensory cortex as previously described (Jacobs, 1996a). Two age groups, immature (P10-15) and mature (P28-35), were used for slice physiology. Standard coronal slices through the malformed region and homotopic control cortex were made. Average caudal/rostral position (measured from bregma) was not different between all cortical slices examined (2.08 mm  $\pm$  0.43 for control and 2.15 mm  $\pm$  0.36 for lesioned cortices). The average position of the sulcus (measured from the midline) in both P0 and P1-lesioned cortices was also not different for either immature or mature malformed cortex (immature: 3.88 mm  $\pm$  0.14 for P0 lesions and 3.90 mm  $\pm$  0.28 for P1 lesions – mature: 4.11 mm  $\pm$  0.18 for P0 lesions and 4.30 mm  $\pm$  0.20 for P1 lesions). There was also not a correlation between the sulcus location and the epileptiform initiation site. These slices were stained with voltage-sensitive dye RH-765 for 30-45 minutes prior to recording. The slice was deemed healthy if a 0.02 uV response was elicited from low-threshold stimulation in normal aCSF containing: (in mM) 126 NaCl, 3 KCl, 2 MgCl<sub>2</sub>, 2 CaCl<sub>2</sub>, 1.25 NaH<sub>2</sub>PO<sub>4</sub>, 10 glucose, and 26 NaHCO<sub>3</sub>. To activate cortical responses, either a train of 5 pulses, (each 100  $\mu$ sec long) with 100 ms inter-pulse interval or a single pulse (100  $\mu$ sec long) was applied to deep layers of neocortex. Voltage sensitive dye imaging (VSD) and local field potential (LFP) responses from a silver-chloride electrode placed in the superficial layers was recorded for 3-10 sec. Pre-low Mg<sup>2+</sup> recordings were averaged across three traces and analyzed as a single trace. After this baseline

period, the aCSF was switched to low  $Mg^{2+}$ , which was the same as normal but without the  $MgCl_2$ . Epileptiform activity was typically observed within 5 minutes after beginning the low  $Mg^{2+}$  for immature cortical slices and 15 minutes for mature cortex. All recordings were made in the following 40 min. Local field potential recordings within layer II/III, ~0.5 mm lateral to the microsulcus and in homotopic control cortex were employed to confirm the health of the slice and the presence of evoked and spontaneous epileptiform activity. **VSD:** For VSD absorbance measurements, slices were illuminated with a tungsten-halogen 100-w lamp passed through a band-pass filter (705 +/- 30 nm, Chroma Technology). The transmitted light was passed through a 4X objective and collected with a Wutech H-469IV photodiode array that is part of the Redshirtimaging integrated Neuroplex II imaging system (176  $\mu m$  resolution between diodes). The data were acquired and analyzed using variable normalization with Neuroplex software. On all VSD heat-mapped images, the scale from blue to red is 0% to 100% of the maximal response at each individual diode.

#### *Immunohistochemical and VSD movie overlay*

Post experiment staining for NeuN (Millipore, 1:500) and BisBenzimide (Sigma, 1:1000) was performed on the imaged slices in order to identify laminar boundaries as well as the outline of the microgyral region. The malformation size was found using two measurements: the distance between both cell sparse zones and the distance between where normal lamination discontinues on either side of the malformation. There was no difference in either measurement for P0 and P1 malformations. The central point within the malformation was used as the 0  $\mu m$  point for distances away from the malformation. Photomicrographs of the stained images were overlaid by selected frames (50ms per frame) from variable scaled movies created from the

optical traces obtaining using the Neuroplex software. To create the supplemental movie files, movies created from Neuroplex were aligned with the stained images in Final Cut Pro (Apple) (1 s of real time = 48.7 ms). Anti-vGlut2 (Synaptic Systems, 1:500) was used to image thalamocortical afferents in P12 P0-, P1-lesioned and control cortex.

### *Data Analysis*

Traces from each diode pertaining to Superficial layers (II/III) and Deep layers (V/VI) in distances of 176  $\mu\text{m}$  away (up to 4.094 mm) from the malformation or corresponding distances in control tissue were imported into Excel (Microsoft) for further analysis. Using a custom macro, the traces from each diode were normalized to the largest response of that diode's response. Time to half-height was used to determine the site of initiation and the speed of propagation of epileptiform activity across the tissue. Most statistical tests used either a two-way ANOVA with a Tukey post hoc test or t-test with bonferroni correction. Statistical tests of proportions used a z-test. Statistically significant differences were P values less than 0.05.

## **Results**

### *Size of Cortical Dysplasia Does Not Change Between P0 and P1*

Two measurements showed that the size of the malformation created from P0 and P1 lesions were not different at either survival time point investigated: the distance between cell sparse zones and the beginning of normal lamination (6-layered cortex) on either side of the malformation (Fig. 4.2A, orange arrows). NeuN, BisBenzimide, and Nissl staining in immature cortex shows that the distance between cell sparse zones for P0-lesioned (Fig. 4.3C, NeuN

staining) cortex was  $194.2 \mu\text{m} \pm 21.1$  and P1-lesioned (Fig. 4.3G, NeuN staining) cortex was  $203.4 \mu\text{m} \pm 23.8$ . The distance between the beginning of normal lamination for P0 was  $858.4 \mu\text{m} \pm 38.3$  and for P1 was  $874.3 \mu\text{m} \pm 28.9$ .

*Horizontal Extent of Cortical Response to Stimulation Greater in P0 but Not P1-lesioned Cortex Compared to Control*

The size of the neuronal response to stimulation was different in the three cortices examined prior to low  $\text{Mg}^{2+}$  was examined. In all immature experiments (24 of 24), a cortical column of neurons, extending from the stimulation site to the pia, became activated in response to stimulation (Fig. 4.1A, C, D). Consequently, the average vertical extent of the neuronal response to stimulation was not different between all cortices examined (Fig. 4.2A – dark bars) ( $6.16 \text{ diodes} \pm 0.24$ ,  $5.60 \text{ diodes} \pm 0.37$ ,  $5.33 \text{ diodes} \pm 0.37$  for control, P0-, and P1-lesioned cortices respectively). The horizontal width of the neuronal response (Fig. 4.2A – light bars) was significantly larger in P0-lesioned cortex ( $12.33 \text{ diodes} \pm 1.23$ ) than either P1-lesioned and control cortex ( $8.33 \text{ diodes} \pm 0.85$  and  $8.27 \text{ diodes} \pm 0.36$ , respectively). Both the horizontal and vertical propagation rate of these responses were not different for all cortices examined (Fig. 4.2B).

*Timing of Freeze Lesion Alters Site of Evoked and Spontaneous Epileptogenesis*

Low threshold stimulation of cortical afferents at the layer VI/corpus collosum interface in the presence of low  $\text{Mg}^{2+}$  aCSF would evoke either a small cortical response similar to pre low  $\text{Mg}^{2+}$  response (Fig. 4.1A,C) or an epileptiform event (Fig. 4.1B,D) that was confirmed by local field potential simultaneous recordings (Fig. 4.1A,B, dashed lines). Epileptiform events



could be evoked in all immature slice (24 of 24) and most mature slices (16 of 21). Both single spike and repetitive spike ictal-like events could be evoked though the initial paroxysmal spike (Fig. 4.1B, left, dark portion) was used as the initial epileptiform spike. Spontaneously generated epileptiform activity was also present in most immature (15 of 24) and approximately half of mature slices (12 of 21). There were no differences between experimental groups (P0-1 lesioned or control cortex) in the proportion of slices capable of generating either evoked or spontaneous epileptiform events.

With a 4x objective, voltage sensitive dye imaging provides a spatial recording area of over 4mm (Fig. 4.1C,D) with a resolution of 178  $\mu\text{m}$ . The optical traces from each diode were scaled independently and exported to Excel (Microsoft Office 2010) for analysis or converted into a heat-mapped image (Fig. 4.1E, F) to visualize the spread of the events. Using this technique, the site of initiation of both evoked and spontaneous epileptiform events was assessed for immature and mature cortex using the time to half-height of the optical response for each diode. Figure 4.3 shows two examples of the optical signal for evoked epileptiform events in cortex lesioned at P0 (A-C) and P1 (D-G). These signals show an event that was initiated (arrows) within the malformation (Fig. 4.3A) and far from the malformation (Fig. 4.3E). To test whether there was a difference in the site of initiation of these events, the distance between the stimulation electrode (1 mm from malformation or analogous site in control and shown in Fig. 4.4B,F) and the site of initiation of the event was compared across P0-, P1-lesioned and control cortex. In relation to the stimulation site, epileptiform events in immature, P0-lesioned cortex were evoked, on average, medial (0.29  $\mu\text{m}$ , +/- 0.15) to the stimulation site (near malformation). In contrast, epileptiform events in both P1-lesioned and control immature cortex were evoked lateral to the simulation site (far from malformation) (P1, immature cortex = -0.53  $\mu\text{m}$ , +/- 0.14)

(control, immature cortex =  $-0.29 \mu\text{m}$ ,  $\pm 0.16$ ). The difference between the sites of epileptiform event initiation between P0 and P1 lesioned cortex was significantly different in immature cortex but not in mature cortex ( $P < 0.05$ , two-way ANOVA, post hoc tukey). This was due to a lateral shift in the P0-lesioned, mature cortex initiation site to a site further from the malformation (Fig. 4.4B, bottom).

To further investigate differences in the epileptiform initiation site between P0 and P1, evoked (Fig. 4.5A-C) and spontaneous (Fig. 4.5D-F) epileptiform events in malformed cortex were divided into two groups: those that originated within the malformation (sulcus) (Fig. 4.3A) and those that were initiated outside of the malformation (PMR) (Fig. 4.3D). The sulcus was defined as being  $400 \mu\text{m}$  from the middle of the malformation.

*Evoked & Spontaneous Epileptiform Events in Immature Cortex:* The cumulative probability plot (Fig. 4.5A) of evoked epileptiform events occurring in distances away from the malformation shows that immature, P0-lesioned cortex is more likely to have an evoked epileptiform event near the sulcus than immature, P1-lesioned cortex, and both mature, P0- and P1-lesioned cortex. The proportion of experiments that had evoked epileptiform events initiated near the sulcus was greater in the P0-lesioned, immature cortex (63.6%, 7 of 11) than the P1-lesioned, immature cortex (15.3%, 2 of 13) (Fig. 4.5C). Further, the initiation site of evoked epileptiform events was significantly closer to the sulcus in P0-lesioned ( $0.80 \mu\text{m} \pm 0.23$ ) than P1-lesioned ( $1.53 \mu\text{m} \pm 0.19$ ) cortex (Fig. 4.5B). The majority of initiation sites for spontaneously generated epileptiform events were outside of the sulcus for both the P0- (71%, 5 of 7) and P1-lesioned (75%, 6 of 8) cortex.

### *Evoked & Spontaneous Epileptiform Events in Mature Cortex*

The proportion of slices with evoked epileptiform events originating within the sulcus in P0 and P1-lesioned cortex did not vary significantly in the mature cortex (Fig. 4.5A-C, solid lines). Additionally, the average distance from the sulcus of initiation of evoked events was not significantly different in P0 ( $1.39 \mu\text{m} \pm 0.57$ ) and P1 ( $1.26 \mu\text{m} \pm 0.33$ ) lesioned mature cortex. Spontaneous epileptiform events were generated predominately outside of the sulcus for both P0 and P1-lesioned cortex (P0: 71%, 5 of 7, P1: 100%, 5 of 5) (Fig. 4.5D,F). Interestingly, the proportion of spontaneous epileptiform events generated outside of the malformation in P1-lesioned cortex was significantly greater than that of P0-lesioned cortex (Fig. 4.5D,F) and the site of initiation was significantly further away from the sulcus in P1-lesioned cortex than mature, P0-lesioned cortex and both immature, P0 and P1-lesioned cortex (Fig. 4.5E).

### *Propagation rates increase near the malformation*

An essential component of epileptiform activity is synchrony of neuronal populations and the degree of synchrony among those populations can change the speed that epileptiform events propagate through the cortex. Using the time to half-height of the epileptiform event and the distance between diodes, the propagation rate was found as epileptiform events spread across the diode array.

### *Propagation of Evoked Epileptiform Activity*

In both P0- and P1-lesioned immature cortex, the rate of propagation was faster near the malformation than in distant sites (Fig. 4.6D: P0 – near:  $49.4 \text{ mm/s} \pm 5.1$  far:  $22.2 \text{ mm/s} \pm 2.1$ ; P1 – near:  $31.2 \text{ mm/s} \pm 3.4$  far:  $19.2 \text{ mm/s} \pm 4.3$ ). Examples of this phenomenon can be

seen in Figure 6 A-C which show the epileptiform event at different sites in distances away from the malformation. Interestingly, the speed of propagation was consistent whether the event was initiated within (Fig. 4.6B) or adjacent (Fig. 4.6C) to the sulcus. In both control immature and mature cortex, the rate did not differ at analogous sites (near and far from malformation) (*immature control* - near: 16.4 mm/s, +/- 3.1 far: 20.4 mm/s, +/- 3.1; *mature control* – near: 12.3 mm/s, +/- 1.6 far: 19.1 mm/s, +/-3.9). The propagation rate in mature P0-lesioned and P1-lesioned cortex near the sulcus was not significantly increased compared to more distant sites (*P0* – near: 34.3 mm/s, +/- 5.4 far: 24.3 mm/s, +/- 4.8; *P1* – near: 29.5 mm/s, +/- 2.9 far: 23.2 mm/s, +/- 3.9).

The propagation rate of evoked epileptiform events was fastest in immature cortex close to the sulcus (<1 mm) in P0-lesioned cortex (Fig. 4.6D, dashed orange) and at sites between 1 and 2 mm away from the sulcus in P1-lesioned cortex (Fig. 4.6D, dashed red). The rate of epileptiform event propagation in immature P0- and P1-lesioned cortex was higher than control cortex at distances 0-1 and 1-2 mm from the sulcus (or analogous distances for control) (Fig. 4.6D, dashed lines). At distant sites (2 to 3 mm), the rate of propagation of evoked events for all cortices examined was the same. In general, the propagation rate tended to be lower in mature cortex when compared to immature cortex but at sites closest to the sulcus (0 to 1mm) the rate for P0- and P1-lesioned cortex was significantly higher than control cortex (Fig. 4.6D, solid lines).

#### *Propagation of Spontaneous Epileptiform Activity*

The rate of propagation for spontaneous epileptiform events did not show a preferential increase near the malformation for either P0- or P1-lesioned immature or mature cortex (Fig.

4.6E). For all cortices examined, the propagation of spontaneous epileptiform events did not change as the events propagated across malformed or control cortex. With the exception of P0-lesioned, mature cortex at 1 to 2 mm from sulcus, there was also no difference in the rate at each location between the different experimental groups (Fig. 4.6D).

*vGlut2 immunohistochemical staining is altered in the paramicrogyrial region*

A preferential increase in the rate that evoked but not spontaneous epileptiform activity spreads near the malformation suggests a mechanism unique to evoked epileptiform events. Stimulation of the layer VI, corpus collosum interface activates cortical afferents, among them are thalamocortical afferents. To test whether an increase in thalamocortical synapses were found in or near the malformed cortex, vGlut2 staining was performed in P12 control (Fig. 4.7A), P0-lesioned (Fig. 4.7B), and P1-lesioned (Fig. 4.7C) cortex. In layer II/III, vGlut2 staining was consistently low at sites within, near, and far from the malformation in P0-, P1-lesioned or control cortex (Fig. 4.7D). In layer IV, the site of greatest thalamocortical innervation – an increase in the density of vGlut2 staining was seen in both P0- and P1-lesioned cortex at the distances 400  $\mu\text{m}$  and 2400  $\mu\text{m}$  from the sulcus (Fig. 4.7E). In deep layers, vGlut2 staining was significantly increased in both lesioned cortices at all distances from the sulcus with the exception of the two most distance sites (Fig. 4.7F).

## **Discussion**

### *Summary*

In this study we have shown that the timing of the creation of a cortical malformation can alter the epileptogenic focus on both the immature and mature cortex. Both the sites of initiation of epileptiform events and the propagation of these events are different depending on the timing of the lesion and the survival age of the animal.

#### *Timing of Lesion Changes Epileptogenicity of Resulting Malformed Cortex*

The epileptogenicity of the cortex in and surrounding the malformation formed by freeze lesion has been investigated for nearly 20 years but the date of freeze lesioning has always been typically defined as “within 48hrs of birth”. As confirmed in the current communication, the histopathology of the P0- and P1 lesioned malformed cortex appeared to be similar (compare: P0 - Redecker, 2000 Fig. 1C (242) and P1 – Jacobs, 1999 Fig. 4B (138)). This is in contrast to the resulting cortex from *in utero* (280) and P5 (286, 288) freeze lesions which are dramatically different for the typical 4-layered malformation caused by P0 and P1 freeze lesion. In contrast to the similarity in the histopathology of malformations created within 48 hours of birth, there is existing literature that suggests there are differences in the electrophysiopathology of the two malformations. Jacobs, et al. reported that in P1-lesioned animals the epileptogenic focus is adjacent to the malformation and that epileptiform activity persists in the adjacent mature cortex even after the malformation is mechanically separated (138). These results are in contrast to a study conducted by Redecker, et al. which demonstrated that in the P0-lesioned adult animal the epileptogenic focus of nearly 100% of epileptiform activity is generated within the malformation itself (245). Our study replicates Redecker’s finding that the malformation generated from a P0-lesion is more epileptogenic (i.e. is the initiation site of the majority epileptiform events) than the surrounding tissue but only in the immature, not mature, malformed cortex. One possible

explanation for the conflicting results in the mature cortex could be that in the current study only the initial epileptiform event of the typical low  $Mg^{2+}$  seizure-like event was assessed not the 4-10 Hz oscillating responses described by Wu, et al (313). When we assessed these oscillatory events that were not the initial depolarized spike, the initiation site of epileptiform events in the immature, P0-lesioned cortex became less focused (data not shown) in agreement with previous studies (17, 313). Another possible explanation for these differences could be the method of analysis used to determine the site of initiation of the epileptiform event. Redecker, et al used the first diode to reach its max amplitude as the site of initiation but others (185) have shown that the time to  $\frac{1}{2}$  amplitude is a better assessment of activation because a location with higher signal amplitude (also higher signal-to-noise ratio) may reach threshold earlier, even though its onset time was later. Finally, another possible reason why our findings were different might be due to species-specific alterations, as Redecker used wistar and our group has used Sprague-Dawleys.

*Possible mechanisms explaining epileptogenic focus shift in P0- and P1-lesioned animals*

It was our hypothesis that the difference in epileptogenic foci would be due to the differences in innervation patterning of the P0- and P1-lesioned cortex because of the possible survival of layer IV neurons in the P0-lesioned cortex. To test this hypothesis, we stained for the vesicular glutamate transporter 2, vGlut2, a reliable marker for identifying and discriminating thalamic terminals in the adult and developing neocortex (210). While we did find that both lesioned cortices had greater thalamic terminal density in the deep layers than control cortex, no differences between the density of thalamic terminals in P0- and P1-lesioned cortices were observed. Though this does not rule out the possibility of differences in number of location of

functional innervations of thalamic afferents, it suggests that other mechanisms are responsible for the differences between P0- and P1- lesioned cortices described here.

An alternate explanation for the differences in the P0- and P1-lesioned cortical epileptogenic foci is the differential expression of both Cl<sup>-</sup> transporters that set the [Cl<sup>-</sup>]<sub>i</sub> and dictate whether activation of the GABA<sub>A</sub> receptor is depolarizing or hyperpolarizing. During development the NKCC1 cotransporter is down regulated and the NCC2 is upregulated, this transition changes GABAergic responses from depolarizing to hyperpolarizing (33, 34). In the P0-induced malformation but not adjacent cortex, it has been shown that NKCC1 mRNA expression is elevated and NCC2 mRNA expression is depressed (265). This finding suggests that depolarizing GABAergic responses may persist in the malformation but not surrounding cortex – creating a more epileptogenic malformation. Data of the developmental expression of NCC2 and NKCC1 in the P1-lesioned cortex does not exist but the possibility exists that the timing of the insult could differentially effect Cl<sup>-</sup> cotransporter expression.

Another possible explanation for the differences in the epileptogenic foci described in this study is that the timing of the lesions differentially induces cell death in different interneuronal populations resulting in the alteration of the inhibitory circuitry. Neocortical interneurons do not follow the same inside-outside migration that pyramidal neurons follow so the birthday of interneurons does not predict the final cortical laminar position (126, 203). Both medial ganglionic eminence - MGE: mostly parvalbumin and somatostatin staining interneurons (95) - and caudal ganglionic eminence – CGE: mainly vasoactivity intestinal peptide (VIP) staining interneurons (203) - derived interneurons migrate tangentially through the superficial marginal zone (mz) and ventricular zone (vz) during perinatal days, E18 to P4 (202). The positioning of these interneurons around the timing of our freeze lesion (P0 and P1) has been not



explicitly studied but the possibility exists, because of the timing of migration, that lesions at P0 and P1 could differentially affect different subpopulations of interneurons.

### *Evoked vs. Spontaneous Epileptiform Events*

Evoked epileptiform events can be considered a hyperactivation of the normal sensory-evoked event that begins in the cortical sensory representation of the stimulus and propagates into a larger area (37, 314). Spontaneous epileptiform events have been proposed to be generated from either an intrinsic ‘pacemaker’ cell type (IB neurons) or hyperexcitable cell groups (66, 117). How different the mechanisms of initiation of these two different types of epileptiform events are is not entirely clear but our data suggests that different epileptiform event foci can exist for evoked and spontaneous events. This suggests that separate mechanisms for the generation of spontaneous and evoked epileptiform exist. We find that in the immature, P0-induced malformed cortex there is an epileptogenic focus near the malformation for evoked but not spontaneous epileptiform events. This focus disappears in the mature, P0-induced malformed cortex but an epileptogenic focus far from the malformation emerges for spontaneous but not evoked epileptiform events in the mature, P1-induced malformed cortex.

We also find that the propagation rate of evoked, but not spontaneous, epileptiform activity is significantly increased in malformed cortex near the malformation. The mechanism underlying the difference between the propagation rate of these two epileptiform events is unknown but stimulation to cortical afferents appears to activate a synchronizing factor in both P0- and P1- lesioned cortex that is not activated during the initiation and spread of spontaneous epileptiform events. It has been proposed that feed forward inhibition directly contributes to the propagation rate of epileptiform activity and it has been shown that a decrease in feedforward

inhibition dramatically increases the speed of epileptiform activity propagation (292).

Interestingly, an autoradiography study has shown decreased binding to GABA receptors in the areas immediately surrounding the malformation which, together with our findings, suggests that there could be a reduction in the inhibitory network near the malformation (319).

#### *Developmental Changes of the Epileptiform Event Focus*

It has previously been shown before that epileptiform activity can be preferentially generated from a small number of sites in the unlesioned cortex both *in vitro* (294) and *in vivo* (201). The initiation sites in these studies were not correlated to either a malformation, specific cortical laminae (295) or cortical region (201) and therefore could not easily be studied developmentally. Redecker, et al found that the epileptiform event initiation site occurs predominately within the superficial layers of the malformation but only in the adult cortex (244). To our knowledge no one has studied whether epileptogenic foci, or hot spots, in *in vitro* slice preparations, can change with development. We did not have the capability to test whether the epileptogenic foci in individual cortices changed over a period of weeks. We did find that the epileptogenic foci malformation bias of evoked epileptiform events in immature, P0-lesioned cortex shifted in the mature, P0-lesioned cortex and spontaneous epileptiform events initiation PMR bias of P1-lesioned, mature evolved from the moderately PMR bias of the immature, P1-lesioned cortex. Our findings suggest that in addition to the timing of the creation of the malformation affecting epileptogenic foci, the developmental age of the cortex will also affect the epileptogenic foci.

**Figure 4.1** Voltage-sensitive Dyes were Used to Assess Neuronal Network Activity for Distances of Over Four mm: **A-B**) Shown are typical examples of local field potentials (lower, dotted lines) and optical signals (upper, solid lines) for a non-epileptiform (normal) (**A**, black) and an epileptiform (**B**, red) response to stimulation. The initial epileptiform event (light blue shaded area) was followed by smaller repetitive events (dark blue shaded area). **C-D**) Shown are responses at individual diodes for the 464 diode array, overlaid on the image of the slice as seen during the experiment for recordings of normal (**C**) and epileptiform (**D**) events. The stimulating electrode appears black in these images and demonstrates the site of stimulation at the layer VI/white matter border. **E-F**) Conversion of the optical signal to a color-coded heat-map (red = depolarization) shows the spatial spread of the peak response (designated by asterisks in **A** and **B**) for normal (**E**) and epileptiform (**F**) events shown in **C** and **D**, respectively.

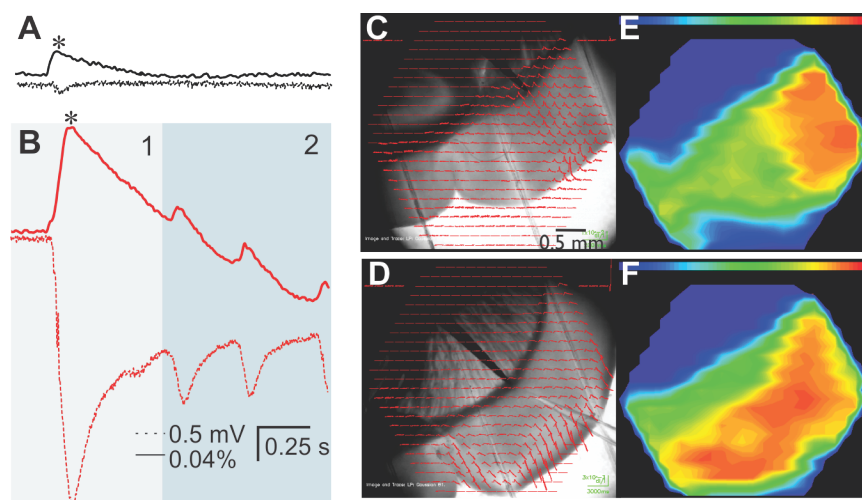


**Figure 4.2** Spatiotemporal Characteristics of Evoked Responses Prior to Low-Mg<sup>2+</sup> in PMR and Control Immature Cortex: Three neuronal responses to stimulation were averaged in order to determine the extent and propagation rate of the average neuronal responses. **A)** The horizontal and vertical extent of the neuronal response to stimulation of the white-grey matter interface, with a significant increase in horizontal extent for P0 lesioned cortex compared to P1-lesioned and control cortex (\*, P < 0.05, 1-way ANOVA, tukey post hoc). **B)** The propagation rate of the neuronal responses in both the vertical and horizontal directions, no differences found between any of the groups.

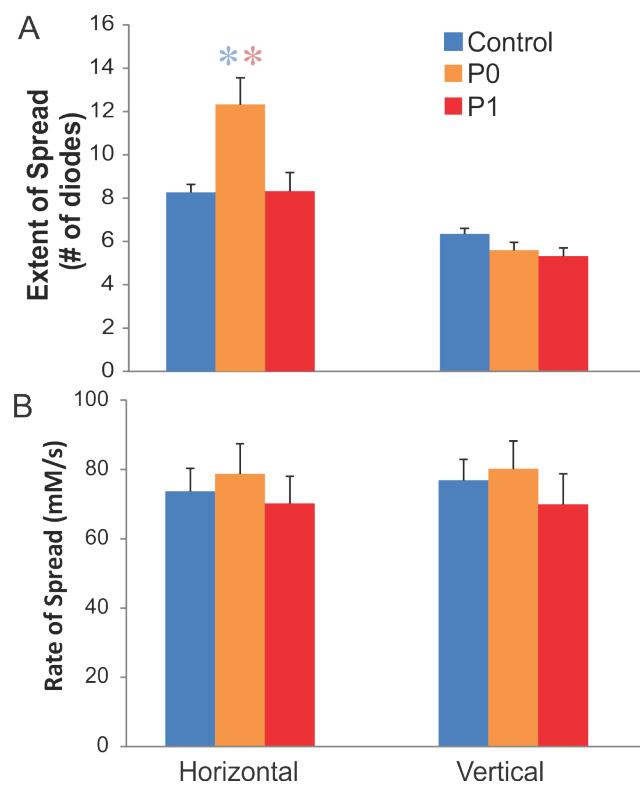


**Figure 4.3** Examples of MG- (A-C) and PMR-initiated (D-F) Epileptiform Activity: **A)** Successive heat-map images (30 ms per frame) of epileptiform activity in a slice in which the malformation was induced at P0. Red colors indicate highest level of depolarization. Asterisk indicates time of stimulation. Black arrow indicates frame showing initiation of epileptiform activity. **B)** Frame indicated by arrow in A is overlaid on the image of the slice, as seen at the time of recording. Stimulating electrode at border of layer VI and white matter appears black in image. **C)** Same slice as that shown in B, with Neun staining. **D)** Heat-map images of epileptiform activity in a slice in which the malformation was induced at P1. **E)** Frame indicated by arrow in D is overlaid on the image of the slice. **F)** Same slice as that shown in E, with NeuN staining

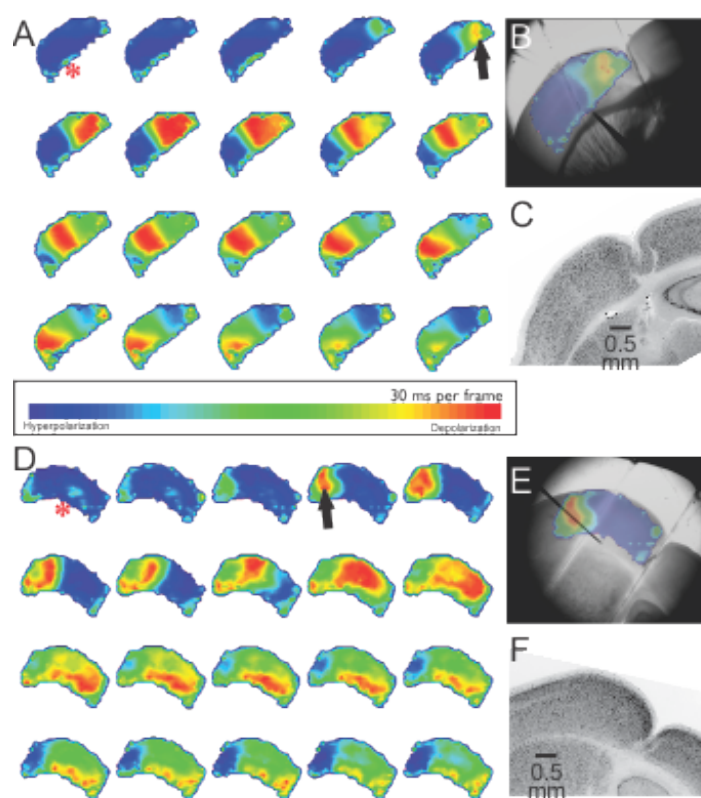




**Figure 4.4** Influence of Malformation Induction Timing on Evoked Epileptiform Activity

Initiation Site: **A)** Example of a NeuN-stained slice from a P0-lesioned rat after survival to P12. The stimulating electrode was located ~ 1 mm to the sulcus. The distance from the stimulation site to the initiation of evoked epileptiform activity was then measured, with positive numbers reflecting initiation sites medial to the stimulation and negative numbers reflecting lateral initiation sites. The dotted hexagon indicates the dimensions of the photodiode array. Gray dashed lines on either side of the sulcus indicate extent of the malformed region, used in subsequent calculations. **B)** For measurements from slices of immature rats, the initiation site was medial to the stimulation site in P0- and lateral to it in P1-lesioned cortex, with a significant difference between the two (\*,  $p < 0.05$ , 1-way ANOVA, Tukey post hoc). In mature cortex the difference between these groups was no longer significant.

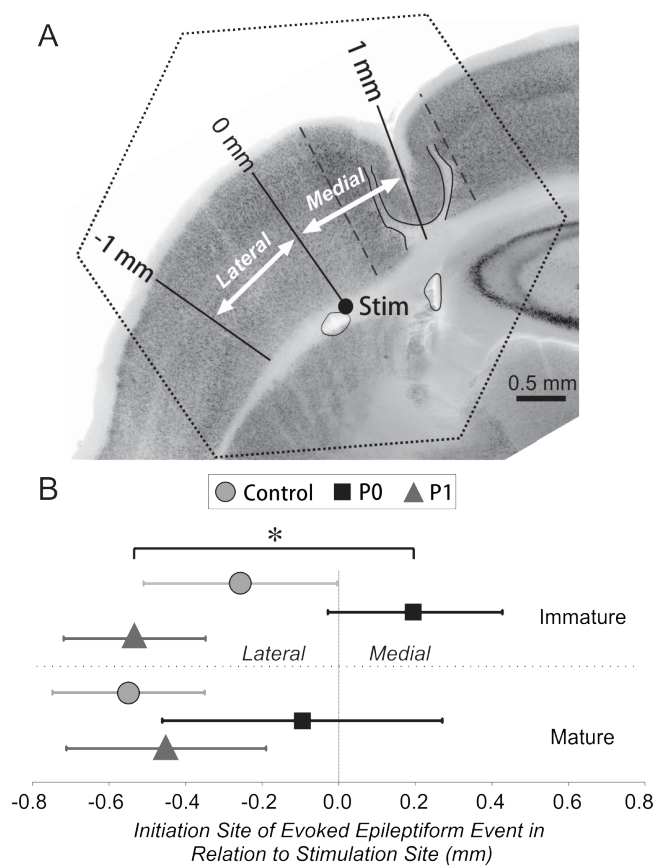


**Figure 4.5** The Location of Epileptiform Activity Initiation Site Relative to the Induced Sulcus Varies Depending on the Timing of Malformation Induction: **A-C)** Timing of malformation induction affects initiation site of evoked epileptiform activity for immature survival ages. **A)** Shown are cumulative probability plots for the distance between the sulcus and evoked epileptiform initiation site in P0- (orange) and P1-lesioned (red) cortex for immature (dashed) and mature survival times. **B)** The mean distance of evoked epileptiform activation site from sulcus is significantly farther for P1- relative to P0-lesioned cortex for immature survival times (\* =  $p < 0.05$ , t-test with Bonferroni correction). **C)** The percentage of events evoked within the malformation (green) or outside of it (purple) are shown for immature (shaded) and mature (solid) survival ages. For slices from P0-lesioned cortex, most epileptiform events were evoked within the microgyrus at immature survival ages. For slices from P1-lesioned cortex, most epileptiform events, and significantly more than for P0-lesioned cortex, were evoked within the PMR at immature survival ages (\* =  $p < 0.05$ , z-test). **D)** Shown are cumulative probability plots for spontaneous epileptiform activity. **E)** The mean distance of the initiation site of spontaneous epileptiform activity is significantly farther from the sulcus for cortex lesioned on P1 surviving to mature ages relative to both immature ages and P0-lesioned cortex at any age (\* =  $p < 0.05$ , t-test with Bonferroni correction). **F)** The percentage of spontaneous epileptiform events initiated with the MG was significantly more for P0- than P1-lesioned cortex at mature survival ages (\* =  $p < 0.05$ , z-test).

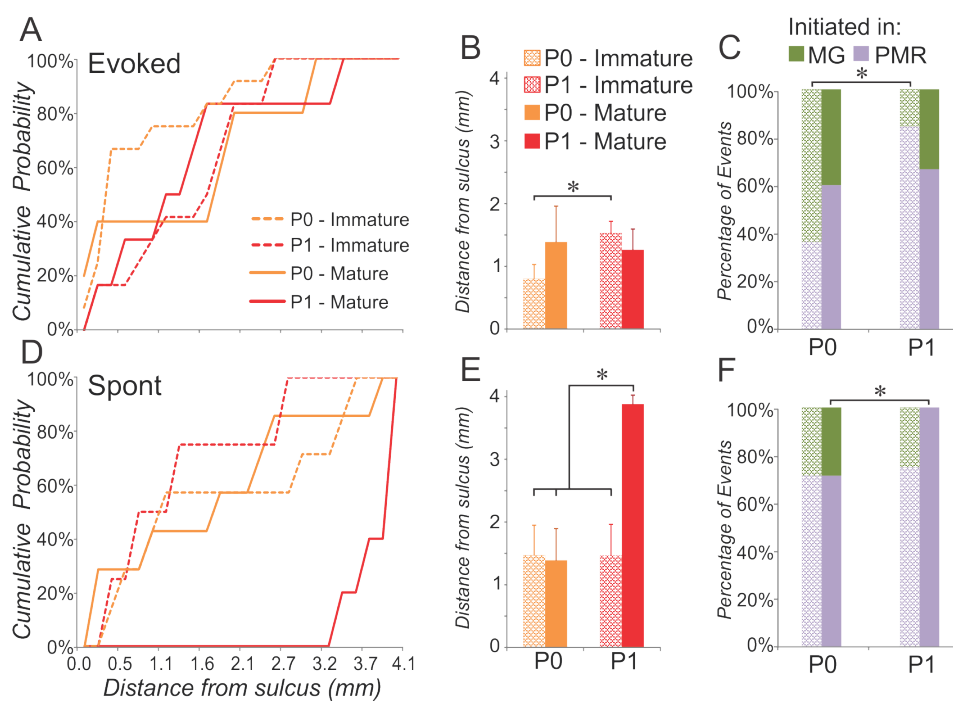


**Figure 4.6** The Propagation Rate of Evoked Epileptiform Activity is Faster Near the Malformation: **A-C)** Examples of the optical responses within superficial cortical layers for various distances from the sulcus (color-coded, mean lateral distance of sulcus in all freeze lesions was used for control distance 0). **D-E)** The time difference between responses at adjacent diodes was calculated at half-peak and averaged for all diodes within 1 mm blocks. Activity was faster at sites up to 2 mm from the sulcus compared to more distant sites for evoked epileptiform activity from both P0- and P1-lesioned cortex at all survival ages ( $*=p<0.05$ , 1-way ANOVA, Tukey post-hoc). For spontaneous epileptiform activity, only the P0-lesioned cortex showed an increased rate at mature survival ages, for the region adjacent to the malformation, compared to more distant sites ( $*=p<0.05$ , 1-way ANOVA, Tukey post-hoc).

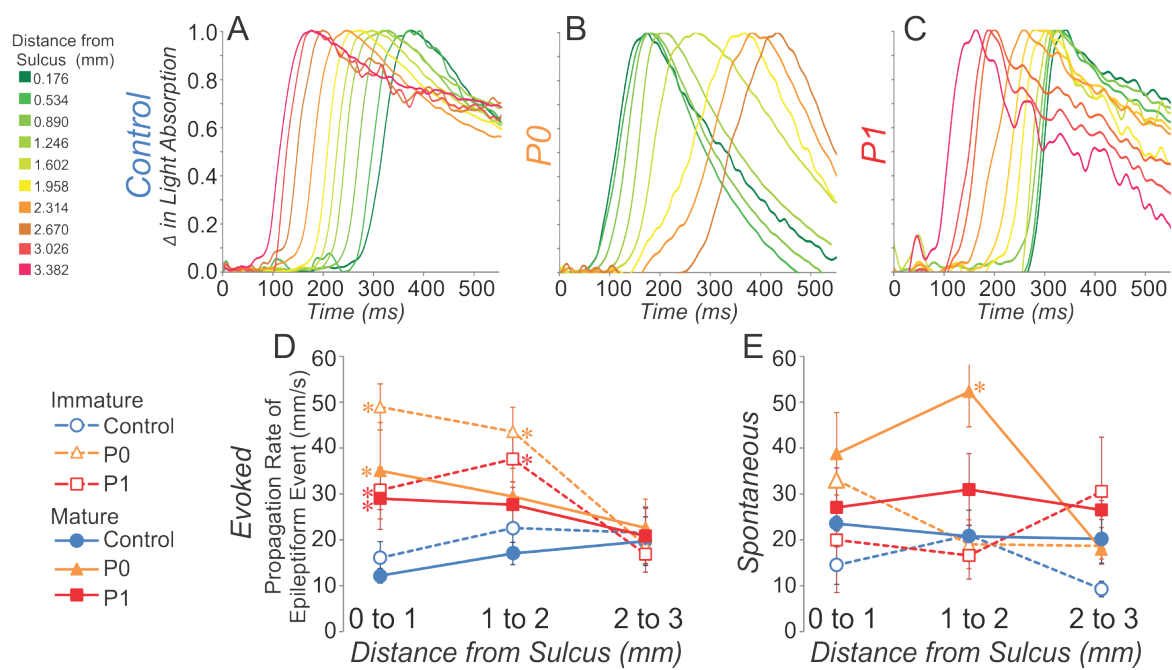
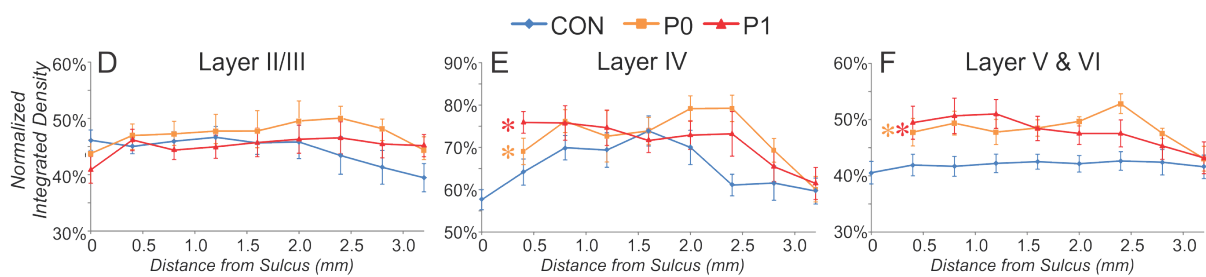
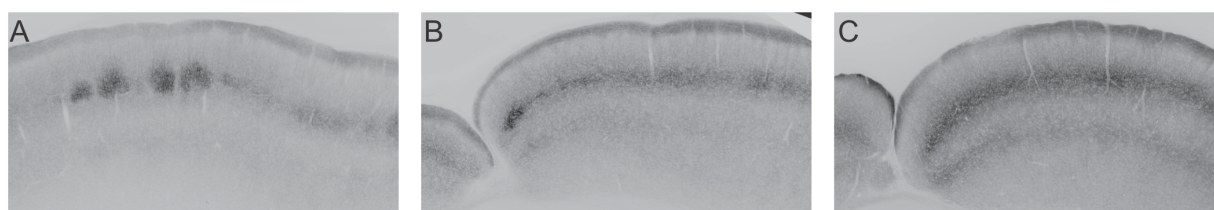


**Figure 4.7** Density of vGlut2 Immunohistochemical Staining is Higher in PMR Cortex than in Control for Middle and Deep Layers. **A-C)** Examples of vGlut2 staining for control (A) and P0- (B) P1-lesioned (C) cortex. **D-F)** The density of vGlut2 staining was integrated within 0.4 mm wide bins within the following layers determined by depth from pia: superficial (D, 150-350  $\mu\text{m}$ ); middle (E, 350-650  $\mu\text{m}$ ); and deep (F, 750-1250  $\mu\text{m}$ ). Both lesion groups were showed significantly greater vGlut2 staining than control (\* =  $p < 0.05$ , 2-way ANOVA).





## Chapter 5

### General Discussion

Decades of epilepsy treatment and research have focused on the treatment of seizures. Despite great advances in the diagnosis and treatment of epilepsy, neocortical hyperexcitability in some patients cannot be treated with anti-epilepsy drugs. Recent studies suggest that complex, complementary mechanisms of hyperexcitability likely explain why current anti-epilepsy drug treatments are ineffective for these patients (186, 198). The experiments described here focus on the characterization of the pre-epileptogenesis period because anti-epilepsy drug treatment for patients with intractable epilepsy may only be possible with the prevention of the onset of seizures. The results of these studies suggest that, in addition to studying the mechanisms of epileptogenesis, research should be done on the mechanisms associated with the development of seizure susceptibility. This final chapter will discuss the implications and limitations of the findings contained in these studies.

#### *Low Mg<sup>2+</sup> Model*

An essential component of the experiments reviewed in this dissertation is the utilization of low Mg<sup>2+</sup> aCSF to reliably generate epileptogenic conditions in both malformed and control cortex. Although the freeze-lesioned cortex is capable of generating evoked interictal-like epileptiform events, spontaneous ictal-like epileptiform events have not been recorded (137, 260). Utilizing low Mg<sup>2+</sup> aCSF enables us to test how ictal-like activity manifests itself in

malformed cortex. As previously described in chapter 2, we believe that low  $Mg^{2+}$  represents a potential ‘second hit’ that is akin to hyperthermia-induced seizures in patients. Low  $Mg^{2+}$  aCSF was used in this study because the form of epileptiform activity it generates is similar to clinical form. However, the author recognizes that the model is not an all-inclusive representation of *in vivo* seizures. Evidence suggests that the kindling method may affect the susceptibility for seizures in the freeze lesion microgyria model. Malformed animals are more susceptible to hyperthermia-induced seizures than control animals, but are not more susceptible to seizures induced by bicuculline injections (151, 260).

The seizure-like events (SLEs) described in chapter 4 are near identical to the EEG recordings of tonic-clonic seizures (see review (196)), but with some caveats. The ictal-like activity generated in the low  $Mg^{2+}$  model is unlike other *in vitro* methods of generating epileptiform activity (i.e. 5-AP, bicuculline application) because inhibitory networks are functional. This results in significantly slower propagation speeds, presumably because inhibitory networks are left functional, and perhaps even enhanced. Impaired inhibitory networks near the malformation could explain the propagation rate increases that were reported in chapter 4. Whether the low  $Mg^{2+}$  generated ictal-like events uncovered a characteristic of all propagating epileptiform events in malformed cortex is uncertain. However, the study reviewed in chapter 4 serves as the first example of how a developmental cortical malformation can cause an increase the propagation rate of evoked epileptiform activity near but not far from the malformation. Further studies in the freeze lesion model utilizing other methods of generating seizure-like events must be done to understand whether the propagation rate increases reported here are representative of other seizure models. From a clinical prospective, in addition to reporting initiating sites of seizures, clinical studies should also assess the rate of propagation of

epileptiform events near and around malformations because this information may better guide surgical resection of the epileptogenic zone.

*Dissertation Findings Emphasize Importance of Developmental Timing*

The studies reviewed in this dissertation, particularly chapter 4, highlight the importance of reexamining previous studies and questioning discrepancies in existing published results. The epileptogenicity of polymicrogyria has been modeled in the rat for nearly 25 years by freeze lesioning the somatosensory cortex *around postnatal day zero and one*. Each year research groups utilizing this model publish results using different lesion dates and make the assumption that the malformed cortex resulting from a P0 and P1 lesion is similar. Chapter 4 demonstrates that the timing of the lesion, even within the first 48 hours after birth, clearly can alter the neuronal networks near and surrounding the malformation created by freeze lesion. The results in chapter 4 highlight the importance of being mindful of the timing of the lesion and will hopefully inspire more targeted experiments and greater caution in extending conclusions on the P0-lesioned cortex to the P1-lesioned cortex and vice versa.

In addition to highlighting the importance of the timing of the freeze lesion, this study also highlights the difference between studying mechanisms associated with epileptiform activity and the mechanisms associated with the development of epileptiform activity. In an *in vitro* model of acquired epileptogenesis that does not exhibit spontaneous seizures (151), one must ask whether the model is most useful for studying the mechanisms associated with the generation of an epileptogenic cortex than the mechanisms of epileptiform activity. Study of acquired epileptiform activity assumes that the brain has already acquired the capacity to become epileptogenic. Research on mechanisms of epileptogenesis following kindling is important for

the development of new anti-epilepsy drugs, but is not as useful for understanding how the brain becomes susceptible to epileptiform activity. A greater understanding of the latter is essential for caring for cortical malformation patients with intractable epilepsy. It is unclear whether the alterations to the cellular, subcellular, and network characteristics prior to epileptogenesis are equally as important as the alterations found in the epileptogenic brain (187). A goal of this study was to characterize the susceptibility of the malformed cortex prior to the time that cortex acquires innate epileptogenicity. We found that the malformed cortex is more susceptible to epileptiform activity as early as P7 and the possibility exists that malformed cortex could be more susceptible even earlier. Future studies should be designed to determine if the susceptibility begins nearly instantaneously after the freeze lesion insult, and whether there is a compound effect of multiple, complimentary epileptogenic mechanisms prior to the onset of epileptogenesis.

#### *Network Activity Recording and Future Studies*

The studies contained in this dissertation examine the cooperative actions of many neurons. Local field potentials and voltage sensitive dye imaging were used to compare the network activity of the malformed and control cortex. Local field potential recordings have been an essential tool in the study of both *in vivo* and *in vitro* cortical oscillations (including epileptiform activity) for the last three decades (149, 200, 239, 262). This is because the recordings relate the sum of all suprathreshold activity from many neurons surrounding a recording electrode (200). Interictal-like and ictal-like events are the result of near synchronous activation and this activation can be clearly identified with local field potential recordings. However, because of the nature of the local field potential signal, the spatial characteristics of a

network event cannot be located without complicated current-source density analysis (2, 211). In addition to the spatial limitation, local field potential recordings reflect suprathreshold activity and do a poor job of reflecting subthreshold activity. Subthreshold activity has been shown to play a large role in cortical oscillations as well as other synaptic communication (230, 290). Because of these limitations, local field potential recordings were utilized as a binary device, providing a method to determine whether an epileptiform event occurred rather than a method to determine the spatiotemporal identity of epileptiform activity.

Voltage sensitive dye imaging was used to gain a greater understanding of the spatiotemporal nature of epileptiform signals. The initiation of epileptiform activity, a point of emphasis in chapter 4, is best determined by the first cells to activate, not the first cells to reach maximum excitation. Voltage sensitive dye imaging allows for recording of subthreshold fluctuations and provides good spatiotemporal resolution of the epileptiform events (312, 313). However, while voltage sensitive dye imaging provides good spatial resolution of neuronal activity, the actual resolution of the technique is dependent on the imaging objective used. In order to visualize the largest section of tissue possible, we used a 4X objective that gave a large area to image but only provided us with 176  $\mu\text{m}$  of resolution. This means that our ability to discern the initiation site of epileptiform activity was limited to a 176 square bin. Now that we have shown the spatial characteristics of epileptogenesis in large networks surrounding malformed cortex, future studies can isolate smaller cortical areas using voltage sensitive dye imaging with higher power objectives and/or calcium imaging techniques. In combination with genetic tools to identify cell types, calcium imaging of single cells would provide not only great spatial resolution, but cell subtype specific resolution. This will be essential to understanding the

role that different cell types play in the generation, persistence, and termination of epileptiform activity.

### *Stimulation Protocol and Future Studies*

An essential component of the studies in this dissertation was the use of stimulation to the grey-white matter interface to evoke both normal cortical responses, as well as epileptiform events. This method of stimulation of cortical events has been used for decades and has proven to be a valid means to activate neuron networks, similar to the way that cortical afferents can activate neuronal networks (65, 264). A limitation of this stimulation protocol is that all afferents under the stimulation electrode are activated. This means that all cortical afferents, including, but not limited to thalamocortical, commissural fibers, and modulatory afferents from subcortical structures, are activated simultaneously. As selective stimulation protocols (optogenetic in particular) become more prevalent, we learn more about how different afferents affect cortical function in different ways (111, 130, 272). The possibility exists that certain cortical afferents may play a larger role than other cortical afferents, but the limitations of our stimulation protocol prevent us from making any of those conclusions. The studies contained in this dissertation identify the age of susceptibility to evoked epileptiform activity in the immature malformed cortex. It is not known which cortical afferents, if any, are responsible for the increases in susceptibility. These studies provide the groundwork for future studies to probe, with more sophisticated stimulation techniques, which afferents contribute the greatest amount to increase susceptibility in the malformed cortex.

### *Translation and Therapeutic Relevance*

Current treatment for patients with epilepsy associated with developmental cortical malformations involves anti-epilepsy drugs followed by surgical resection of the epileptogenic tissue. Most malformations are only found after a patient shows signs of neurological deficit and/or seizure. This makes treating a patient prior to the onset of seizures difficult. However, the latent period between malformation creation and seizure onset could become a therapeutic window by utilizing technological advances that have made imaging malformations less expensive and easier to locate, in conjunction with greater understanding of developmental cortical malformations. Identifying key time points in both the development of seizure susceptibility, as well as the exact timing of epileptogenic mechanisms will be essential components of a clinician's ability to help a polymicrogyria patient avoid seizures from initiating.

Clinical evidence suggests that the same developmental cortical malformation in two different patients can have a different epileptogenic focus. To date, no single animal model of a developmental cortical malformation has been able to replicate these disparate clinical findings. The evidence in chapter 4 suggests that, for the first time, the timing of the creation of a microgyria can alter the epileptogenic focus, mimicking clinical evidence. Unfortunately, in these dissertation studies we were unable to identify a mechanism that causes the differences in the spatiotemporal characteristics of the P0- and P1-lesioned cortex. As discussed earlier, we hypothesized that differential thalamocortical afferentation of the MG and PMR regions in P0- and P1-lesioned cortex might explain the differences in epileptogenic focus. We have shown here that anatomical thalamocortical afferentation of the cortex (evidenced by vGlut2 staining) is not different between P0- and P1-lesioned cortex, but it is possible that functional thalamocortical afferentation differences exist. Experience provides important developmental

signals to the cortex, including the unsilencing of AMPA receptors and the formation of functional thalamocortical synapses on layer IV neurons (12). In chapter 3, we found that the abnormal presence of CRI activity in P9 PMR cortex (lesioned on P1) was due in part to altered AMPA receptor kinetics. Whether the functional thalamocortical afferentation differential affects AMPA receptor kinetics in P0- or P1-lesioned cortex is not known, but future studies could probe this possibility. Hopefully, the new spatiotemporal characteristics of epileptiform activity in microgyria discussed in this dissertation will lead to the development of better-targeted pharmacological and/or surgical solutions for patients with polymicrogyria.



## List of References

### List of References

1. Abuelo D. 2007. Microcephaly syndromes *Seminars in pediatric neurology* 14(3):118–127.
2. Aizenman CD, Kirkwood A, and Bear MF. 1996. A current source density analysis of evoked responses in slices of adult rat visual cortex: implications for the regulation of long-term potentiation. *Cereb Cortex* 6(6):751–758.
3. Akerman CJ and Cline HT. 2007. Refining the roles of GABAergic signaling during neural circuit formation *Trends in Neurosciences* 30(8):382–389.
4. Alberca R and Moreno A. 1996. [Late onset epilepsy] *Neurologia* 11 Suppl 4:72–79.
5. Albertson AJ, Yang J, and Hablitz JJ. 2011. Decreased Hyperpolarization-activated Currents in Layer 5 Pyramidal Neurons Enhances Excitability in Focal Cortical Dysplasia *J Neurophysiol.*
6. Aligianis IA, Morgan NV, Mione M, Johnson CA, Rosser E, Hennekam RC, Adams G, et al. 2006. Mutation in Rab3 GTPase-activating protein (RAB3GAP) noncatalytic subunit in a kindred with Martsolf syndrome *Am J Hum Genet* 78(4):702–707.
7. Allaman I, Bélanger M, and Magistretti PJ. 2011. Astrocyte-neuron metabolic relationships: for better and for worse *Trends in Neurosciences* 34(2):76–87.
8. Allen CB, Celikel T, and Feldman DE. 2003. Long-term depression induced by sensory deprivation during cortical map plasticity in vivo *Nat Neurosci* 6(3):291–299.
9. Altman J. 1969. Autoradiographic and histological studies of postnatal neurogenesis. IV. Cell proliferation and migration in the anterior forebrain, with special reference to

- persisting neurogenesis in the olfactory bulb *J Comp Neurol* 137(4):433–457.
10. Angevine JB and Sidman RL. 1961. Autoradiographic study of cell migration during histogenesis of cerebral cortex in the mouse *Nature* 192:766–768.
  11. Aronica E, Gorter JA, Redeker S, Ramkema M, Spliet WGM, van Rijen PC, Leenstra S, and Troost D. 2005. Distribution, characterization and clinical significance of microglia in glioneuronal tumours from patients with chronic intractable epilepsy *Neuropathol Appl Neurobiol* 31(3):280–291.
  12. Ashby MC and Isaac JTR. 2011. Maturation of a Recurrent Excitatory Neocortical Circuit by Experience-Dependent Unsilencing of Newly Formed Dendritic Spines. *Neuron* 70(3):510–521.
  13. Avoli M. 2001. Do interictal discharges promote or control seizures? Experimental evidence from an in vitro model of epileptiform discharge. *Epilepsia* 42 Suppl 3:2–4.
  14. Avoli M, Bernasconi A, Mattia D, Olivier A, and Hwa GG. 1999. Epileptiform discharges in the human dysplastic neocortex: in vitro physiology and pharmacology. *Ann Neurol* 46(6):816–826.
  15. Avoli M, Drapeau C, Louvel J, Pumain R, Olivier A, and Villemure JG. 1991. Epileptiform activity induced by low extracellular magnesium in the human cortex maintained in vitro. *Ann Neurol* 30(4):589–596.
  16. Baala L, Briault S, Etchevers HC, Laumonnier F, Natiq A, Amiel J, Boddaert N, et al. 2007. Homozygous silencing of T-box transcription factor EOMES leads to microcephaly with polymicrogyria and corpus callosum agenesis *Nat. Genet.* 39(4):454–456.
  17. Bai L, Huang X, Yang Q, and Wu J-Y. 2006. Spatiotemporal patterns of an evoked

- network oscillation in neocortical slices: coupled local oscillators *J Neurophysiol* 96(5):2528–2538.
18. Bandyopadhyay S and Hablitz JJ. 2006. NR2B antagonists restrict spatiotemporal spread of activity in a rat model of cortical dysplasia. *Epilepsy Res* 72(2-3):127–139.
  19. Bandyopadhyay S, Sutor B, and Hablitz JJ. 2006. Endogenous acetylcholine enhances synchronized interneuron activity in rat neocortex. *J Neurophysiol* 95(3):1908–1916.
  20. Baraban SC, Wenzel HJ, Hochman DW, and Schwartzkroin PA. 2000. Characterization of heterotopic cell clusters in the hippocampus of rats exposed to methylazoxymethanol in utero *Epilepsy Res* 39(2):87–102.
  21. Baraban SC and Schwartzkroin PA. 1995. Electrophysiology of CA1 pyramidal neurons in an animal model of neuronal migration disorders: prenatal methylazoxymethanol treatment. *Epilepsy Res* 22(2):145–156.
  22. Barkovich AJ and Kjos BO. 1992. Nonlissencephalic cortical dysplasias: correlation of imaging findings with clinical deficits *AJNR Am J Neuroradiol* 13(1):95–103.
  23. Barkovich AJ, Kuzniecky RI, and Dobyns WB. 2001. Radiologic classification of malformations of cortical development *Curr Opin Neurol* 14(2):145–149.
  24. Barkovich AJ. 2010. Current concepts of polymicrogyria *Neuroradiology* 52(6):479–487.
  25. Barth AL and Malenka RC. 2001. NMDAR EPSC kinetics do not regulate the critical period for LTP at thalamocortical synapses *Nat Neurosci* 4(3):235–236.
  26. Bartolomei F, Gavaret M, Dravet C, Guye M, Bally-Berard JY, Genton P, Raybaud C, Régis J, and Gastaut JL. 1999. Late-onset epilepsy associated with regional brain cortical dysplasia. *Eur Neurol* 42(1):11–16.

27. Bayer SA and Altman J. 1991. *Neocortical development*. 255. Raven Pr.
28. Beck H and Yaari Y. 2008. Plasticity of intrinsic neuronal properties in CNS disorders *Nat Rev Neurosci* 9(5):357–369.
29. Becker AJ, Pitsch J, Sochivko D, Opitz T, Staniek M, Chen C-C, Campbell KP, Schoch S, Yaari Y, and Beck H. 2008. Transcriptional upregulation of Cav3.2 mediates epileptogenesis in the pilocarpine model of epilepsy *J Neurosci* 28(49):13341–13353.
30. Beghi E. 2007. Epilepsy *Curr Opin Neurol* 20(2):169–174.
31. Begley CE, Famulari M, Annegers JF, Lairson DR, Reynolds TF, Coan S, Dubinsky S, et al. 2000. The cost of epilepsy in the United States: an estimate from population-based clinical and survey data *Epilepsia* 41(3):342–351.
32. Bell GS, Mula M, and Sander JW. 2009. Suicidality in people taking antiepileptic drugs: What is the evidence *CNS Drugs* 23(4):281–292.
33. Ben-Ari Y, Cherubini E, Corradetti R, and Gaiarsa JL. 1989. Giant synaptic potentials in immature rat CA3 hippocampal neurones *J Physiol (Lond)* 416:303–325.
34. Ben-Ari Y, Gaiarsa J-L, Tyzio R, and Khazipov R. 2007. GABA: a pioneer transmitter that excites immature neurons and generates primitive oscillations *Physiol Rev* 87(4):1215–1284.
35. Benardete EA and Kriegstein AR. 2002. Increased excitability and decreased sensitivity to GABA in an animal model of dysplastic cortex *Epilepsia* 43(9):970–982.
36. Bender KJ, Allen CB, Bender VA, and Feldman DE. 2006. Synaptic basis for whisker deprivation-induced synaptic depression in rat somatosensory cortex *J Neurosci* 26(16):4155–4165.
37. Benucci A, Frazor RA, and Carandini M. 2007. Standing waves and traveling waves

- distinguish two circuits in visual cortex *Neuron* 55(1):103–117.
38. Berg AT, Berkovic SF, Brodie MJ, Buchhalter J, Cross JH, van Emde Boas W, Engel J, et al. 2010. Revised terminology and concepts for organization of seizures and epilepsies: report of the ILAE Commission on Classification and Terminology, 2005-2009 *Epilepsia* 51(4):676–685.
  39. Berg AT and Scheffer IE. 2011. New concepts in classification of the epilepsies: Entering the 21st century. *Epilepsia* 52(6):1058–1062.
  40. Bertram EH and Cornett J. 1993. The ontogeny of seizures in a rat model of limbic epilepsy: evidence for a kindling process in the development of chronic spontaneous seizures *Brain Res* 625(2):295–300.
  41. Bertram EH and Cornett JF. 1994. The evolution of a rat model of chronic spontaneous limbic seizures *Brain Res* 661(1-2):157–162.
  42. Bien CG, Benninger FO, Urbach H, Schramm J, Kurthen M, and Elger CE. 2000. Localizing value of epileptic visual auras *Brain* 123 ( Pt 2):244–253.
  43. Bladin PF. 2010. *The threshold of the new epileptology: Dr Lennox at the London Congress, 1935* 16–21.
  44. Boer K, Spliet WGM, van Rijen PC, Redeker S, Troost D, and Aronica E. 2006. Evidence of activated microglia in focal cortical dysplasia *J. Neuroimmunol.* 173(1-2):188–195.
  45. Bordey A, Lyons SA, Hablitz JJ, and Sontheimer H. 2001. Electrophysiological characteristics of reactive astrocytes in experimental cortical dysplasia. *J Neurophysiol* 85(4):1719–1731.
  46. Bragin A, Wilson CL, Almajano J, Mody I, and Engel J. 2004. High-frequency

- oscillations after status epilepticus: epileptogenesis and seizure genesis *Epilepsia* 45(9):1017–1023.
47. Bragin DE, Sanderson JL, Peterson S, Connor JA, and Müller WS. 2009. Development of epileptiform excitability in the deep entorhinal cortex after status epilepticus *Eur J Neurosci* 30(4):611–624.
  48. Brill J and Huguenard JR. 2010. Enhanced infragranular and supragranular synaptic input onto layer 5 pyramidal neurons in a rat model of cortical dysplasia *Cereb Cortex* 20(12):2926–2938.
  49. Brodie MJ. 2010. Antiepileptic drug therapy the story so far *Seizure : the journal of the British Epilepsy Association* 19(10):650–655.
  50. Brodtkorb E, Andersen K, Henriksen O, Myhr G, and Skullerud K. 1998. Focal, continuous spikes suggest cortical developmental abnormalities. Clinical, MRI and neuropathological correlates *Acta Neurol. Scand.* 98(6):377–385.
  51. Brodtkorb E, Myhr G, and Gimse R. 2000. Is monozygotic twinning a risk factor for focal cortical dysgenesis *Acta Neurol. Scand.* 102(1):53–59.
  52. Brunelli S, Faiella A, Capra V, Nigro V, Simeone A, Cama A, and Boncinelli E. 1996. Germline mutations in the homeobox gene EMX2 in patients with severe schizencephaly *Nat. Genet.* 12(1):94–96.
  53. Campbell SL and Hablitz JJ. 2008. Decreased glutamate transport enhances excitability in a rat model of cortical dysplasia. *Neurobiology of Disease* 32(2):254–261.
  54. Caronia-Brown G and Grove EA. 2011. Timing of cortical interneuron migration is influenced by the cortical hem *Cereb Cortex* 21(4):748–755.
  55. Catterall WA, Dib-Hajj S, Meisler MH, and Pietrobon D. 2008. Inherited neuronal ion

- channelopathies: new windows on complex neurological diseases *J Neurosci* 28(46):11768–11777.
56. Caviness VS. 1982. Early events of neocortical assembly: experimental studies and human pathology *Int. J. Neurol.* 16-17:102–109.
  57. Cepeda C, André VM, Levine MS, Salamon N, Miyata H, Vinters HV, and Mathern GW. 2006. Epileptogenesis in pediatric cortical dysplasia: the dysmature cerebral developmental hypothesis. *Epilepsy & behavior : E&B* 9(2):219–235.
  58. Chassoux F, Landre E, Rodrigo S, Beuvon F, Turak B, Semah F, and Devaux B. 2008. Intralesional recordings and epileptogenic zone in focal polymicrogyria *Epilepsia* 49(1):51–64.
  59. Cheetham CEJ, Hammond MSL, Edwards CEJ, and Finnerty GT. 2007. Sensory experience alters cortical connectivity and synaptic function site specifically *J Neurosci* 27(13):3456–3465.
  60. Chevassus-Au-Louis N and Represa A. 1999. The right neuron at the wrong place: biology of heterotopic neurons in cortical neuronal migration disorders, with special reference to associated pathologies *Cell Mol Life Sci* 55(10):1206–1215.
  61. Chu Y, Parada I, and Prince DA. 2009. Temporal and topographic alterations in expression of the alpha3 isoform of Na<sup>+</sup>, K<sup>(+)</sup>-ATPase in the rat freeze lesion model of microgyria and epileptogenesis. *Neuroscience* 162(2):339–348.
  62. Chudotvorova I, Ivanov A, Rama S, Hübner CA, Pellegrino C, Ben-Ari Y, and Medina I. 2005. Early expression of KCC2 in rat hippocampal cultures augments expression of functional GABA synapses *J Physiol (Lond)* 566(Pt 3):671–679.
  63. Clarke DF, Otsubo H, Weiss SK, Chitoku S, Chuang SH, Logan WJ, Smith M-L, et al.



2003. The significance of ear plugging in localization-related epilepsy *Epilepsia* 44(12):1562–1567.
64. Cobos I, Calcagnotto ME, Vilaythong AJ, Thwin MT, Noebels JL, Baraban SC, and Rubenstein JLR. 2005. Mice lacking *Dlx1* show subtype-specific loss of interneurons, reduced inhibition and epilepsy. *Nat Neurosci* 8(8):1059–1068.
65. Cogan SF. 2008. Neural Stimulation and Recording Electrodes. *Annu. Rev. Biomed. Eng.* 10(1):275–309.
66. Connors BW and Gutnick MJ. 1990. Intrinsic firing patterns of diverse neocortical neurons. *Trends in Neurosciences* 13(3):99–104.
67. Cui C, Sakata-Haga H, Ohta K-I, Nishida M, Yashiki M, Sawada K, and Fukui Y. 2006. Histological brain alterations following prenatal methamphetamine exposure in rats *Congenit Anom (Kyoto)* 46(4):180–187.
68. Curia G, Longo D, Biagini G, Jones RSG, and Avoli M. 2008. The pilocarpine model of temporal lobe epilepsy *J Neurosci Methods* 172(2):143–157.
69. D'Arcangelo G, Miao GG, Chen SC, Soares HD, Morgan JI, and Curran T. 1995. A protein related to extracellular matrix proteins deleted in the mouse mutant *reeler* *Nature* 374(6524):719–723.
70. Daras M, Papakostas G, and Tuchman AI. 1994. *Epilepsy and the ancient world: from the magic beliefs of the Babylonians to the Hippocratic scientific thinking* 233–236.
71. Das K, Banerjee M, Mondal GP, Devi LG, Singh OP, and Mukherjee BB. 2007. Evaluation of socio-economic factors causing discontinuation of epilepsy treatment resulting in seizure recurrence: a study in an urban epilepsy clinic in India *Seizure : the journal of the British Epilepsy Association* 16(7):601–607.

72. de Curtis M and Avanzini G. 2001. Interictal spikes in focal epileptogenesis. *Prog Neurobiol* 63(5):541–567.
73. De Felipe J, Marco P, Fairén A, and Jones EG. 1997. Inhibitory synaptogenesis in mouse somatosensory cortex *Cereb Cortex* 7(7):619–634.
74. DeDiego I, Smith-Fernández A, and Fairén A. 1994. Cortical cells that migrate beyond area boundaries: characterization of an early neuronal population in the lower intermediate zone of prenatal rats *Eur J Neurosci* 6(6):983–997.
75. Defazio RA and Hablitz JJ. 1999. Reduction of zolpidem sensitivity in a freeze lesion model of neocortical dysgenesis. *J Neurophysiol* 81(1):404–407.
76. Defazio RA and Hablitz JJ. 2000. Alterations in NMDA receptors in a rat model of cortical dysplasia. *J Neurophysiol* 83(1):315–321.
77. DeFazio T and Hablitz JJ. 1998. Zinc and zolpidem modulate mIPSCs in rat neocortical pyramidal neurons. *J Neurophysiol* 80(4):1670–1677.
78. Dhamija R, Moseley BD, Cascino GD, and Wirrell EC. 2011. A population-based study of long-term outcome of epilepsy in childhood with a focal or hemispheric lesion on neuroimaging *Epilepsia* 52(8):1522–1526.
79. Di Rocco F, Giannetti S, Gaglini P, Di Rocco C, and Granato A. 2002. Dendritic architecture of corticothalamic neurons in a rat model of microgyria. *Childs Nerv Syst* 18(12):690–693.
80. Dobyns WB, Reiner O, Carrozzo R, and Ledbetter DH. 1993. Lissencephaly. A human brain malformation associated with deletion of the LIS1 gene located at chromosome 17p13 *JAMA* 270(23):2838–2842.
81. Dobyns WB, Mirzaa G, Christian SL, Petras K, Roseberry J, Clark GD, Curry CJR, et

- al. 2008. Consistent chromosome abnormalities identify novel polymicrogyria loci in 1p36.3, 2p16.1-p23.1, 4q21.21-q22.1, 6q26-q27, and 21q2 *Am J Med Genet A* 146A(13):1637–1654.
82. Dubeau F, Tampieri D, Lee N, Andermann E, Carpenter S, Leblanc R, Olivier A, Radtke R, Villemure JG, and Andermann F. 1995. Periventricular and subcortical nodular heterotopia. A study of 33 patients *Brain* 118 ( Pt 5):1273–1287.
83. Dudek FE and Staley KJ. 2011. The time course of acquired epilepsy: implications for therapeutic intervention to suppress epileptogenesis *Neurosci Lett* 497(3):240–246.
84. Dudek FE and Staley KJ. 2011. Seizure probability in animal models of acquired epilepsy: A perspective on the concept of the preictal state *Epilepsy Res.*
85. During MJ and Spencer DD. 1993. Extracellular hippocampal glutamate and spontaneous seizure in the conscious human brain *Lancet* 341(8861):1607–1610.
86. Dvorak K and Feit J. 1977. Migration of neuroblasts through partial necrosis of the cerebral cortex in newborn rats-contribution to the problems of morphological development and developmental period of cerebral microgyria. Histological and autoradiographical study. *Acta Neuropathol* 38(3):203–212.
87. Dvorak K, Feit J, and Juránková Z. 1978. Experimentally induced focal microgyria and status verrucosus deformis in rats--pathogenesis and interrelation. Histological and autoradiographical study. *Acta Neuropathol* 44(2):121–129.
88. Dzhala VI and Staley KJ. 2003. Excitatory actions of endogenously released GABA contribute to initiation of ictal epileptiform activity in the developing hippocampus *J Neurosci* 23(5):1840–1846.
89. Dzhala VI, Talos DM, Sdrulla DA, Brumback AC, Mathews GC, Benke TA, Delpire E,

- Jensen FE, and Staley KJ. 2005. NKCC1 transporter facilitates seizures in the developing brain *Nat Med* 11(11):1205–1213.
90. Englund C, Folkerth RD, Born D, Lacy JM, and Hevner RF. 2005. Aberrant neuronal-glial differentiation in Taylor-type focal cortical dysplasia (type IIA/B) In *Acta neuropathologica*, 109: 519–533.
91. Feldman DE and Brecht M. 2005. Map plasticity in somatosensory cortex *Science* 310(5749):810–815.
92. Finardi A, Gardoni F, Bassanini S, Lasio G, Cossu M, Tassi L, Caccia C, et al. 2006. NMDA receptor composition differs among anatomically diverse malformations of cortical development *J Neuropathol Exp Neurol* 65(9):883–893.
93. Fisher RS, van Emde Boas W, Blume W, Elger C, Genton P, Lee P, and Engel J. 2005. Epileptic seizures and epilepsy: definitions proposed by the International League Against Epilepsy (ILAE) and the International Bureau for Epilepsy (IBE) *Epilepsia* 46(4):470–472.
94. Fitch RH, Brown CP, Tallal P, and Rosen GD. 1997. Effects of sex and MK-801 on auditory-processing deficits associated with developmental microgyric lesions in rats *Behav. Neurosci.* 111(2):404–412.
95. Fogarty M, Grist M, Gelman D, Marín O, Pachnis V, and Kessar N. 2007. Spatial genetic patterning of the embryonic neuroepithelium generates GABAergic interneuron diversity in the adult cortex *J Neurosci* 27(41):10935–10946.
96. Fox JW, Lamperti ED, Ekşioğlu YZ, Hong SE, Feng Y, Graham DA, Scheffer IE, et al. 1998. Mutations in filamin 1 prevent migration of cerebral cortical neurons in human periventricular heterotopia *Neuron* 21(6):1315–1325.

97. Frantz GD and McConnell SK. 1996. Restriction of late cerebral cortical progenitors to an upper-layer fate *Neuron* 17(1):55–61.
98. Friede RL and Mikolasek J. 1978. Postencephalitic porencephaly, hydranencephaly or polymicrogyria. A review *Acta Neuropathol* 43(1-2):161–168.
99. Fujiwara-Tsukamoto Y, Isomura Y, Nambu A, and Takada M. 2003. Excitatory GABA input directly drives seizure-like rhythmic synchronization in mature hippocampal CA1 pyramidal cells. *Neuroscience* 119(1):265–275.
100. Galaburda AM, Sherman GF, Rosen GD, Aboitiz F, and Geschwind N. 1985. Developmental dyslexia: four consecutive patients with cortical anomalies. *Ann Neurol* 18(2):222–233.
101. Ge S, Goh ELK, Sailor KA, Kitabatake Y, Ming G-L, and Song H. 2006. GABA regulates synaptic integration of newly generated neurons in the adult brain *Nature* 439(7076):589–593.
102. George AL and Jacobs KM. 2011. Altered intrinsic properties of neuronal subtypes in malformed epileptogenic cortex. *Brain Res* 1374:116–128.
103. Germano IM, Sperber EF, Ahuja S, and Moshé SL. 1998. Evidence of enhanced kindling and hippocampal neuronal injury in immature rats with neuronal migration disorders. *Epilepsia* 39(12):1253–1260.
104. Giannetti S, Gaglini P, Di Rocco F, Di Rocco C, and Granato A. 2000. Organization of cortico-cortical associative projections in a rat model of microgyria *Neuroreport* 11(10):2185–2189.
105. Giannetti S, Gaglini P, Granato A, and Di Rocco C. 1999. Organization of callosal connections in rats with experimentally induced microgyria *Childs Nerv Syst* 15(9):444–

- 8; discussion 449–50.
106. Glaser T, Jepeal L, Edwards JG, Young SR, Favor J, and Maas RL. 1994. PAX6 gene dosage effect in a family with congenital cataracts, aniridia, anophthalmia and central nervous system defects *Nat. Genet.* 7(4):463–471.
  107. Gloveli T, Albrecht D, and Heinemann U. 1995. Properties of low Mg<sup>2+</sup> induced epileptiform activity in rat hippocampal and entorhinal cortex slices during adolescence. *Brain Res Dev Brain Res* 87(2):145–152.
  108. Golden JA. 2001. Cell migration and cerebral cortical development *Neuropathol Appl Neurobiol* 27(1):22–28.
  109. González JL, Russo CJ, Goldowitz D, Sweet HO, Davisson MT, and Walsh CA. 1997. Birthdate and cell marker analysis of scrambler: a novel mutation affecting cortical development with a reeler-like phenotype *J Neurosci* 17(23):9204–9211.
  110. Gorter JA, van Vliet EA, Aronica E, and Lopes da Silva FH. 2001. Progression of spontaneous seizures after status epilepticus is associated with mossy fibre sprouting and extensive bilateral loss of hilar parvalbumin and somatostatin-immunoreactive neurons *Eur J Neurosci* 13(4):657–669.
  111. Gradinaru V, Mogri M, Thompson KR, Henderson JM, and Deisseroth K. 2009. Optical deconstruction of parkinsonian neural circuitry. *Science* 324(5925):354–359.
  112. Grant AC and Rho JM. 2002. Ictal EEG patterns in band heterotopia *Epilepsia* 43(4):403–407.
  113. Gressens P. 2000. Mechanisms and disturbances of neuronal migration *Pediatr. Res.* 48(6):725–730.
  114. Gressens P, Marret S, and Evrard P. 1996. Developmental spectrum of the excitotoxic

- cascade induced by ibotenate: a model of hypoxic insults in fetuses and neonates. *Neuropathol Appl Neurobiol* 22(6):498–502.
115. Guerrini R and Parrini E. 2010. Neuronal migration disorders *Neurobiology of Disease* 38(2):154–166.
116. Guerrini R, Sicca F, and Parmeggiani L. 2003. Epilepsy and malformations of the cerebral cortex *Epileptic Disord* 5 Suppl 2:S9–26.
117. Gutnick MJ, Connors BW, and Prince DA. 1982. Mechanisms of neocortical epileptogenesis in vitro. *J Neurophysiol* 48(6):1321–1335.
118. Hagemann G, Kluska MM, Redecker C, Luhmann HJ, and Witte OW. 2003. Distribution of glutamate receptor subunits in experimentally induced cortical malformations *Neuroscience* 117(4):991–1002.
119. Hauser WA. 1994. The prevalence and incidence of convulsive disorders in children *Epilepsia* 35 Suppl 2:S1–6.
120. Hauser WA, Annegers JF, and Kurland LT. 1993. Incidence of epilepsy and unprovoked seizures in Rochester, Minnesota: 1935-1984 *Epilepsia* 34(3):453–468.
121. Hellier JL, Patrylo PR, Buckmaster PS, and Dudek FE. 1998. Recurrent spontaneous motor seizures after repeated low-dose systemic treatment with kainate: assessment of a rat model of temporal lobe epilepsy *Epilepsy Res* 31(1):73–84.
122. Hellier JL, Patrylo PR, Dou P, Nett M, Rose GM, and Dudek FE. 1999. Assessment of inhibition and epileptiform activity in the septal dentate gyrus of freely behaving rats during the first week after kainate treatment *J Neurosci* 19(22):10053–10064.
123. Hensch TK. 2005. Critical period plasticity in local cortical circuits *Nat Rev Neurosci* 6(11):877–888.

124. Herman AE, Galaburda AM, Fitch RH, Carter AR, and Rosen GD. 1997. Cerebral microgyria, thalamic cell size and auditory temporal processing in male and female rats *Cereb Cortex* 7(5):453–464.
125. Herman ST. 2002. Epilepsy after brain insult: targeting epileptogenesis *Neurology* 59(9 Suppl 5):S21–6.
126. Hevner RF, Daza RAM, Englund C, Kohtz J, and Fink A. 2004. Postnatal shifts of interneuron position in the neocortex of normal and reeler mice: evidence for inward radial migration *Neuroscience* 124(3):605–618.
127. Hjelmstad GO, Isaac JT, Nicoll RA, and Malenka RC. 1999. Lack of AMPA receptor desensitization during basal synaptic transmission in the hippocampal slice *J Neurophysiol* 81(6):3096–3099.
128. Hoffman SN, Salin PA, and Prince DA. 1994. Chronic neocortical epileptogenesis in vitro. *J Neurophysiol* 71(5):1762–1773.
129. Holmes GL, Sarkisian M, Ben-Ari Y, Liu Z, and Chevassus-Au-Louis N. 1999. Consequences of cortical dysplasia during development in rats. *Epilepsia* 40(5):537–544.
130. Hooks BM, Hires SA, Zhang Y-X, Huber D, Petreanu L, Svoboda K, and Shepherd GMG. 2011. Laminar analysis of excitatory local circuits in vibrissal motor and sensory cortical areas. *Plos Biol* 9(1):e1000572.
131. Humphreys P, Rosen GD, Press DM, Sherman GF, and Galaburda AM. 1991. Freezing lesions of the developing rat brain: a model for cerebrocortical microgyria. *J Neuropathol Exp Neurol* 50(2):145–160.
132. Igelstrom KM, Shirley CH, and Heyward PM. 2011. Low-magnesium medium induces



- epileptiform activity in mouse olfactory bulb slices *J Neurophysiol*.
133. Ignacio M, Kimm E, Kageyama G, and Yu J. 1995. Postnatal migration of neurons and formation of laminae in rat cerebral cortex. *Anatomy and ...*.
  134. Innocenti GM and Berbel P. 1991. Analysis of an experimental cortical network: I). Architectonics of visual areas 17 and 18 after neonatal injections of ibotenic acid; similarities with human microgyria. *Journal of neural transplantation & plasticity* 2(1):1–28.
  135. Isaev D, Isaeva E, Shatskih T, Zhao Q, Smits NC, Shworak NW, Khazipov R, and Holmes GL. 2007. Role of extracellular sialic acid in regulation of neuronal and network excitability in the rat hippocampus *J Neurosci* 27(43):11587–11594.
  136. Isaeva E, Isaev D, Savrasova A, Khazipov R, and Holmes GL. 2010. Recurrent neonatal seizures result in long-term increases in neuronal network excitability in the rat neocortex. *Eur J Neurosci* 31(8):1446–1455.
  137. Jacobs KM, Gutnick MJ, and Prince DA. 1996. Hyperexcitability in a model of cortical maldevelopment. *Cereb Cortex* 6(3):514–523.
  138. Jacobs KM, Hwang BJ, and Prince DA. 1999. Focal epileptogenesis in a rat model of polymicrogyria *J Neurophysiol* 81(1):159–173.
  139. Jacobs KM, Mogensen M, Warren E, and Prince DA. 1999. Experimental microgyri disrupt the barrel field pattern in rat somatosensory cortex. *Cereb Cortex* 9(7):733–744.
  140. Jacobs KM and Prince DA. 2005. Excitatory and inhibitory postsynaptic currents in a rat model of epileptogenic microgyria. *J Neurophysiol* 93(2):687–696.
  141. Jaglin XH, Poirier K, Saillour Y, Buhler E, Tian G, Bahi-Buisson N, Fallet-Bianco C, et al. 2009. Mutations in the beta-tubulin gene TUBB2B result in asymmetrical

- polymicrogyria *Nat. Genet.* 41(6):746–752.
142. Jansen A and Andermann E. 2005. Genetics of the polymicrogyria syndromes. *J Med Genet* 42(5):369–378.
  143. Jefferys JGR. 2003. Models and mechanisms of experimental epilepsies. *Epilepsia* 44 Suppl 12:44–50.
  144. Jones EG. 2009. The origins of cortical interneurons: mouse versus monkey and human *Cereb Cortex* 19(9):1953–1956.
  145. Juenger H, de Haan B, Krägeloh-Mann I, Staudt M, and Karnath H-O. 2011. Early determination of somatosensory cortex in the human brain. *Cereb Cortex* 21(8):1827–1831.
  146. Jung S, Jones TD, Lugo JN, Sheerin AH, Miller JW, D'Ambrosio R, Anderson AE, and Poolos NP. 2007. Progressive dendritic HCN channelopathy during epileptogenesis in the rat pilocarpine model of epilepsy *J Neurosci* 27(47):13012–13021.
  147. Kale R. 2002. Global Campaign Against Epilepsy:the treatment gap *Epilepsia* 43 Suppl 6:31–33.
  148. Kanekar S and Gent M. 2011. Malformations of cortical development *Semin. Ultrasound CT MR* 32(3):211–227.
  149. Keller CJ, Truccolo W, Gale JT, Eskandar E, Thesen T, Carlson C, Devinsky O, et al. 2010. Heterogeneous neuronal firing patterns during interictal epileptiform discharges in the human cortex *Brain* 133(Pt 6):1668–1681.
  150. Kellinghaus C, Loddenkemper T, Najm IM, Wyllie E, Lineweaver T, Nair DR, and Lüders HO. 2004. Specific epileptic syndromes are rare even in tertiary epilepsy centers: a patient-oriented approach to epilepsy classification. *Epilepsia* 45(3):268–275.

151. Kellinghaus C, Möddel G, Shigeto H, Ying Z, Jacobsson B, Gonzalez-Martinez J, Burrier C, Janigro D, and Najm IM. 2007. Dissociation between in vitro and in vivo epileptogenicity in a rat model of cortical dysplasia. *Epileptic Disord* 9(1):11–19.
152. Khazipov R, Khalilov I, Tyzio R, Morozova E, Ben-Ari Y, and Holmes GL. 2004. Developmental changes in GABAergic actions and seizure susceptibility in the rat hippocampus *Eur J Neurosci* 19(3):590–600.
153. Kilb W, Sinning A, and Luhmann HJ. 2007. Model-specific effects of bumetanide on epileptiform activity in the in-vitro intact hippocampus of the newborn mouse. *Neuropharmacology* 53(4):524–533.
154. Kilb W, Hartmann D, Saftig P, and Luhmann HJ. 2004. Altered morphological and electrophysiological properties of Cajal-Retzius cells in cerebral cortex of embryonic Presenilin-1 knockout mice. *Eur J Neurosci* 20(10):2749–2756.
155. Ko J, Humbert S, Bronson RT, Takahashi S, Kulkarni AB, Li E, and Tsai LH. 2001. p35 and p39 are essential for cyclin-dependent kinase 5 function during neurodevelopment *J Neurosci* 21(17):6758–6771.
156. Kobayashi E, Bagshaw AP, Jansen A, Andermann F, Andermann E, Gotman J, and Dubeau F. 2005. Intrinsic epileptogenicity in polymicrogyric cortex suggested by EEG-fMRI BOLD responses. *Neurology* 64(7):1263–1266.
157. Kobayashi K, Ohtsuka Y, Ohno S, Tanaka A, Hiraki Y, and Oka E. 2001. Age-related clinical and neurophysiologic characteristics of intractable epilepsy associated with cortical malformation. *Epilepsia* 42 Suppl 6:24–28.
158. Kolb B and Cioe J. 2003. Recovery from early cortical damage in rats. IX. Differential behavioral and anatomical effects of temporal cortex lesions at different ages of neural

- maturation. *Behav Brain Res* 144(1-2):67–76.
159. Kondo S and Kawaguchi Y. 2001. Slow synchronized bursts of inhibitory postsynaptic currents (0.1-0.3 Hz) by cholinergic stimulation in the rat frontal cortex in vitro. *Neuroscience* 107(4):551–560.
160. Kostović I and Judas M. 2010. The development of the subplate and thalamocortical connections in the human foetal brain *Acta Paediatr.* 99(8):1119–1127.
161. Köhling R, Vreugdenhil M, Bracci E, and Jefferys JG. 2000. Ictal epileptiform activity is facilitated by hippocampal GABAA receptor-mediated oscillations *J Neurosci* 20(18):6820–6829.
162. Krägeloh-Mann I. 2004. Imaging of early brain injury and cortical plasticity *Exp Neurol* 190 Suppl 1:S84–90.
163. Kuzniecky R, Murro A, King D, Morawetz R, Smith J, Powers R, Yaghmai F, Faught E, Gallagher B, and Snead OC. 1993. Magnetic resonance imaging in childhood intractable partial epilepsies: pathologic correlations *Neurology* 43(4):681–687.
164. Lasztóczy B, Antal K, Nyikos L, Emri Z, and Kardos J. 2004. High-frequency synaptic input contributes to seizure initiation in the low-[Mg<sup>2+</sup>] model of epilepsy. *Eur J Neurosci* 19(5):1361–1372.
165. Lasztóczy B and Kardos J. 2006. Cyclothiazide prolongs low [Mg<sup>2+</sup>]-induced seizure-like events. *J Neurophysiol* 96(6):3538–3544.
166. Laurie DJ, Wisden W, and Seeburg PH. 1992. The distribution of thirteen GABAA receptor subunit mRNAs in the rat brain. III. Embryonic and postnatal development *J Neurosci* 12(11):4151–4172.
167. Lavdas AA, Grigoriou M, Pachnis V, and Parnavelas JG. 1999. The medial ganglionic

- eminence gives rise to a population of early neurons in the developing cerebral cortex *J Neurosci* 19(18):7881–7888.
168. Lee AC, Wong RKS, Chuang S-C, Shin H-S, and Bianchi R. 2002. Role of synaptic metabotropic glutamate receptors in epileptiform discharges in hippocampal slices *J Neurophysiol* 88(4):1625–1633.
169. Lee KS, Schottler F, Collins JL, Lanzino G, Couture D, Rao A, Hiramatsu K, et al. 1997. A genetic animal model of human neocortical heterotopia associated with seizures *J Neurosci* 17(16):6236–6242.
170. Leger P-L, Souville I, Boddaert N, Elie C, Pinard JM, Plouin P, Moutard ML, et al. 2008. The location of DCX mutations predicts malformation severity in X-linked lissencephaly *Neurogenetics* 9(4):277–285.
171. Leventer RJ, Guerrini R, and Dobyns WB. 2008. Malformations of cortical development and epilepsy *Dialogues Clin Neurosci* 10(1):47–62.
172. Leweke FM, Louvel J, Rausche G, and Heinemann U. 1990. Effects of pentetrazol on neuronal activity and on extracellular calcium concentration in rat hippocampal slices *Epilepsy Res* 6(3):187–198.
173. Li G, Adesnik H, Li J, Long J, Nicoll RA, Rubenstein JLR, and Pleasure SJ. 2008. Regional distribution of cortical interneurons and development of inhibitory tone are regulated by Cxcl12/Cxcr4 signaling *J Neurosci* 28(5):1085–1098.
174. Lim CCT, Yin H, Loh NK, Chua VGE, Hui F, and Barkovich AJ. 2005. Malformations of cortical development: high-resolution MR and diffusion tensor imaging of fiber tracts at 3T *AJNR Am J Neuroradiol* 26(1):61–64.
175. Loddenkemper T, Kellinghaus C, Wyllie E, Najm IM, Gupta A, Rosenow F, and Lüders

- HO. 2005. A proposal for a five-dimensional patient-oriented epilepsy classification  
*Epileptic Disord* 7(4):308–316.
176. Lojková-Janecková D, Ng J, and Mares P. 2009. Antagonists of group I metabotropic glutamate receptors and cortical afterdischarges in immature rats. *Epilepsia* 50(9):2123–2129.
177. Lothman EW, Bertram EH, Bekenstein JW, and Perlin JB. 1989. Self-sustaining limbic status epilepticus induced by “continuous” hippocampal stimulation: electrographic and behavioral characteristics *Epilepsy Res* 3(2):107–119.
178. López-Bendito G, Sánchez-Alcañiz JA, Pla R, Borrell V, Picó E, Valdeolmillos M, and Marín O. 2008. Chemokine signaling controls intracortical migration and final distribution of GABAergic interneurons *J Neurosci* 28(7):1613–1624.
179. Lubke J, Egger V, Sakmann B, and Feldmeyer D. 2000. Columnar Organization of Dendrites and Axons of Single and Synaptically Coupled Excitatory Spiny .... *J Neurosci*.
180. Luhmann HJ, Huston JP, and Hasenöhr RU. 2005. Contralateral increase in thigmotactic scanning following unilateral barrel-cortex lesion in mice. *Behav Brain Res* 157(1):39–43.
181. Luhmann HJ, Karpuk N, Qü MS, and Zilles K. 1998. Characterization of neuronal migration disorders in neocortical structures. II. Intracellular in vitro recordings. *J Neurophysiol* 80(1):92–102.
182. Luhmann HJ and Prince DA. 1990. Control of NMDA receptor-mediated activity by GABAergic mechanisms in mature and developing rat neocortex. *Brain Res Dev Brain Res* 54(2):287–290.

183. Luhmann HJ and Prince DA. 1991. Postnatal maturation of the GABAergic system in rat neocortex. *J Neurophysiol* 65(2):247–263.
184. Luhmann HJ and Raabe K. 1996. Characterization of neuronal migration disorders in neocortical structures: I. Expression of epileptiform activity in an animal model. *Epilepsy Res* 26(1):67–74.
185. Ma H-T, Wu C-H, and Wu J-Y. 2004. Initiation of spontaneous epileptiform events in the rat neocortex in vivo *J Neurophysiol* 91(2):934–945.
186. Malphrus AD and Wilfong AA. 2007. Use of the newer antiepileptic drugs in pediatric epilepsies *Curr Treat Options Neurol* 9(4):256–267.
187. Mani R, Pollard J, and Dichter MA. 2011. Human clinical trails in antiepileptogenesis *Neurosci Lett* 497(3):251–256.
188. Marín O and Rubenstein JL. 2001. A long, remarkable journey: tangential migration in the telencephalon. *Nat Rev Neurosci* 2(11):780–790.
189. Marín O and Rubenstein JLR. 2003. Cell migration in the forebrain *Annu Rev Neurosci* 26:441–483.
190. Marret S, Mukendi R, Gadisseux JF, Gressens P, and Evrard P. 1995. Effect of ibotenate on brain development: an excitotoxic mouse model of microgyria and posthypoxic-like lesions *J Neuropathol Exp Neurol* 54(3):358–370.
191. Mathern GW, Leiphart JL, De Vera A, Adelson PD, Seki T, Neder L, and Leite JP. 2002. Seizures decrease postnatal neurogenesis and granule cell development in the human fascia dentata. *Epilepsia* 43 Suppl 5:68–73.
192. Mattia D, Olivier A, and Avoli M. 1995. Seizure-like discharges recorded in human dysplastic neocortex maintained in vitro. *Neurology* 45(7):1391–1395.

193. Mazarati A, Bragin A, Baldwin R, Shin D, Wilson C, Sankar R, Naylor D, Engel J, and Wasterlain CG. 2002. Epileptogenesis after self-sustaining status epilepticus *Epilepsia* 43 Suppl 5:74–80.
194. McBride MC and Kemper TL. 1982. Pathogenesis of four-layered microgyric cortex in man *Acta Neuropathol* 57(2-3):93–98.
195. McConnell SK and Kaznowski CE. 1991. Cell cycle dependence of laminar determination in developing neocortex *Science* 254(5029):282–285.
196. McCormick DA and Contreras D. 2001. On the cellular and network bases of epileptic seizures *Annu. Rev. Physiol.* 63:815–846.
197. McEvelly RJ, de Diaz MO, Schonemann MD, Hooshmand F, and Rosenfeld MG. 2002. Transcriptional regulation of cortical neuron migration by POU domain factors *Science* 295(5559):1528–1532.
198. McTague A and Appleton R. 2011. Treatment of difficult epilepsy *Arch. Dis. Child.* 96(2):200–204.
199. Merlin LR and Wong RK. 1997. Role of group I metabotropic glutamate receptors in the patterning of epileptiform activities in vitro *J Neurophysiol* 78(1):539–544.
200. Mitzdorf U. 1985. Current source-density method and application in cat cerebral cortex: investigation of evoked potentials and EEG phenomena *Physiol Rev* 65(1):37–100.
201. Miyakawa N, Yazawa I, Sasaki S, Momose-Sato Y, and Sato K. 2003. Optical analysis of acute spontaneous epileptiform discharges in the in vivo rat cerebral cortex *Neuroimage* 18(3):622–632.
202. Miyoshi G and Fishell G. 2011. GABAergic interneuron lineages selectively sort into specific cortical layers during early postnatal development *Cereb Cortex* 21(4):845–852.



203. Miyoshi G, Hjerling-Leffler J, Karayannis T, Sousa VH, Butt SJB, Battiste J, Johnson JE, Machold RP, and Fishell G. 2010. Genetic fate mapping reveals that the caudal ganglionic eminence produces a large and diverse population of superficial cortical interneurons *J Neurosci* 30(5):1582–1594.
204. Momin A, Cadiou H, Mason A, and McNaughton PA. 2008. Role of the hyperpolarization-activated current  $I_h$  in somatosensory neurons. *J Physiol (Lond)* 586(24):5911–5929.
205. Moroni RF, Inverardi F, Regondi MC, Panzica F, Spreafico R, and Frassoni C. 2008. Altered spatial distribution of PV-cortical cells and dysmorphic neurons in the somatosensory cortex of BCNU-treated rat model of cortical dysplasia *Epilepsia* 49(5):872–887.
206. Moser J, Kilb W, Werhahn K-J, and Luhmann HJ. 2006. Early developmental alterations of low-Mg<sup>2+</sup> -induced epileptiform activity in the intact corticohippocampal formation of the newborn mouse in vitro. *Brain Res* 1077(1):170–177.
207. Moser J, Kilb W, Werhahn K-J, and Luhmann HJ. 2006. Early developmental alterations of low-Mg<sup>2+</sup> -induced epileptiform activity in the intact corticohippocampal formation of the newborn mouse in vitro. *Brain Res* 1077(1):170–177.
208. Möddel G, Jacobson B, Ying Z, Janigro D, Bingaman W, Gonzalez-Martinez J, Kellinghaus C, Prayson RA, and Najm IM. 2005. The NMDA receptor NR2B subunit contributes to epileptogenesis in human cortical dysplasia *Brain Res* 1046(1-2):10–23.
209. Nadarajah B and Parnavelas JG. 2002. Modes of neuronal migration in the developing cerebral cortex. *Nat Rev Neurosci* 3(6):423–432.
210. Nahmani M and Erisir A. 2005. VGluT2 immunocytochemistry identifies thalamocortical

- terminals in layer 4 of adult and developing visual cortex *J Comp Neurol* 484(4):458–473.
211. Nicholson C and Freeman JA. 1975. Theory of current source-density analysis and determination of conductivity tensor for anuran cerebellum. *J Neurophysiol* 38(2):356–368.
212. Noctor SC, Palmer SL, Hasling T, and Juliano SL. 1999. Interference with the development of early generated neocortex results in disruption of radial glia and abnormal formation of neocortical layers. *Cereb Cortex* 9(2):121–136.
213. Ogawa M, Miyata T, Nakajima K, Yagyu K, Seike M, Ikenaka K, Yamamoto H, and Mikoshiba K. 1995. The reeler gene-associated antigen on Cajal-Retzius neurons is a crucial molecule for laminar organization of cortical neurons *Neuron* 14(5):899–912.
214. Ohshima T, Ward JM, Huh CG, Longenecker G, Veeranna, Pant HC, Brady RO, Martin LJ, and Kulkarni AB. 1996. Targeted disruption of the cyclin-dependent kinase 5 gene results in abnormal corticogenesis, neuronal pathology and perinatal death *Proc Natl Acad Sci USA* 93(20):11173–11178.
215. Olafsson E, Hauser WA, Ludvigsson P, and Gudmundsson G. 1996. Incidence of epilepsy in rural Iceland: a population-based study *Epilepsia* 37(10):951–955.
216. Olivier C, Cobos I, Perez Villegas EM, Spassky N, Zalc B, Martinez S, and Thomas JL. 2001. Monofocal origin of telencephalic oligodendrocytes in the anterior entopeduncular area of the chick embryo *Development* 128(10):1757–1769.
217. Otis T, Zhang S, and Trussell LO. 1996. Direct measurement of AMPA receptor desensitization induced by glutamatergic synaptic transmission *J Neurosci* 16(23):7496–7504.

218. Palmer SL, Noctor SC, Jablonska B, and Juliano SL. 2001. Laminar specific alterations of thalamocortical projections in organotypic cultures following layer 4 disruption in ferret somatosensory cortex *Eur J Neurosci* 13(8):1559–1571.
219. Palmini A, Andermann F, Olivier A, Tampieri D, Robitaille Y, Melanson D, and Ethier R. 1991. Neuronal migration disorders: a contribution of modern neuroimaging to the etiologic diagnosis of epilepsy. *The Canadian journal of neurological sciences Le journal canadien des sciences neurologiques* 18(4 Suppl):580–587.
220. Palmini A, Gambardella A, Andermann F, Dubeau F, da Costa JC, Olivier A, Tampieri D, Gloor P, Quesney F, and Andermann E. 1995. Intrinsic epileptogenicity of human dysplastic cortex as suggested by corticography and surgical results *Ann Neurol* 37(4):476–487.
221. Panayiotopoulos CP. 2010. *Atlas of Epilepsies*. 1910. Springer Verlag.
222. Park C-K, Kim S-K, Wang K-C, Hwang Y-S, Kim KJ, Chae JH, Chi JG, Choe G-Y, Kim NR, and Cho B-K. 2006. Surgical outcome and prognostic factors of pediatric epilepsy caused by cortical dysplasia. *Childs Nerv Syst* 22(6):586–592.
223. Payne BR and Lomber SG. 2001. Reconstructing functional systems after lesions of cerebral cortex *Nat Rev Neurosci* 2(12):911–919.
224. Peiffer AM, Fitch RH, Thomas JJ, Yurkovic AN, and Rosen GD. 2003. Brain weight differences associated with induced focal microgyria. *BMC Neurosci* 4:12.
225. Peiffer AM, McClure MM, Threlkeld SW, Rosen GD, and Fitch RH. 2004. Severity of focal microgyria and associated rapid auditory processing deficits. *Neuroreport* 15(12):1923–1926.
226. Pekny M and Nilsson M. 2005. Astrocyte activation and reactive gliosis *Glia* 50(4):427–

- 434.
227. Perucca E. 2007. Treatment of epilepsy in developing countries *BMJ* 334(7605):1175–1176.
228. Piao X, Chang BS, Bodell A, Woods K, Benzeev B, Topcu M, Guerrini R, et al. 2005. Genotype-phenotype analysis of human frontoparietal polymicrogyria syndromes *Ann Neurol* 58(5):680–687.
229. Polleux F, Whitford KL, Dijkhuizen PA, Vitalis T, and Ghosh A. 2002. Control of cortical interneuron migration by neurotrophins and PI3-kinase signaling *Development* 129(13):3147–3160.
230. Poulet JFA and Petersen CCH. 2008. Internal brain state regulates membrane potential synchrony in barrel cortex of behaving mice. *Nature* 454(7206):881–885.
231. Powell KL, Ng C, O'Brien TJ, Xu SH, Williams DA, Foote SJ, and Reid CA. 2008. Decreases in HCN mRNA expression in the hippocampus after kindling and status epilepticus in adult rats *Epilepsia* 49(10):1686–1695.
232. Prince DA. 1985. Physiological mechanisms of focal epileptogenesis *Epilepsia* 26 Suppl 1:S3–14.
233. Quilichini PP, Diabira D, Chiron C, Ben-Ari Y, and Gozlan H. 2002. Persistent epileptiform activity induced by low Mg<sup>2+</sup> in intact immature brain structures. *Eur J Neurosci* 16(5):850–860.
234. Quilichini PP, Diabira D, Chiron C, Milh M, Ben-Ari Y, and Gozlan H. 2003. Effects of antiepileptic drugs on refractory seizures in the intact immature corticohippocampal formation in vitro. *Epilepsia* 44(11):1365–1374.
235. Rademacher J, Aulich A, Reifenberger G, Kiwit JC, Langen KJ, Schmidt D, and Seitz

- RJ. 2000. Focal cortical dysplasia of the temporal lobe with late-onset partial epilepsy: serial quantitative MRI. *Neuroradiology* 42(6):430–435.
236. Rakic P. 1972. Mode of cell migration to the superficial layers of fetal monkey neocortex. *J Comp Neurol* 145(1):61–83.
237. Rakić P and Sidman RL. 1969. Telencephalic origin of pulvinar neurons in the fetal human brain *Z Anat Entwicklungsgesch* 129(1):53–82.
238. RamachandranNair R, Otsubo H, Ochi A, Rutka J, and Donner EJ. 2006. Mirror movements following cortical resection of polymicrogyria in a child with intractable epilepsy. *Pediatr Neurol* 34(2):135–138.
239. Rasch MJ, Gretton A, Murayama Y, Maass W, and Logothetis NK. 2008. Inferring spike trains from local field potentials. *J Neurophysiol* 99(3):1461–1476.
240. Rattka M, Brandt C, Bankstahl M, Bröer S, and Löscher W. 2011. Enhanced susceptibility to the GABA antagonist pentylenetetrazole during the latent period following a pilocarpine-induced status epilepticus in rats *Neuropharmacology* 60(2-3):505–512.
241. Raymond AA, Fish DR, Sisodiya SM, Alsanjari N, Stevens JM, and Shorvon SD. 1995. Abnormalities of gyration, heterotopias, tuberous sclerosis, focal cortical dysplasia, microdysgenesis, dysembryoplastic neuroepithelial tumour and dysgenesis of the archicortex in epilepsy. Clinical, EEG and neuroimaging features in 100 adult patients *Brain* 118 ( Pt 3):629–660.
242. Redecker C, Luhmann HJ, Hagemann G, Fritschy JM, and Witte OW. 2000. Differential downregulation of GABAA receptor subunits in widespread brain regions in the freeze-lesion model of focal cortical malformations *J Neurosci* 20(13):5045–5053.

243. Redecker C, Lutzenburg M, Gressens P, Evrard P, Witte OW, and Hagemann G. 1998. Excitability changes and glucose metabolism in experimentally induced focal cortical dysplasias *Cereb Cortex* 8(7):623–634.
244. Redecker C, Hagemann G, Köhling R, Straub H, Witte OW, and Speckmann E-J. 2005. Optical imaging of epileptiform activity in experimentally induced cortical malformations *Exp Neurol* 192(2):288–298.
245. Redecker C, Hagemann G, Köhling R, Straub H, Witte OW, and Speckmann E-J. 2005. Optical imaging of epileptiform activity in experimentally induced cortical malformations. *Exp Neurol* 192(2):288–298.
246. Roll P, Rudolf G, Pereira S, Royer B, Scheffer IE, Massacrier A, Valenti M-P, et al. 2006. SRPX2 mutations in disorders of language cortex and cognition *Hum. Mol. Genet.* 15(7):1195–1207.
247. Roper SN, Eisenschenk S, and King MA. 1999. Reduced density of parvalbumin- and calbindin D28-immunoreactive neurons in experimental cortical dysplasia. *Epilepsy Res* 37(1):63–71.
248. Roper SN, Gilmore RL, and Houser CR. 1995. Experimentally induced disorders of neuronal migration produce an increased propensity for electrographic seizures in rats. *Epilepsy Res* 21(3):205–219.
249. Rosen GD, Sherman GF, and Galaburda AM. 1994. Radial glia in the neocortex of adult rats: effects of neonatal brain injury *Brain Res Dev Brain Res* 82(1-2):127–135.
250. Rosen GD, Burstein D, and Galaburda AM. 2000. Changes in efferent and afferent connectivity in rats with induced cerebrocortical microgyria. *J Comp Neurol* 418(4):423–440.

251. Rosen GD, Herman AE, and Galaburda AM. 1999. Sex differences in the effects of early neocortical injury on neuronal size distribution of the medial geniculate nucleus in the rat are mediated by perinatal gonadal steroids. *Cereb Cortex* 9(1):27–34.
252. Rosen GD, Press DM, Sherman GF, and Galaburda AM. 1992. The development of induced cerebrocortical microgyria in the rat. *J Neuropathol Exp Neurol* 51(6):601–611.
253. Rosen GD, Sherman GF, and Galaburda AM. 1996. Birthdates of neurons in induced microgyria. *Brain Res* 727(1-2):71–78.
254. Rosen GD, Windzio H, and Galaburda AM. 2001. Unilateral induced neocortical malformation and the formation of ipsilateral and contralateral barrel fields. *Neuroscience* 103(4):931–939.
255. Rosenow F and Lüders H. 2001. Presurgical evaluation of epilepsy *Brain* 124(Pt 9):1683–1700.
256. Salanova V, Andermann F, Rasmussen T, Olivier A, and Quesney LF. 1995. Tumoural parietal lobe epilepsy. Clinical manifestations and outcome in 34 patients treated between 1934 and 1988 *Brain* 118 ( Pt 5):1289–1304.
257. Samuels BA and Tsai L-H. 2004. Nucleokinesis illuminated *Nat Neurosci* 7(11):1169–1170.
258. Sancini G, Franceschetti S, Battaglia G, Colacitti C, Di Luca M, Spreafico R, and Avanzini G. 1998. Dysplastic neocortex and subcortical heterotopias in methylazoxymethanol-treated rats: an intracellular study of identified pyramidal neurones. *Neurosci Lett* 246(3):181–185.
259. Scantlebury MH, Gibbs SA, Foadjo B, Lema P, Psarropoulou C, and Carmant L. 2005. Febrile seizures in the predisposed brain: a new model of temporal lobe epilepsy. *Ann*

- Neurol* 58(1):41–49.
260. Scantlebury MH, Ouellet P-L, Psarropoulou C, and Carmant L. 2004. Freeze lesion-induced focal cortical dysplasia predisposes to atypical hyperthermic seizures in the immature rat. *Epilepsia* 45(6):592–600.
261. Scher MS, Barabas RE, and Barmada MA. 1996. Clinical examination findings in neonates with the absence of electrocerebral activity: an acute or chronic encephalopathic state *J Perinatol* 16(6):455–460.
262. Scherberger H, Jarvis MR, and Andersen RA. 2005. Cortical local field potential encodes movement intentions in the posterior parietal cortex. *Neuron* 46(2):347–354.
263. Schmidt S, Bruehl C, Hagemann G, Witte OW, and Redecker C. 2006. Impairment of functional inhibition in the contralateral cortex following perinatally acquired malformations in rats. *Exp Neurol* 201(1):270–274.
264. SEGUNDO JP, NAQUET R, and BUSER P. 1955. Effects of cortical stimulation on electro-cortical activity in monkeys *J Neurophysiol* 18(3):236–245.
265. Shimizu-Okabe C, Okabe A, Kilb W, Sato K, Luhmann HJ, and Fukuda A. 2007. Changes in the expression of cation-Cl<sup>-</sup> cotransporters, NKCC1 and KCC2, during cortical malformation induced by neonatal freeze-lesion *Neurosci Res* 59(3):288–295.
266. Shoykhet M and Simons DJ. 2008. Development of thalamocortical response transformations in the rat whisker-barrel system *J Neurophysiol* 99(1):356–366.
267. Sisodiya SM. 2000. Surgery for malformations of cortical development causing epilepsy. *Brain* 123 ( Pt 6):1075–1091.
268. Sisodiya SM. 2000. Surgery for malformations of cortical development causing epilepsy *Brain* 123 ( Pt 6):1075–1091.



269. Sisodiya SM, Free SL, Williamson KA, Mitchell TN, Willis C, Stevens JM, Kendall BE, et al. 2001. PAX6 haploinsufficiency causes cerebral malformation and olfactory dysfunction in humans *Nat. Genet.* 28(3):214–216.
270. Sisodiya SM. 2000. Surgery for malformations of cortical development causing epilepsy. *Brain* 123 ( Pt 6):1075–1091.
271. Smyth MD, Barbaro NM, and Baraban SC. 2002. Effects of antiepileptic drugs on induced epileptiform activity in a rat model of dysplasia *Epilepsy Res* 50(3):251–264.
272. Sohal VS, Zhang F, Yizhar O, and Deisseroth K. 2009. Parvalbumin neurons and gamma rhythms enhance cortical circuit performance. *Nature* 459(7247):698–702.
273. Squier W and Jansen A. 2010. Abnormal development of the human cerebral cortex *J. Anat.* 217(4):312–323.
274. Staley KJ, White A, and Dudek FE. 2011. Interictal spikes: harbingers or causes of epilepsy *Neurosci Lett* 497(3):247–250.
275. Stern EA, Maravall M, and Svoboda K. 2001. Rapid development and plasticity of layer 2/3 maps in rat barrel cortex in vivo *Neuron* 31(2):305–315.
276. Sun Q-Q, Huguenard JR, and Prince DA. 2005. REORGANIZATION OF BARREL CIRCUITS LEADS TO THALAMICALLY-EVOKED CORTICAL EPILEPTIFORM ACTIVITY. *Thalamus & related systems* 3(4):261–273.
277. Supèr H, Pérez Sust P, and Soriano E. 1997. Survival of Cajal-Retzius cells after cortical lesions in newborn mice: a possible role for Cajal-Retzius cells in brain repair *Brain Res Dev Brain Res* 98(1):9–14.
278. Swann JW, Smith KL, and Brady RJ. 1993. Localized excitatory synaptic interactions mediate the sustained depolarization of electrographic seizures in developing

- hippocampus *J Neurosci* 13(11):4680–4689.
279. Takahashi T, Goto T, Miyama S, Nowakowski RS, and Caviness VS. 1999. Sequence of neuron origin and neocortical laminar fate: relation to cell cycle of origin in the developing murine cerebral wall *J Neurosci* 19(23):10357–10371.
280. Takase K-I, Shigeto H, Suzuki SO, Kikuchi H, Ohyagi Y, and Kira J-I. 2008. Prenatal freeze lesioning produces epileptogenic focal cortical dysplasia *Epilepsia* 49(6):997–1010.
281. Tanaka D, Nakaya Y, Yanagawa Y, Obata K, and Murakami F. 2003. Multimodal tangential migration of neocortical GABAergic neurons independent of GPI-anchored proteins *Development* 130(23):5803–5813.
282. Tassi L, Colombo N, Garbelli R, Francione S, Russo Lo G, Mai R, Cardinale F, et al. 2002. Focal cortical dysplasia: neuropathological subtypes, EEG, neuroimaging and surgical outcome. *Brain* 125(Pt 8):1719–1732.
283. Teixeira KCS, Montenegro MA, Cendes F, Guimarães CA, Guerreiro CAM, and Guerreiro MM. 2007. Clinical and electroencephalographic features of patients with polymicrogyria. *J Clin Neurophysiol* 24(3):244–251.
284. Tezer FI, Yildiz G, Oguz KK, Elibol B, and Saygi S. 2008. Newly diagnosed polymicrogyria in the eighth decade. *Epilepsia* 49(1):181–183.
285. Threlkeld SW, Hill CA, Rosen GD, and Fitch RH. 2009. Early acoustic discrimination experience ameliorates auditory processing deficits in male rats with cortical developmental disruption. *Int J Dev Neurosci* 27(4):321–328.
286. Threlkeld SW, McClure MM, Rosen GD, and Fitch RH. 2006. Developmental timeframes for induction of microgyria and rapid auditory processing deficits in the rat

- Brain Res* 1109(1):22–31.
287. Threlkeld SW, Penley SC, Rosen GD, and Fitch RH. 2008. Detection of silent gaps in white noise following cortical deactivation in rats. *Neuroreport* 19(8):893–898.
288. Threlkeld SW, Rosen GD, and Fitch RH. 2007. Age at developmental cortical injury differentially alters corpus callosum volume in the rat. *BMC Neurosci* 8:94.
289. Tinuper P, D'Orsi G, Bisulli F, Zaniboni A, Piraccini A, Bernardi B, and Baruzzi A. 2003. Malformation of cortical development in adult patients. *Epileptic Disord* 5 Suppl 2:S85–90.
290. Traub RD, Contreras D, and Whittington MA. 2005. Combined experimental/simulation studies of cellular and network mechanisms of epileptogenesis in vitro and in vivo *J Clin Neurophysiol* 22(5):330–342.
291. Traub RD, Jefferys JG, and Whittington MA. 1994. Enhanced NMDA conductance can account for epileptiform activity induced by low Mg<sup>2+</sup> in the rat hippocampal slice. *J Physiol (Lond)* 478 Pt 3:379–393.
292. Trevelyan A, Sussillo D, and Yuste R. 2007. Feedforward Inhibition Contributes to the Control of Epileptiform Propagation Speed. *J Neurosci*.
293. Trotter SA, Kapur J, Anzivino MJ, and Lee KS. 2006. GABAergic synaptic inhibition is reduced before seizure onset in a genetic model of cortical malformation *J Neurosci* 26(42):10756–10767.
294. Tsau Y, Guan L, and Wu JY. 1998. Initiation of spontaneous epileptiform activity in the neocortical slice *J Neurophysiol* 80(2):978–982.
295. Tsau Y, Guan L, and Wu JY. 1999. Epileptiform activity can be initiated in various neocortical layers: an optical imaging study *J Neurophysiol* 82(4):1965–1973.

296. Uylings HB and van Eden CG. 1990. Qualitative and quantitative comparison of the prefrontal cortex in rat and in primates, including humans *Prog Brain Res* 85:31–62.
297. van Zundert B, Yoshii A, and Constantine-Paton M. 2004. Receptor compartmentalization and trafficking at glutamate synapses: a developmental proposal *Trends in Neurosciences* 27(7):428–437.
298. Velisek L, Velísková J, Chudomel O, Poon K-L, Robeson K, Marshall B, Sharma A, and Moshé SL. 2008. Metabolic environment in substantia nigra reticulata is critical for the expression and control of hypoglycemia-induced seizures *J Neurosci* 28(38):9349–9362.
299. Vezzani A, Conti M, De Luigi A, Ravizza T, Moneta D, Marchesi F, and De Simoni MG. 1999. Interleukin-1beta immunoreactivity and microglia are enhanced in the rat hippocampus by focal kainate application: functional evidence for enhancement of electrographic seizures *J Neurosci* 19(12):5054–5065.
300. Vezzani A, Moneta D, Richichi C, Aliprandi M, Burrows SJ, Ravizza T, Perego C, and De Simoni MG. 2002. Functional role of inflammatory cytokines and antiinflammatory molecules in seizures and epileptogenesis *Epilepsia* 43 Suppl 5:30–35.
301. Világi I, Tarnawa I, and Banczerowski-Pelyhe I. 1991. Changes in seizure activity of the neocortex during the early postnatal development of the rat: an electrophysiological study on slices in Mg(2+)-free medium. *Epilepsy Res* 8(2):102–106.
302. Walton NY and Treiman DM. 1992. Valproic acid treatment of experimental status epilepticus *Epilepsy Res* 12(3):199–205.
303. Wendling F, Hernandez A, Bellanger J-J, Chauvel P, and Bartolomei F. 2005. Interictal to ictal transition in human temporal lobe epilepsy: insights from a computational model of intracerebral EEG. *J Clin Neurophysiol* 22(5):343–356.

304. Wenzel HJ, Robbins CA, Tsai LH, and Schwartzkroin PA. 2001. Abnormal morphological and functional organization of the hippocampus in a p35 mutant model of cortical dysplasia associated with spontaneous seizures *J Neurosci* 21(3):983–998.
305. White EL, Weinfeld L, and Lev DL. 1997. A survey of morphogenesis during the early postnatal period in PMBSF barrels of mouse SmI cortex with emphasis on barrel D4 *Somatosens Mot Res* 14(1):34–55.
306. White R, Hua Y, Scheithauer B, Lynch DR, Henske EP, and Crino PB. 2001. Selective alterations in glutamate and GABA receptor subunit mRNA expression in dysplastic neurons and giant cells of cortical tubers *Ann Neurol* 49(1):67–78.
307. Wichterle H, Turnbull DH, Nery S, Fishell G, and Alvarez-Buylla A. 2001. In utero fate mapping reveals distinct migratory pathways and fates of neurons born in the mammalian basal forebrain *Development* 128(19):3759–3771.
308. Widdess-Walsh P, Kellinghaus C, Jeha L, Kotagal P, Prayson R, Bingaman W, and Najm IM. 2005. Electro-clinical and imaging characteristics of focal cortical dysplasia: correlation with pathological subtypes. *Epilepsy Res* 67(1-2):25–33.
309. Williams PA, Hellier JL, White AM, Staley KJ, and Dudek FE. 2007. Development of spontaneous seizures after experimental status epilepticus: implications for understanding epileptogenesis *Epilepsia* 48 Suppl 5:157–163.
310. Williams PA, White AM, Clark S, Ferraro DJ, Swiercz W, Staley KJ, and Dudek FE. 2009. Development of spontaneous recurrent seizures after kainate-induced status epilepticus *J Neurosci* 29(7):2103–2112.
311. Wong M and Yamada KA. 2001. Developmental characteristics of epileptiform activity in immature rat neocortex: a comparison of four in vitro seizure models *Brain Res Dev*

- Brain Res* 128(2):113–120.
312. Wu JY, Guan L, Bai L, and Yang Q. 2001. Spatiotemporal properties of an evoked population activity in rat sensory cortical slices *J Neurophysiol* 86(5):2461–2474.
313. Wu JY, Guan L, and Tsau Y. 1999. Propagating activation during oscillations and evoked responses in neocortical slices *J Neurosci* 19(12):5005–5015.
314. Xu W, Huang X, Takagaki K, and Wu J-Y. 2007. Compression and reflection of visually evoked cortical waves *Neuron* 55(1):119–129.
315. Yashiro K and Philpot BD. 2008. Regulation of NMDA receptor subunit expression and its implications for LTD, LTP, and metaplasticity *Neuropharmacology* 55(7):1081–1094.
316. Yoneshima H, Nagata E, Matsumoto M, Yamada M, Nakajima K, Miyata T, Ogawa M, and Mikoshiba K. 1997. A novel neurological mutant mouse, yotari, which exhibits reeler-like phenotype but expresses CR-50 antigen/reelin *Neurosci Res* 29(3):217–223.
317. Zeng L-H, Rensing NR, Zhang B, Gutmann DH, Gambello MJ, and Wong M. 2011. Tsc2 gene inactivation causes a more severe epilepsy phenotype than Tsc1 inactivation in a mouse model of tuberous sclerosis complex *Hum. Mol. Genet.* 20(3):445–454.
318. Zhang CL, Gloveli T, and Heinemann U. 1994. Effects of NMDA- and AMPA-receptor antagonists on different forms of epileptiform activity in rat temporal cortex slices. *Epilepsia* 35 Suppl 5:S68–73.
319. Zilles K, Qü MS, Schleicher A, and Luhmann HJ. 1998. Characterization of neuronal migration disorders in neocortical structures: quantitative receptor autoradiography of ionotropic glutamate, GABA(A) and GABA(B) receptors. *Eur J Neurosci* 10(10):3095–3106.

320. Zsombok A and Jacobs KM. 2007. Postsynaptic currents prior to onset of epileptiform activity in rat microgyria. *J Neurophysiol* 98(1):178–186.
321. Zurolo E, Iyer A, Maroso M, Carbonell C, Anink JJ, Ravizza T, Fluiter K, et al. 2011. Activation of Toll-like receptor, RAGE and HMGB1 signalling in malformations of cortical development *Brain* 134(Pt 4):1015–1032.
322. 2002. Wyllie 2000-Surgical treatment of epilepsy in. 1–5.

### **Vita**

Lloyd Andrew Bell IV was born on February 5, 1985, in Greensboro, North Carolina. He graduated from Bishop Kenny High School in 2001. He received his Bachelor of Arts in English and Psychology from Hampden-Sydney College, Hampden-Sydney, Virginia in 2005. He spent a year working with Dr. Steve Sawyer in the Pharmacology-Toxicology Department at Virginia Commonwealth University before entering the Ph.D. program at Virginia Commonwealth University.